Shock Tube Testing

Ted A. Erikson

Armour Research Foundation of Illinois Institute of Technology
Technology Center
Chicago 16, Illinois

INTRODUCTION

A shock tube[1,2] consists of a high-pressure (driver) section and a low-pressure (driven) section which are separated from each other by a rupture diaphragm. When the diaphragm is ruptured, the compression wave quickly generates a shock wave into the low-pressure medium. The transient zone of shock-heated and shock-compressed driven gas produced in this manner can be utilized to cause the initiation of condensed-phase, unstable (explosive) systems.

This paper indicates the background and nature of such shock tube techniques and briefly summarizes the technique employed in pure environmental shock tests (PEST) at the Armour Research Foundation.

GENERAL BACKGROUND

The first application of a shock tube technique for assessing the explosive sensitivity of condensed-phase systems was reported by Gey and Bennett in 1955.[3] For many years the Foundation has employed this technique in qualitative[4,5] tests of the explosive sensitivity of various unstable materials, and more recently in a quantitative study of the initiation of lead azide.[6] Other investigators[7,8,9,10] have reported the use of the shock tube for the initiation of several composite propellants. Currently the Foundation is extending these studies to liquid monopropellant systems.

Briefly, the shock tube is used as a research tool for producing a transient zone of shock-heated and shock-compressed driven gas which can be made to contact the surface of a condensed-phase, unstable system. Under certain conditions, a time delay can be measured from shock contact to the detection of an explosive response or reaction runaway.

A shock tube is operated by adjusting the driven gas pressure and slowly increasing the driver (usually helium) gas pressure until the diaphragm ruptures. The compression wave rapidly generates a shock wave which propagates at nearly constant velocity into the low-pressure medium. State properties of the driven gas behind the incident and the reflected shock front can be calculated from the driver-to-driven gas pressure ratio at the instant of diaphragm rupture and the initial state of the driven gas. The calculated properties can be experimentally confirmed with suitable instrumentation to measure shock pressures, shock temperatures and traverse velocities between two or more fixed stations.

The surface of a test sample may be exposed to a quiescent or a flowing shocked gas environment wherein conductive and forced convective heating effects are respectively enhanced. An ideal quiescent condition can be generated by flush-mounting a test sample on the end plate of a shock tube. In this location, the sample surface is exposed to the twice shocked (incident and reflected) driven gas environment, which remains essentially static until the rarefaction wave arrives from the driver section. A flowing condition is generated by mounting a test sample

aerodynamically in the center or along the periphery, of the shock tube. In such positions, the sample is exposed to the transient zone of shocked gas environment which sweeps across the surface.

When the surface of a condensed-phase, unstable system is exposed to the quiescent or flowing shocked gas environment, the following experimental data are known or can be calculated or measured at time of contact:

C - composition of the driven gas

T_g - temperature of the shock-heated driven gas

P_g - pressure of the shock-compressed driven gas

T_o - surface temperature of the condensed-phase system.

A time delay to explosive response can be measured, during which interval it is practically impossible to monitor the infinitesimal variations in T_g, P_g, and T_t (the surface temperature at time t), or the extent of decomposition near the surface. Basically then, the experimental data that are measured or controlled in such shock testing techniques include: (1) a definition of the state of the shocked driven gas in terms of say, composition, temperature, and pressure (2) the initial surface temperature of the test sample exposed to said environment and (3) a time interval (delay) from moment of contact to detection of explosive response.

Explosive response can be determined by various experimental techniques. For example, the time at which pressure, electrical conductivity, or luminosity transitions occur can be recorded respectively by pressure transducers, conductivity probes, and a photographic (or photocell) record of flame luminosity. The Foundation has employed the detection of the generated explosion "noise" or vibration upon the end plate mount as a simple technique for identifying an explosive response. It should also be mentioned that the resulting time delay should be within the relatively constant conditions of the first incident and/or reflected shock exposure, so that the analytical complications that can be incurred because of subsequent shocks of diminished intensity can be avoided.

Based on a heat transfer analysis, T_t can be estimated. The correlation of T_t with the time delay, t_d, then serves to indicate reaction mechanisms by permitting the identification of runaway temperatures, activation energies, and other initiating phenomena. Whether the ignition mechanism involves a runaway reaction in the condensed-phase, as developed by Hicks,[11] or the establishment of a gaseous reaction zone adjacent to the surface, as suggested by McAlevy, et al.,[9] appears to be in doubt. The difficulty in these approaches is the assumption that T_t can be adequately estimated by a heat transfer analysis. Severe complications can arise due to surface irregularities in the case of solids (unless single crystal faces are employed), and to vapor pressure and vaporization phenomena in the case of liquids.

Recently, a number of thermodynamic models have been proposed[12] for various steady-rate processes. These models utilize the arguments of ordinary thermodynamics to relate the flow of mass, volume and heat to the properties (chemical potential, pressure and temperature) of terminal parts of a system which are linked by a gradient region or part-on-the-line. A simplified application of this procedure is in order for the problem of explosion initiation, or sensitivity, because of the likelihood that definable stationary states exist across the gradient regions of steady-rate flames.

One objective of studies conducted at the Foundation is based on the premise that the order of explosive response (i.e., sustaining decomposition, deflagration and detonation) for an unstable system is characterized by a unique energetic situation. Thus, contact of an energy-rich zone (e.g., the flame zone or an

artificial environment) with a potentially energy-rich zone (e.g., a layer of relatively undisturbed explosive) can result in a characteristic time delay for a subsequent rate of propagation. By varying the magnitude, rate, and mode of energy release from an artificial environment to the surface of an unstable medium, it should be possible to evaluate specific energetic susceptibilities of unstable systems.

For example, in the pure environmental shock test, relative measures of the magnitude, rate and mode of energy release from the shocked driven gas environment to the surface of a condensed-phase system might be ascertained from the shock intensity, the pressure, and the composition of the driven gas (varying degrees of freedom), respectively.

EXPERIMENTAL

A schematic diagram of the shock tube used for a study of the initiation of lead azide at the Armour Research Foundation is shown in Fig. 1,* which also indicates a detailed time-distance sequence of events. The sample was positioned on the back plate of the shock tube as shown in Fig. 2, which indicates the composite array of equipment, instrumentation and electrical circuitry.

Transient shock pressures were recorded by photographing the output of a Kistler PZ-6 miniature pressure transducer and PT-6 amplifier-calibrator unit on a Tektronix 535 oscilloscope. Triggering of the Tektronix 535 oscilloscope was effected internally by the reception of the shock pressure output from the Kistler gage, and both the pressure and the V_2 voltage of the conductivity circuit (see Fig. 2) were simultaneously displayed at the 100-kc chopping rate of a Tektronix 53/54-c dual preamplifier.

Triggering of the Tektronix 545 oscilloscope sweep was effected by less than a 0.1-volt rise in V_1 (of the conductivity circuit), and both the negative voltage output of the Kistler gage and V_1 were displayed at the 100-kc chopping rate of a CA dual preamplifier unit. This was done as a means of obtaining magnified records of the extremely fast conductivity transient.

The criterion of explosion response was the characteristic "ring" of the Kistler gage output when explosion noise was generated at the sample site and transmitted through the end plate and wall of the shock tube to the gage position. The response time was calibrated by spark initiation of lead azide samples.

The results of typical tests are shown in Fig. 3. Photographs of oscilloscope traces with and without azide samples are included to enable the identification of the respective traces. It can be seen that the shock pressure, a time delay (due to "ring"), and conductivity voltage transients are recorded. The data for these tests are summarized in Table 1. Since the driver-to-driven gas pressure ratio (P_4/P_1) was accurately measured, this value was used to define the Mach number of the incident shock, M_s, from a report by Alpher and White.[13] From M_s, the values of the reflected shock pressure and temperature, P_g and T_g (the former usually being confirmed by the oscilloscope record), were obtained by the use of tables.[14] Tests have been conducted with nitrogen, helium, argon and carbon dioxide as driven gases over Mach numbers ranging from about 2 to 7.

---

*Final Reports on Contract No. DA-11-022-501-ORD-2731, June, 1959, and Contract No. DA-11-022-ORD-3120, June, 1960. Supported by the Picatinny Arsenal.

Table 1

DATA FROM PURE ENVIRONMENTAL SHOCK TESTS WITH LEAD AZIDE AND NITROGEN DRIVEN GAS

Test No.	P_1, psia	P_4/P_1	M_s	T_g, °K	P_g, psia	t_d, μsec
115	0.467	500	5.09	3100	97.5	103
116	0.460	517	5.11	3200	100	-
119	0.767	301	4.69	2700	134	69
120	0.770	304	4.69	2700	135	-
131	1.55	150	4.18	2220	206	24
132	1.545	156	4.19	2230	206	-

DISCUSSION OF RESULTS

The data from our pure environmental shock testing of polycrystalline lead azide can be simply represented by plotting the logarithm of the product of the square of the reflected shock pressure and the time delay, log $(P_g^2 t_d)$, as a function of the reciprocal of the reflected shock temperature, $1/T_g$. Figure 4 displays such a plot for shock test data obtained with nitrogen as a driven gas. Additional data with other driven gases are presented in this form in Fig. 5. Attempts were made to evaluate the data by a heat transfer analysis based on published data[15] and independent calculations at the Foundation. The increase in surface temperature was estimated to vary from 10 to 50°C. The difficulty with such analyses is that a flat planar surface must be assumed, which is experimentally inadequate unless single crystal faces are exposed to the shock environment.

The vaporization of fuel and a subsequent gas phase runaway reaction mechanism[9] appears to explain the results obtained in solid propellant tests; however the possibility of such a mechanism being operative in the decomposition of lead azide seems remote. Further conjecture regarding the interpretation of shock tube results is inappropriate at this time. A more sophisticated analysis must be delayed until sufficient data are available for the development of composite views.

REFERENCES

1. Bleakney, W., Weimer, D. K., and Fletcher, C. H., "The Shock Tube - A Facility for Investigations in Fluid Dynamics," Rev. Sci. Instr. 20, 807 (1949).

2. Resler, E., Lin, S., and Kantrowitz, A., "The Production of High Temperature Gases in Shock Tubes," J. Appl. Phys. 23, 1390 (1952).

3. Gey, W. E., and Bennett, A., "Sensitivity of Explosives to Pure Shocks," J. Chem. Phys. 23, 1979 (1955).

4. Erikson, T. A., "Pure Shock Testing," Paper presented at the Second Explosive Sensitivity Conference, Silver Spring, Maryland, September, 1957.

5. Erikson, T. A., "Pure Environmental Shock Testing of Condensed-Phase, Unstable Materials," ARS Journal 30, 190 (1960).

6. Erikson, T. A., "Pure Environmental Shock Testing of Condensed Phases," ONR Symposium Report, ACR-52, Vol. 1, pp. 24-41, September 26-28, 1960.

7. Summerfield, M., and McAlevy, R., "Shock Tube as a Tool for Solid Propellant Research," Jet Prop. 28, 478 (1958).

8. Baer, A. O., Ryan, N. W., and Salt, D. L., "Propellant Ignition by High Convective Heat Fluxes," Paper presented at ARS Solid Propellant Conference, Princeton, N. J., January 28-29, 1960.

9. McAlevy, R. F., Cowan, P. L., and Summerfield, M., "Mechanism of Ignition of Composite Solid Propellants," Paper presented at ARS Solid Propellant Conference, Princeton, N. J., January 28-29, 1960.

10. Solid Propellant Rocket Research, Vol. 1, October, 1960, Academic Press, New York, edited by Martin Summerfield, Princeton University.

11. Hicks, B. L., "Theory of Ignition Considered as a Thermal Reaction," J. Chem. Phys. 22, 414 (1954).

12. Tykodi, R. J., and Erikson, T. A., "Thermodynamics, Stationary States and Steady-Rate Processes (series of six papers)," J. Chem. Phys. 31, 1506-1525 (1959); 33, 40-49 (1960).

13. Alpher, R. A., and White, D. R., "Ideal Theory of Shock Tubes with Area Change Near Diaphragm," General Electric Report No. 57-RL-1664, January, 1957, Schenectady, New York.

14. Strehlow, R., "One Dimensional Step Shock Calculations for Ideal Gases," Ballistic Research Laboratory Report No. 978, April, 1956, Aberdeen Proving Ground, Maryland.

15. Rose, P., "Development of a Calorimeter Heat Transfer Gage for Use in Shock Tubes," Avco Research Laboratory Report No. 17, February, 1958.

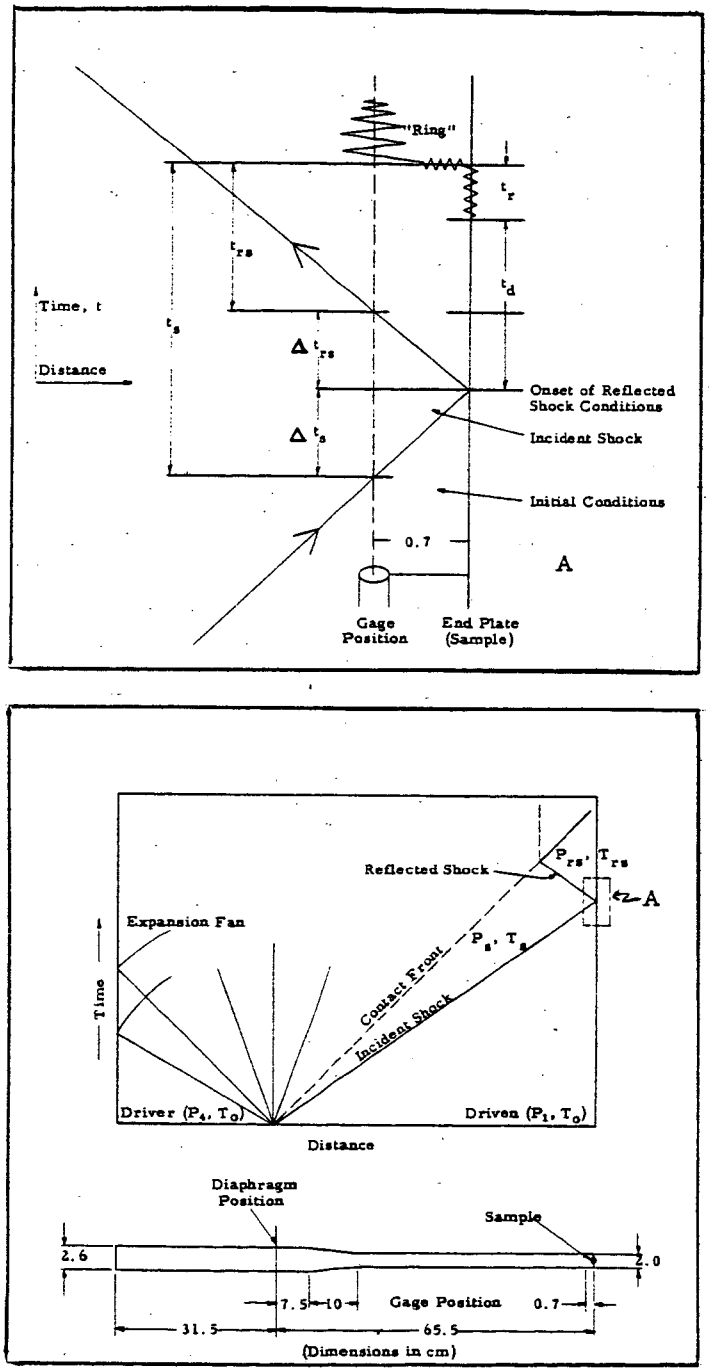

Fig. 1 Shock Tube Profile and Schematic of Time-Distance Events

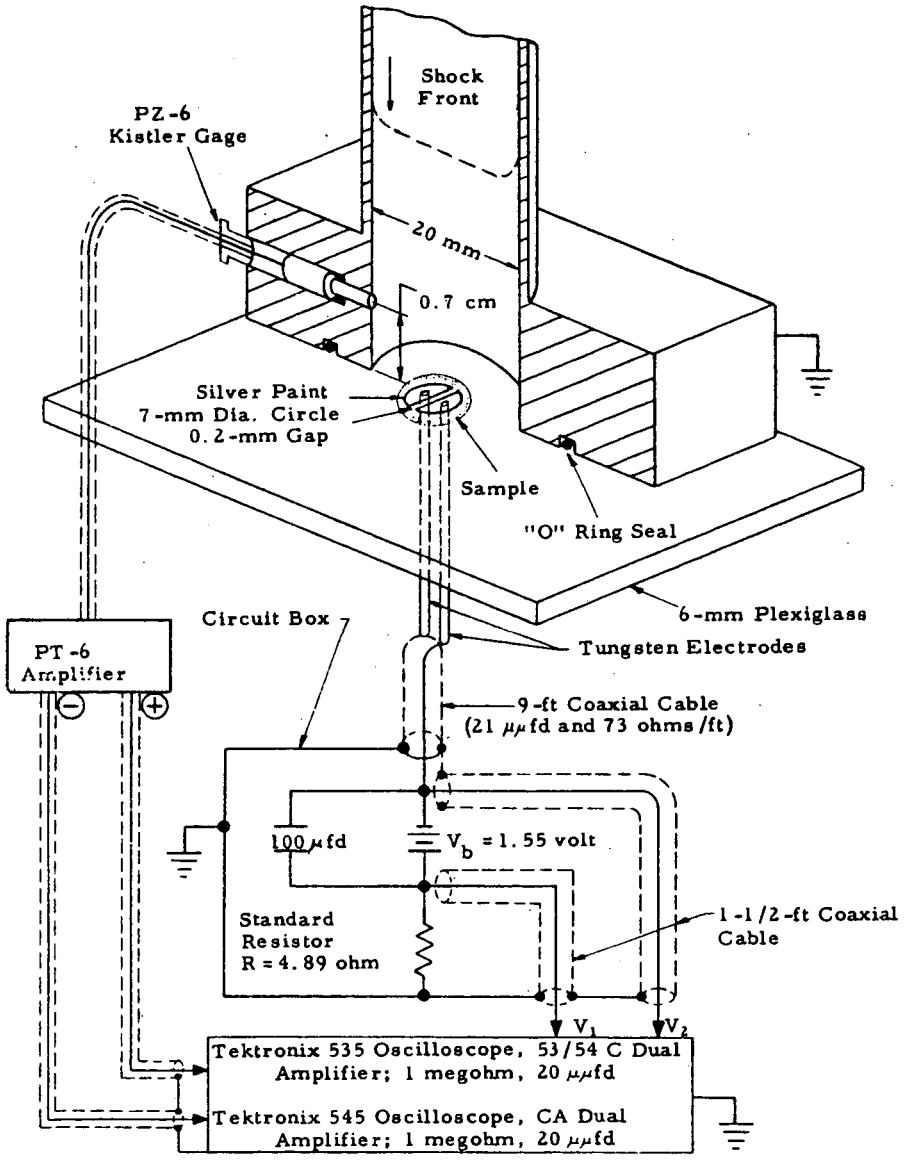

Fig. 2 Composite Details of Shock Test Set-Up

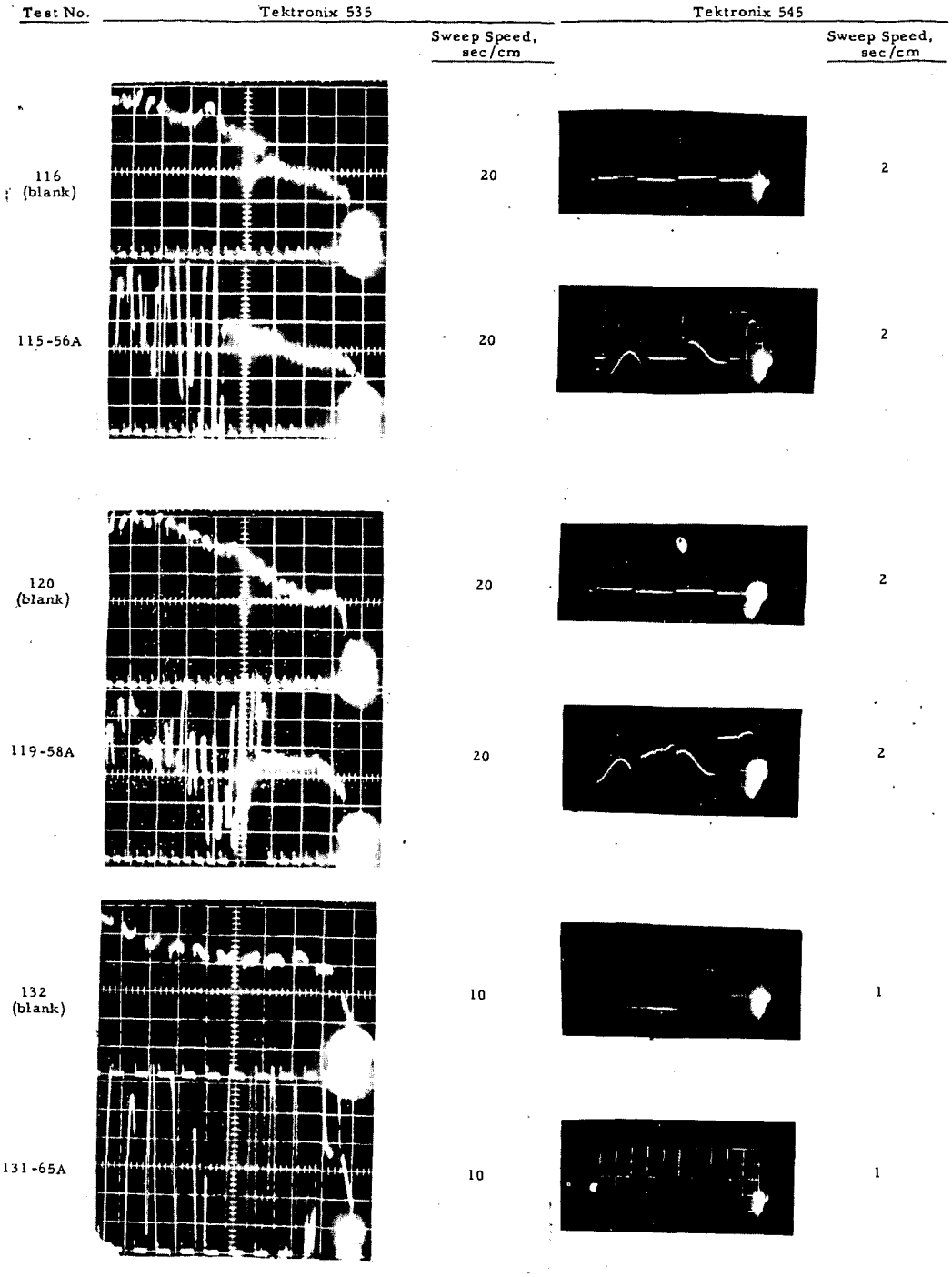

Fig. 3 Photographs of Pressure-Voltage Transients in Shock Tube Testing

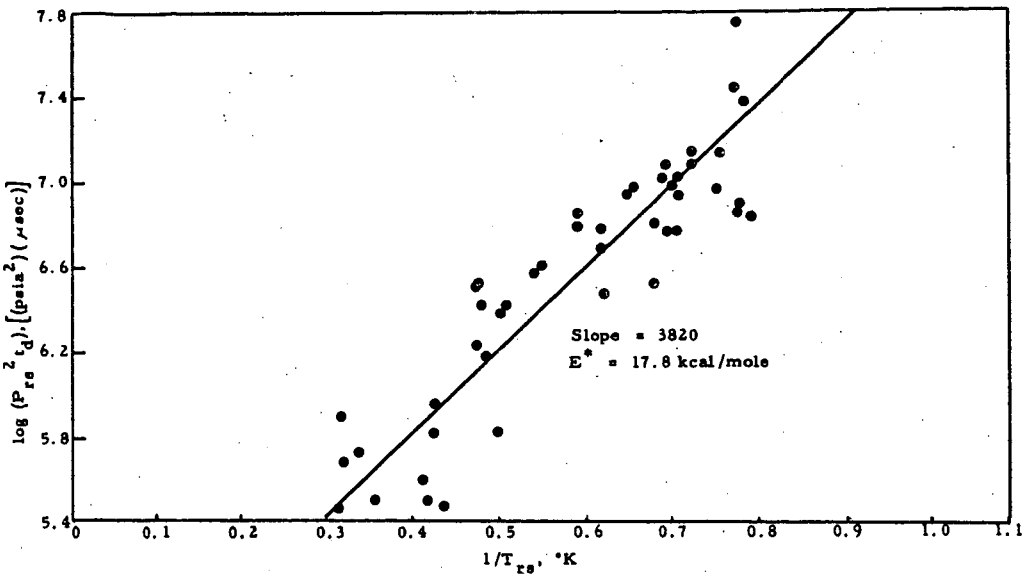

Fig. 4 Log ($P_{rs}^2 t_d$) as a Function of 1/T_{rs} for Shock Test Data Obtained with Unpressed Lead Azide and Nitrogen

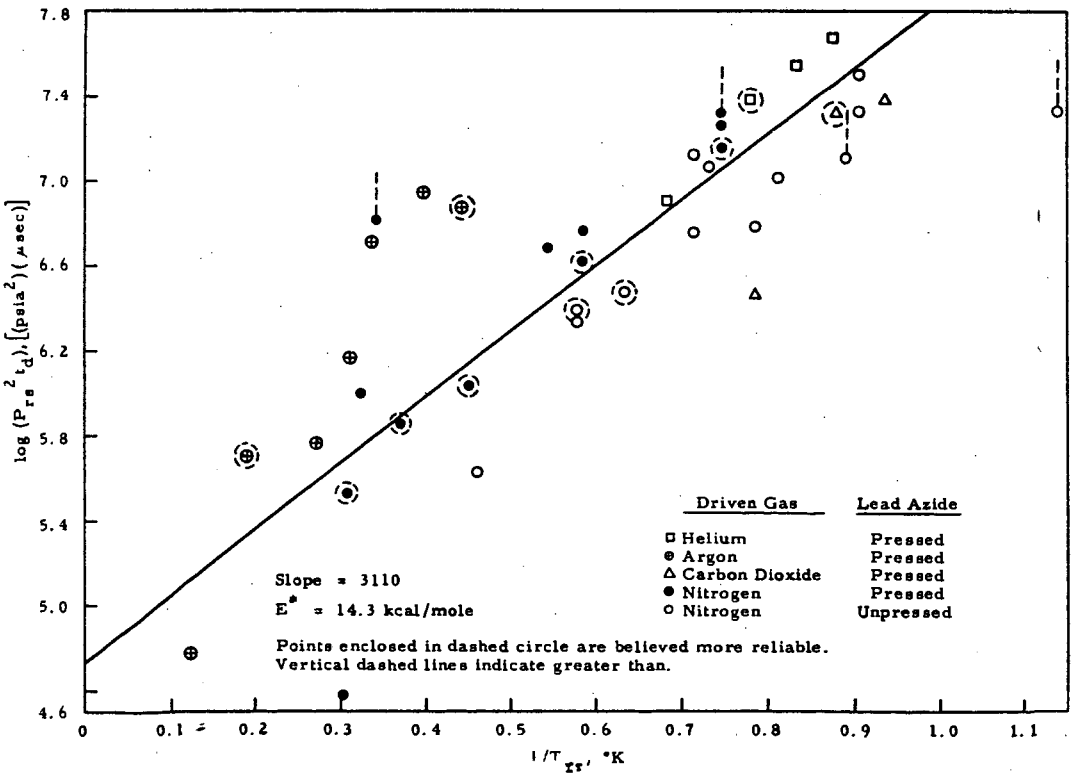

Fig. 5 Log ($P_{rs}^2 t_d$) as a Function of 1/T_{rs} for Shock Test

SHOCK TUBE STUDIES OF IGNITION CHARACTERISTICS OF SOME LIQUID HYDROCARBONS

Earl W. Malmberg
Research and Development Division, Sun Oil Company
Marcus Hook, Pennsylvania

The high temperatures and high exothermicity of combustion reactions in general have made the experimental study of these reactions especially difficult. When problems arise in the manifold practical applications of combustion, the lack of fundamental information on the processes which are involved leave only empirical methods with which to arrive at a solution. Some of the unique characteristics of the shock tube make it especially useful in overcoming the experimental difficulties in combustion studies. A number of investigations have already been made in which advantage has been taken of this device.

For the spark-ignition engine, knock, surface ignition, and rumble are some specific problems which would profit from appropriate fundamental studies. Two characteristics of the shock tube which make it useful for these applications are the freedom from surface effects and the instantaneous heating to a selected high temperature which is possible. Because of these advantages, a shock tube study of the ignition of hydrocarbon-oxygen mixtures was begun.

The earlier work in this area by Gay and others is listed by Steinberg and Kaskan[1]; thia paper, and the discussion thereto, very well delineates the pitfalls and necessary precautions for the study of ignitions in the shock tube. The more satisfactory results with ignition by the reflected shock wave and the importance of surface discontinuities in causing anomalous behavior are described. Ignition in a reflected shock wave has been used to investigate ignition of a spray of Diesel fuel[2]. A study of the high-temperature ignition characteristics of different fuels was made by Mullins[3] in a system in which was designed to approximate combustion conditions in a jet engine. The differences between a number of liquid fuels in reaction with oxygen in a shock tube at intermediate temperatures has been studied by Malmberg and Wellman. In the present investigation, various characteristics of the ignition of several liquid hydrocarbons with oxygen were studied in the reflected shock wave.

EXPERIMENTAL

Some earlier experiments had shown that the response of a piezoelectric pressure pickup is noticeably different to an explosion as compared to an initial and reflected shock wave. The apparatus was constructed to utilize the reflected shock wave, with, in general, the detecting elements located in the endplate of the reaction section.

The shock tube was made from one-inch Schedule 40 stainless steel pipe, with necessary connections for evacuation, filling, and instrumentation. Helium was used as a driver gas. Mylar film, ranging in thickness from 0.0035 to 0.030 inch was used for the diaphragms. The tube was designed with a factor of safety of ten; the peak pressures observed in explosions corresponded with the peak pressure calculated by assuming instantaneous liberation of the energy. For most of these experiments, a four-foot driver section and a three-foot reaction section was used. With the pressures used in these experiments, the time available for reaction at the far end of

the reaction section (before arrival of the rarefaction or a re-reflection from the contact front) was always greater than the longest ignition delays measured.

A miniature SLM quartz piezoelectric pressure pickup and a quartz window were mounted in the endplate; the window, which led to a 1P28 photomultiplier tube looked down the shock tube toward the high pressure section. With the photomultiplier housing rigidly attached to the shock tube, anomalous deflections can be obtained at the time of breaking of the diaphragm and somewhat less pronounced at the time of reflection. Shock-proof mounting of the tube solved this problem. The first deflection is presumably shock transmitted through the metal of the tube. This behavior may be the explanation of the "light" observed by Steinberg and Kaskan in initial shock waves in which there was no ignition.

The output from the pressure pickup was sent into a Kistler Piezo calibrator and thence to one input of a Tektronix 531 oscilloscope with a Type CA dual-trace plug-in unit. A single sweep of the oscilloscope was triggered from the breaking of the diaphragm.

The explosive mixtures were made by the method used by Steinberg and Kaskan[1], flow of oxygen and the fuel vapor each through a critical velocity orifice flowmeter. The method was modified so that mixtures could be made from liquid hydrocarbons. The orifices, a reservoir for hydrocarbon vapor, and a pressure gauge on the reservoir were held in a constant-temperature oven at 125°. After the gases were mixed, the hydrocarbon was below its vapor pressure at room temperature so that it could be led into the evacuated shock tube.

The temperatures which are used in the discussion of results are read from a curve made for each hydrocarbon; the temperature was calculated from the diaphragm pressure ratio by the usual shock wave relations. The specific heat ratio for the components was assumed constant, and the values of temperature may be as much as 20 percent high. The necessary data, in general, are not available for more accurate calculations for these hydrocarbons. However, for our purposes, the relative values are the point of interest, and there should be no important deviation in that respect.

The measurement of length of time before ignition, the "ignition delay", was made on the two simultaneous traces. An example is shown in Figure 1A. The lower trace is of the pressure transducer; the small initial rise is the arrival-reflection of the shock. The second sharp high rise is the explosion, sometimes called a "retonation wave". The upper trace, recorded by the photomultiplier, confirms the occurence of the explosion. Variations in this trace will be discussed later.

RESULTS

The measurement of delay time was characterized by a relatively large scatter of points, similar to earlier results[1]. Two examples are shown, Figures 2 and 3, isooctane and benzene respectively. The large number of points are available for benzene because a number of auxiliary studies were made with that hydrocarbon. The photomultiplier trace shown in Figure 1A is for a high temperature; i.e., a short delay. The small or non-existent "overshoot" of initial emission of light is characteristic of the high temperature. As the temperature is lowered, the amount of overshoot is much greater preceding the leveling off which seems to characterize the explosion (Figure 1B). Hence, for benzene, a number of points are shown in which flame was observed almost exclusively (Figure 1C), plus a number with a large amount of flame, plus some explosion. The consistent behavior in a large number of experiments, including the useful data from the pressure transducer, the results of experiments with a second pressure transducer in the side wall six inches from the end, and experiments with a quite slow writing speed, all confirm these interpretations. The high luminosity of the flame compared to the explosion is quite striking

when the relative rates of the reactions are compared. Rough measurements indicate that the time required for the explosion to reach the pressure transducer six inches from the end is roughly one-tenth the time required for the reflected shock to arrive.

Whether explosion or flame was observed, the lowest temperature at which reaction would occur was quite characteristic of a given hydrocarbon. The results for a limited number of fuels are given in Table I. The behavior of these fuels in high-temperature ignition is remarkably parallel to the tendency to produce rumble; hence, the LIB number for each fuel is given in the table as well (Isooctane, high resistance to rumble, LIB number equals 100; benzene, zero).

TABLE I

MINIMUM TEMPERATURE OF IGNITION FOR STOICHIOMETRIC MIXTURES OF VARIOUS FUELS WITH OXYGEN

Fuel	Minimum Temperature* of Ignition, °K	LIB Number **
Pentane	1350	***
Isooctane	1340	100
Toluene	1220	50
Benzene	1155	0
Benzene-isooctane 1:1	1250	50
Toluene-isooctane	1250	
Benzene-water 1:1	1350	

* Conditions under which ignition occurred in about half the attempts.
** LIB numbers are determined with lead necessarily present. The benzene isooctane 1:1 mixture is LIB = 50 by definition of the scale.
*** Not measurable because of its octane number; probably about 100.

A number of experiments were performed to determine the effect of volatile additives on the minimum temperature of ignition of benzene-oxygen mixtures. The number of experiments in each case is not large enough for an accurate determination of the 50 percent point, but the following preliminary observations were made. Conventional motor mix with tetraethyl lead has a relatively small effect on the minimum temperature of ignition. The temperature was raised appreciably with tertiarybutyl acetate present in 0.5 percent amount. Tetramethyl lead in a motor mix quite definitely increased the minimum temperature of ignition.

DISCUSSION

The ignition delay and the minimum temperature of ignition are measures of reactions between hydrocarbons and oxygen which lead to a condition that engenders rapid combustion by flame or explosion. The values of the ignition delay are not particularly useful experimental results because of the large amount of scatter, although there is appreciably less scatter for the aromatics. Part of the data from benzene-oxygen experiments was used for calculation of rate constants. From data such as shown in Figure 2, the rate constants will necessarily have a range of values. However, good agreement was obtained among the rate constants which were calculated when the rate expression included only fuel concentration to the first power as compared to the values when the product of the fuel and oxygen concentrations each to the first power was used. This result is not surprising when it is considered that the reaction under study is an initiation and the mixture is stoichiometric; i.e., 7.5 moles of oxygen per mole of hydrocarbon. The data in Figures 2, 3 and 4, are presented as Arrhenius plots for convenience and for comparison to results of others. An activation energy calculated from the slope of

the best "line" is based on the assumption that this initiation reaction leads to a critical concentration of some active species, and this concentration is the same at all temperatures. Values from 10 to 40 kcal/mole are obtained; clearly, the assumption is not generally valid in these cases. The values of the temperatures are in error to a certain extent, as already discussed. However, in some earlier work[4] in which the temperature was obtained by a more accurate method, the beginning of the reversal of the relative ease of oxidation of aromatic, as compared to paraffin hydrocarbons, was observed at 900-950°K. The approximate calculated temperatures in the present work fit this general pattern within the possible error. In addition, these results in the "crossing over" region are in agreement with the findings of the present investigation.

The minimum temperature of ignition is shown on Figures 2, 3, and 4, because it demonstrates more concretely the reality and validity of this number. There are a few isolated cases of explosion below the limit; however, these were found in a large number of experiments in which no reaction occurred. In addition, when ignition did occur below this borderline area, it usually was marked by some quite different characteristics.

As the representative traces in Figure 1 indicate, the explosion in general seems to develop from a flame, except at high temperatures the preliminary spike is almost lost. These combustion reactions are necessarily homogeneous. The known facts of surface ignition and LIB requirements may be examined from this viewpoint. The correlation of the minimum temperature of ignition with the LIB number suggests that the characteristic tendency of aromatic fuels to produce rumble may result from a greater ease of the undesired premature ignition from an area of deposit which is active in surface ignition. This ignition need result only from a local heating. If this interpretation is valid, the complexity of the problem of surface ignition may be considerably reduced in that the fuel need not necessarily enter directly into the reactions in the deposit. Rather, the interaction of the deposit and oxygen is paramount. This view is consistent with results from the measurements of temperature of ignition of engine deposits in an atmosphere of oxygen; a low temperature of ignition is correlated with a high LIB requirement for the engine in the test in which the deposit was formed.[5] A fuel is not present in these experiments.

The experiments with one mole of water present with benzene in the stoichiometric mixture with oxygen confirms the importance of the homogeneous reaction in rumble. In an engine, the addition of this amount of water to the benzene fuel eliminates the rumble. In the shock ignition experiments, correspondingly, the presence of water increased the minimum temperature of ignition for benzene to the value for isooctane. Even at very high temperatures, the presence of water caused many of the ignitions to be largely flame rather than explosion.

The experiments with additives were not as definitive as would be desired, largely because a reliable determination requires a relatively high number of individual determinations. Also, a diaphragm-breaking apparatus, now being built, will allow more flexibility in the control of the diaphragm-breaking pressure. This method in general offers considerable promise as a means of studying in more detail the conditions leading to explosion. If, for example, in the borderline region differences can be detected spectroscopically or by some other method between mixtures that explode rather than burn with a flame, very useful information would be forthcoming.

In general, other aspects of the investigation are similar to results already described. Almost all of the experiments were run with 100 mm pressure in the reaction section. Small changes in reaction pressure and small changes from stoichiometric composition had only small effects. The exposed surface of the miniature pressure pickup had rather sharp corrugations. The surface discontinuities at this point and small irregularities around the window were very satisfactorily eliminated by smoothing on Apiezon Sealing Compound Q. A number of experiments were performed with pentane and air rather than oxygen. The delay times were, in general,

a bit longer, as might be expected, but otherwise these limited experiments showed no important differences.

ACKNOWLEDGMENTS

The author wishes to acknowledge helpful suggestions and discussions with Dr. James L. Lauer. Preliminary experiments were performed by Mr. Robert Zeto; Mr. Robert Ledley, III, assisted in a large amount of the experimental work. The permission of the Sun Oil Company to publish this work is gratefully acknowledged.

REFERENCES

1) M. Steinberg and W. E. Kaskan, Fifth Symposium.

2) G. J. Mullaney, Ind. Eng. Chem. 50 53 (1958).

3) B. P. Mullins, Fuel, 363 (1953).

4) W. E. Wellman, Ph.D. Dissertation, The Ohio State University, 1960.

5) J. L. Lauer, Paper presented before the Eighth International Combustion Symposium, Pasadena, California, August, 1960.

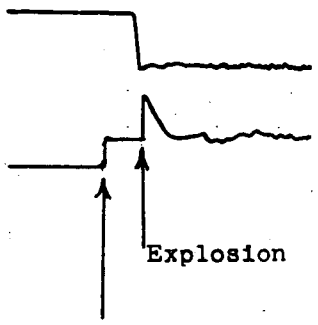

A. High temperature: short delay time, explosion

B. Intermediate temperature: flame appears initially

C. Low temperature: mostly flame, weak explosion

Fig. 1. Representative oscilloscope traces from which delay time and other experimental variables were determined. Writing speed, 200 μsec./cm; trace 10 cm in length. Vertical amplification unchanged in these experiments.

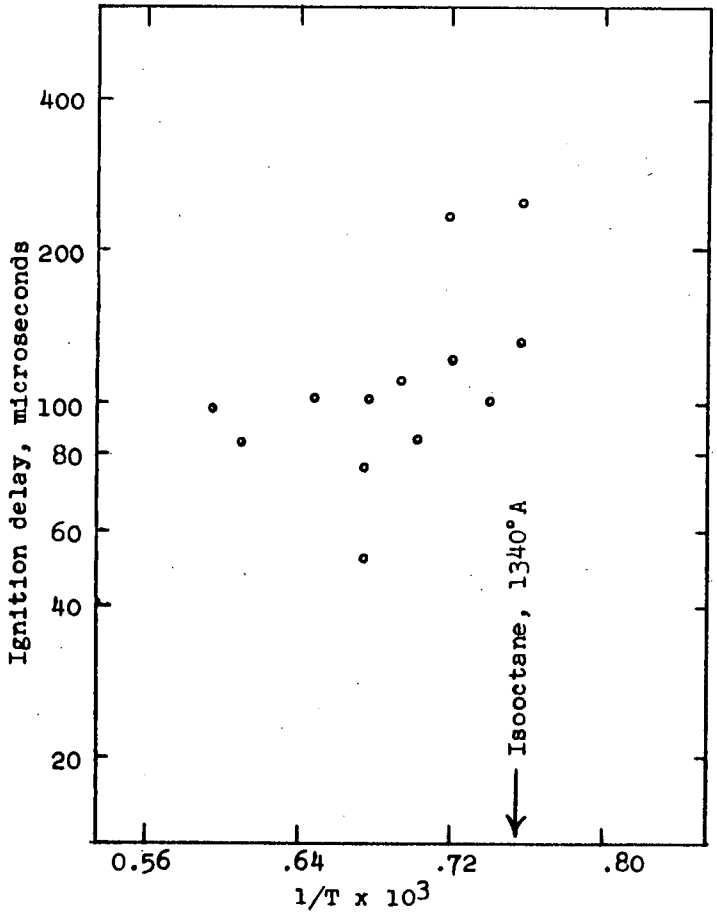

Fig. 2. Characteristic results in the ignition of isooctane-oxygen; logarithm of the ignition delay versus reciprocal of the absolute temperature.

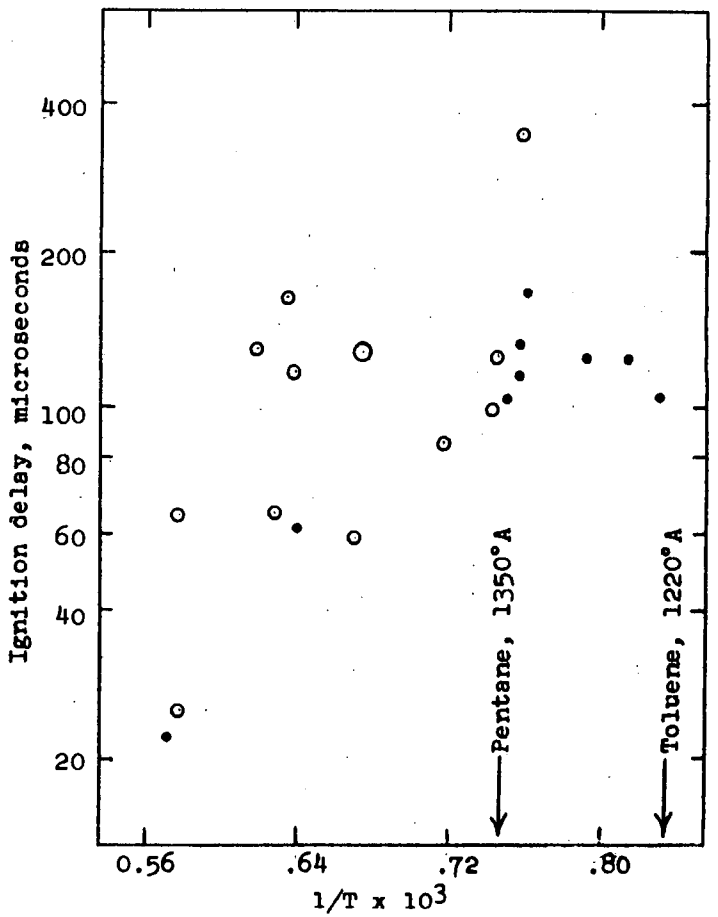

Fig. 4. Ignition of pentane-oxygen and toluene-oxygen; logarithm of the ignition delay versus the reciprocal of the absolute temperature. O Pentane; • Toluene

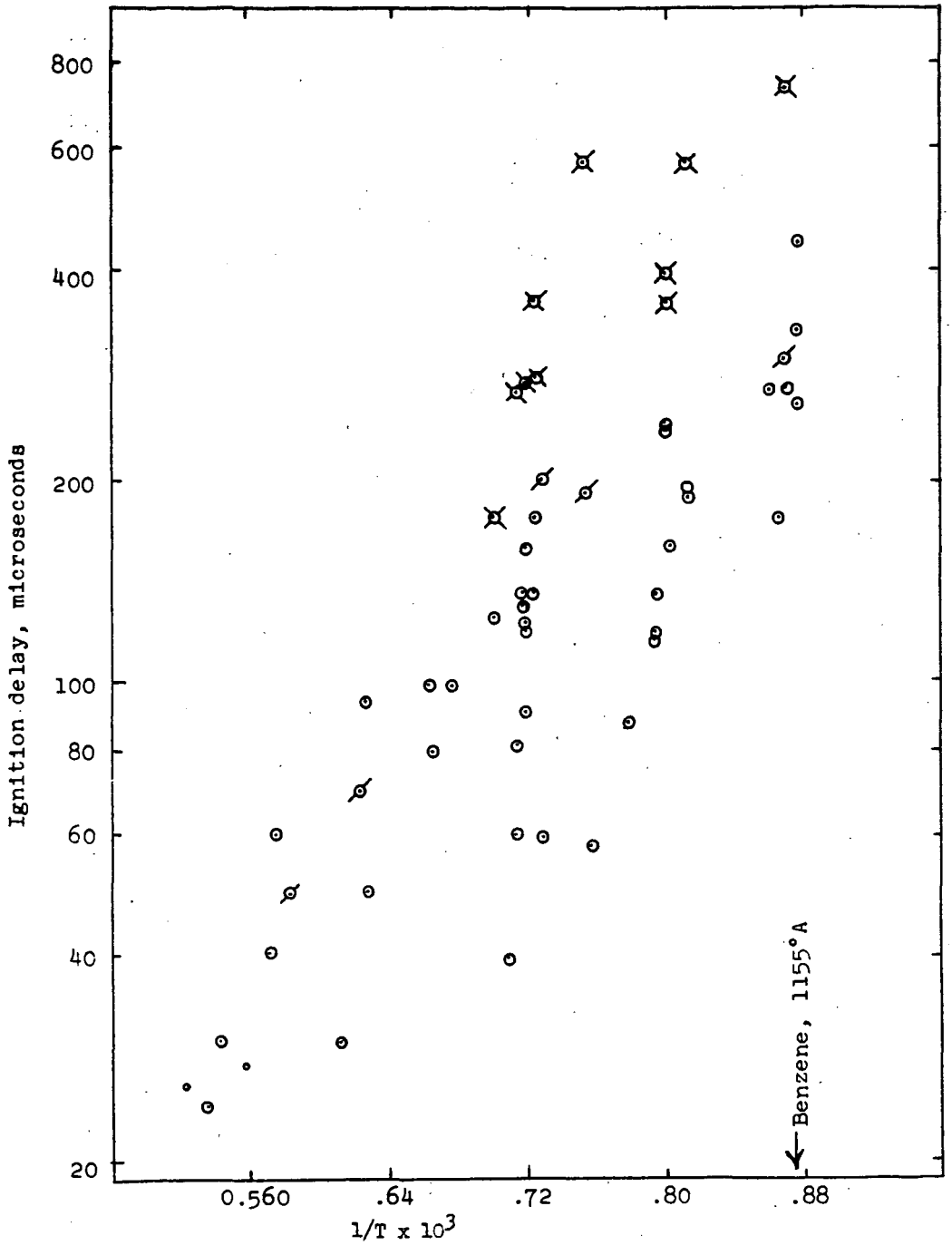

Fig. 3. Ignition of benzene-oxygen; logarithm of ignition delay versus the reciprocal of the absolute temperature. o Explosion; ⌀ flame and explosion; ⌘ mostly flame.

A SHOCK TUBE TECHNIQUE FOR STUDYING THE KINETICS OF HIGHLY EXOTHERMIC REACTIONS---SHOCK INITIATED DETONATIONS.

Roger A. Strehlow*
Aeronautical Engineering Department
University of Illinois
Urbana, Illinois

and

Arthur Cohen
Ballistics Research Laboratories
Aberdeen Proving Ground, Maryland

INTRODUCTION

The incident shock techniques which are so well adapted to the study of endothermic reactions[1], are in general, not applicable to the study of highly exothermic reactions. This is because an exothermic reaction occurring in a small region of a flowing gas causes an increase of the local pressure and in the case of shock wave heating this pressure increase occurs behind and close to the shock front. Since this region is subsonic the pressure increase will propagate as a wave to the front and increase the velocity of the front, thereby increasing the temperature of the next element of gas heated by shock compression. This process is self accelerating and in general a steady state wave will not be obtained until the wave is traveling at or above the Chapman-Jouget detonation velocity for the mixture. Since in all reaction kinetics work one must follow the history of a fixed element of gas, incident techniques will only work if the wave is truly steady state in time. Therefore highly exothermic systems may be studied by incident techniques only in the limit as steady detonation waves.

In the endothermic case the reaction locally lowers the pressure behind the shock wave thereby slightly lowering shock velocity. A steady shock wave followed by a reaction wave can therefore be generated and studied. Schott and Kinsey[2] have demonstrated that steady waves can also be generated and studied in weakly exothermic mixtures.

A different situation exists for the region behind a reflected shock. Here the gas is essentially quiescent at the back wall and fixed station observations should yield meaningful results. Furthermore the reflected shock provides nicely controllable initial conditions for observing the details of the accelerating process.

---

*On leave from the Ballistics Research Laboratories as a Ford Foundation Visiting Professor.

Recently, we observed that a highly exothermic reaction occurring behind the reflected shock can quite reproducibly generate one dimensional accelerating waves that are either: 1) "detonation" waves which eventually overtake and interact with the reflected shock wave, or, 2) pressure waves which cause a simple acceleration of the reflected shock.[3] This paper describes our conclusions concerning design limitations for the reflected shock technique, some of our further observations of the acceleration phenomena in the hydrogen-oxygen system, and our observations of adiabatic explosion delays in hydrogen-oxygen mixtures.

DESIGN LIMITATIONS

The step reflected shock produced at the end of a conventional shock tube is, within certain limitations, well suited for the study of highly exothermic reactions. These limitations are:

1. Reflected shock heating is clean (i.e. truly one dimensional) only if the heat capacity ratio of the gas mixture is greater than 1.4 over the temperature range used in the experiment.[4]

2. Only reactions which occur rapidly at high temperatures may be studied. Only at the higher temperatures is the reflected shock temperature sufficiently above the shock temperature to allow rapid reaction in this region with no earlier reaction behind the incident shock.[4] A rapid reaction is defined here as one in which the events of interest occur in the time range 10 to 1000 microseconds.

3. The explosive mixture must be separated from the diaphragm by an inert gas mixture of similar properties (buffer gas) and the interface between the two gases must not generate reflected shocks when the incident shock traverses the boundary. Once again local reflected shocks in the explosive mixture could trigger early detonation.[5]

4. Small cracks and crevices in the tube wall must be entirely absent. These produce local reflected shock waves which could trigger early detonation.[6]

5. In general the reflected shock is not as ideal as the incident shock wave.[4,7] In pure argon the best current estimate is that the reflected shock gas temperature is approximately 30^{o} to 50^{o} below theoretical in the range $1500^{o}K < T_{rs} < 3000^{o}K$.

EXPERIMENTAL

A four inch i.d. stainless steel shock tube with a 50 inch compression section, an 88 inch buffer section and a 164 inch test section was used in these experiments. The buffer section was separated from the test section by a four inch stainless steel ball valve (a six and one half inch sphere with a four

inch hole bored through it) which allowed undisturbed passage of the shock when in the open position. When closed the valve was vacuum tight and allowed us to place an inert gas, of the same density as the explosive gas, in the section near the diaphragm and in the bore of the valve. Pressure differential across the valve was adjusted to zero externally and the valve was opened about 10-20 seconds before firing the tube. This effectively prevented any premature detonations initiated by non-ideal diaphragm burst. Also, the test section was constructed to eliminate all internal crevices at the joints and window mountings in order to eliminate premature detonations caused by local reflected shocks. Strip photographs (x-t) of reflected shock behavior were taken with an eight inch schlieren system through 8" X 0.025" slit windows at the back wall. Other experimental details are given in a previous paper.(4)

One dimensional steady state shock wave and detonation calculations were performed on the Ballistic Research Laboratories' high speed computer, the EDVAC. Thermodynamic data for the gases was taken from recent Bureau of Standards tables. Shock calculations were performed with the assumption of no reaction or dissociation but rapid vibrational relaxation in the shock. Detonation calculations were performed by assuming complete thermodynamic equilibrium in the wave. The C-J velocity was calculated using the frozen equilibrium velocity of sound.

RESULTS

Schlieren strip film (x-t) photographs of the reflected shock region were taken in stoichiometric hydrogen-oxygen mixtures diluted with 70%, 85% and 94% argon. In the range $2.14 < M_s < 2.8$ ($920^{\circ}K < T_{rs} < 1820^{\circ}K$) reaction was evident behind the reflected shock. All our photographs indicated that the initial reaction was typical of a homogeneous adiabatic explosion with a finite delay. Delays ranged from 12 to 880 microseconds. In addition we observed that the wave nature of the heating cycle produced a reaction wave which traveled away from the back wall at or above the reflected shock velocity.

Two types of accelerating wave behavior were observed in hydrogen-oxygen-argon mixtures. Figure 1 illustrates the case where the reaction generates a weak pressure wave which travels to the reflected shock causing it to accelerate to a new steady velocity. During this process the reaction zone also accelerates and eventually reaches a new position closer to the reflected shock wave. Figure 2 is typical of the other type of behavior observed. Here the pressure wave steepens into a shock wave before it reaches the reflected shock. This reaction shock is followed by a narrow dark zone (i.e. no gradients) and then a strong rarefaction wave (gradients opposite to that in the shock). This wave pattern accelerates and grows more compact as it travels away from the back wall of the tube and finally interacts with the reflected shock, producing a new high strength shock (now closely followed by the rarefaction zone). The interaction with the reflected shock also produces a contact discontinuity which is traveling away from the back wall initially but quickly decelerates to zero

velocity and a sometimes observed weak rarefaction wave which travels toward the back wall of the shock tube at a constant velocity. The shock-rarefaction pattern which we observe, both before and after interaction with the reflected shock wave, suggests a detonation wave. The steady velocity of this wave in the incident gas agrees well with C-J calculations. However, wave velocities measured ahead of the interaction show that these accelerating waves are traveling at approximately one half the C-J velocity for this region. It is interesting that this non-steady wave has never exhibited any of the characteristics of spinning detonation. Occasionally we have observed slightly non-one-dimensional behavior at the start of wave formation but in every case these non-idealities were rapidly damped and the wave quickly became a strictly one dimensional wave perpendicular to the wall of the four inch shock tube.

In all cases where reaction was observed behind the reflected shock wave the delay to adiabatic explosion at the back wall was measured by extrapolating the wave motions to the back wall. These delays are compared to Schott and Kinsey's[2] recent data in Figure 3. Their data line represents the delay to the first appearance of OH radicals in absorption while ours represents the delay to the actual adiabatic explosion. Dr. Schott has indicated in a private communication that their delays to maximum OH concentration were about one and one-half times longer than their appearance delays. Our delays are, on the average, 1.2 to 2.0 times longer than Schott and Kinsey's delays. This indicates that at the back wall we are indeed observing an exothermic reaction under well controllable and calculable conditions free from the complications of the acceleration process.

THE MECHANISM OF DETONATION INITIATION

In the "detonation" case described above it is obvious that we are dealing with a very special and interesting case of detonation initiation. It is an interesting case because it is so nicely one dimensional and reproducible. It is special because the wave that is generated behind the reflected shock has all the gross characteristics of a detonation but travels at approximately half the calculated C-J velocity.

The qualitative behavior of this wave system may be described if we first make some assumptions concerning the reaction and then mentally remove them one at a time. Let us assume that: 1) the reaction starts after a finite delay time τ which is constant for every element of gas, 2) the reaction rate is infinite (i.e. $t < \tau$, no reaction; $t > \tau$, complete equilibrium), 3) no heat evolution or molecular weight change occurs during the reaction. With the above assumptions the reaction would appear as a reaction wave traveling at the same velocity as the reflected shock. In Figure 4 the dotted line $(RW)_o$ represents this situation. If we remove condition three and allow the reaction to liberate a quantity of heat, the reaction wave will separate regions of low and high temperature. The continuity equations of gas dynamics predict that for this simple situation you will observe a centered wave pattern consisting of a shock wave (reaction shock) followed by

the reaction wave (RW). These waves separate steady state regions and the shock strength is determined by the exothermicity of the reaction and the added condition that the particle velocity be equal to zero at the back wall. The shock which is produced is identical to that obtained with a piston motion drawn as the equivalent piston path in Figure 4. The light lines represent a particle path through the idealized centered wave pattern.

Removing assumption number two and allowing finite reaction rates will cause the shock wave to appear some distance from the back wall. This is equivalent to a slow acceleration of the piston instead of the impulsive motion illustrated in Figure 4, and it causes the wave to accelerate near the region of wave formation. This acceleration will lead to a terminal shock velocity which can be calculated from the equilibrium properties of the gas and the reflected shock strength. Removal of assumption number two therefore allows one to predict that an approximately centered constant velocity expanding wave pattern will appear some distance from the back wall. A close look at this wave pattern shows that assumption number one (constant τ) becomes less and less valid as the pattern expands. Heating by the reaction shock soon causes an appreciable decrease in the delay and the wave system becomes self accelerating. One additional feature, the observed rarefaction wave, is undoubtably produced because the gas leaving the accelerated reaction wave has a net velocity away from the back wall and must therefore be decelerated to zero velocity.

The intersection of the accelerating wave pattern and the reflected shock produces the interaction described in the results section. This behavior is adequately predicted by one dimensional gas dynamics. A momentum balance on this interaction shows that the forward traveling resultant shock will be moving faster than the calculated CJ velocity for this region. One would therefore expect the resultant wave to decelerate to the velocity of a high order detonation. This is what is observed experimentally.

SUMMARY AND CONCLUSIONS

Reaction mechanisms may be studied using a reflected shock technique even for the case of highly exothermic reactions. Fixed station observations near the back wall will allow the study of chemical species for the case of homogeneous adiabatic explosions. Furthermore, if the range of reaction time and the geometry of the system is carefully chosen one should be able to study the reaction without the bothersome influence of wall effects. The time history of the explosion will be slightly different than in a closed vessel: first because the reaction will in general be truly homogeneous, and second, because the gas dynamics allows the volume of the "vessel" to increase during reaction. The application of this technique should allow the direct study of the details of many exothermic reactions in the temperature range of current interest (i.e. flame temperatures).

The accelerating waves observed during our investigation are even more interesting. We observe a wave pattern reminiscent of a

detonation under conditions where the "reaction wave" is passed through a combustible mixture at an arbitrary velocity determined by the reflected shock velocity. (This arbitrary velocity is much higher than the normal flame propagation velocity for these mixtures.) The general features of this wave pattern can be explained qualitatively using one dimensional gas dynamics with heat addition. An exact treatment of the wave development will require the use of the method of characteristics and a knowledge of the rate of heat release in the reaction zone and the effect of shock heating on the delay time

From the brief analysis given above it is evident that these nicely one dimensional accelerating waves are "uncoupled" or "weakly coupled" when first produced. That is, the reaction wave is physically well removed from the shock wave. Hirschfelder and Curtiss[8] have recently discussed the "coupling" of the shock wave and reaction zone in steady detonation waves. A detailed study of this initiation process for a variety of exothermic reactions should yield a great deal of information on the structure of stable detonation waves for specific explosive mixtures.

REFERENCES

1. H. Pritchard, Quarterly Reviews, 14, 46-61, 1960;
   A. Hertzberg, Appl. Mech. Rev., 9, 505, (1960);
   T. Carrington and N. Davidson, J. Phys. Chem., 57, 418, (1953).

2. G. Schott and J. Kinsey, J. Chem. Phys., 29, 1177-82, (1958).

3. R. Strehlow and A. Cohen, Phys. of Fluids, 3, 320, (1960).

4. R. Strehlow and A. Cohen, J. Chem. Phys., 30, 257-65, (1959).

5. J. Fay, Some Experiments on the Initiation of Detonation in $2H_2 - O_2$ Mixtures by Uniform Shock Waves, 4th Symposium (International) on Combustion, 501-7, Williams and Wilkens, Baltimore (1953).

6. M. Steinberg and W. Kaskan, The Ignition of Combustible Mixtures by Shock Waves, 5th Symposium (International) on Combustion, 664-71, Reinhold, New York (1955).

7. G. Skinner, J. Chem. Phys., 31, 268, (1959).

8. J. Hirschfelder and C. Curtiss, J. Chem. Phys., 28, 1130-51, (1958).

Figure 1. (x-t) Schlerien photograph of adiabatic explosion leading to simple acceleration of the reflected wave. Time increases toward the right. Back wall of shock tube at top. Vertical line is stationary slit image. 70% argon, P_o = 1 cm Hg, M_s = 2.76, T_{rs} = 1570°K, delay at back wall is 31.5 microseconds.

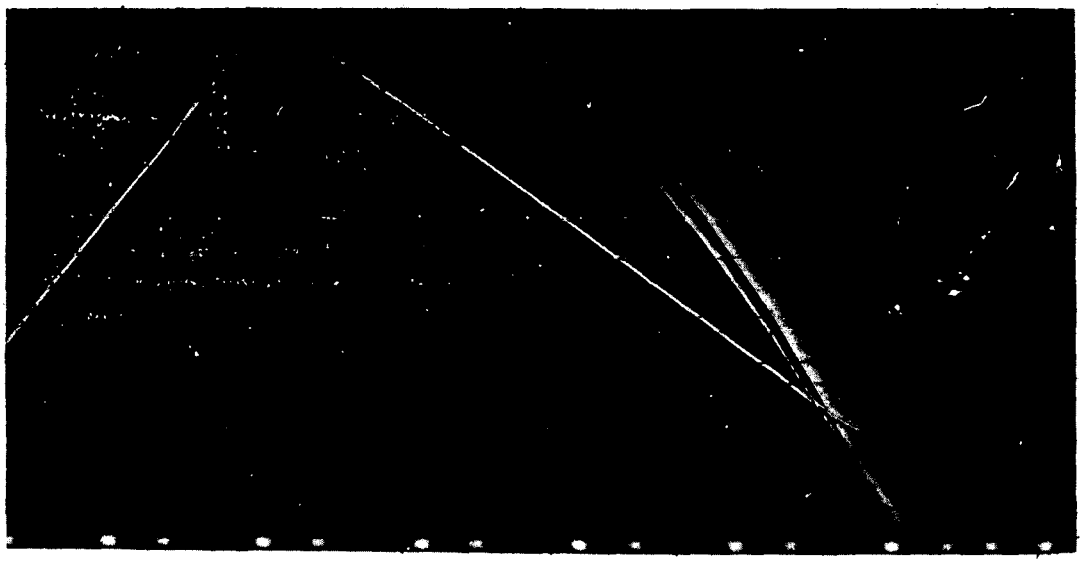

Figure 2. (x-t) Schlerien photograph of the initiation of detonation behind the reflected wave. Notice the interaction of the developing detonation and the reflected wave. Time increases to the right. Back wall of shock tube at top. 85% argon, P_o = 4 cm Hg, M_s = 2.22, T_{rs} = 1160°K, delay at back wall is 135 microseconds.

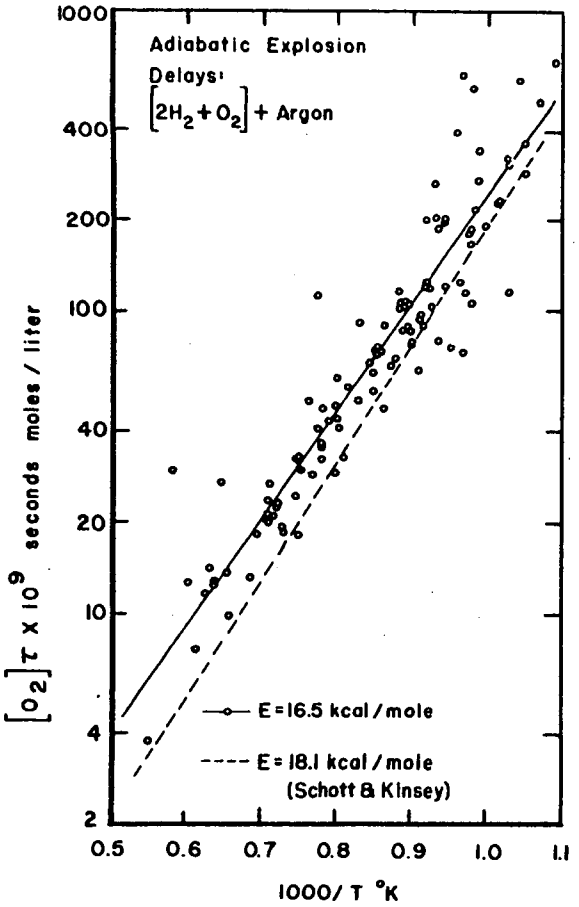

Figure 3. Adiabatic explosion delays measured for stoichiometric hydrogen-oxygen mixtures diluted with argon. Temperatures are calculated from incident shock velocities and one-dimensional theory.

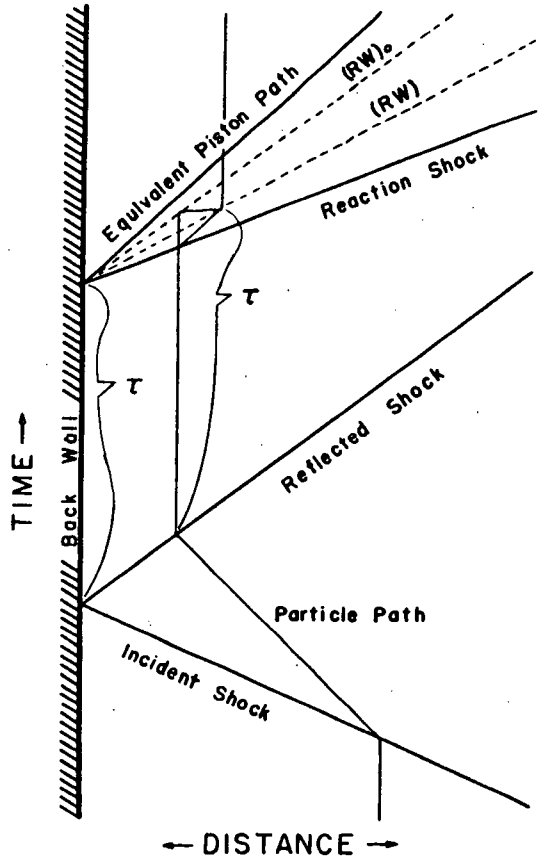

Figure 4. Schematic (x-t) diagram illustrating the mechanism of shock formation for a delayed exothermic reaction occurring behind the reflected shock.

A Study of Combustion and Other Free Radical Processes in the Chemical Shock Tube

William E. Lee* and Earl W. Malmberg**

Department of Chemistry, The Ohio State University, Columbus, Ohio
Present address: *Eastman Kodak Co., Rochester, N. Y.
**Sun Oil Co., Marcus Hook, Pa.

The difficulties which are inherent in the study of certain thermal reactions and in combustion research are well known: difficulty of initiation, the very high rate of reaction once begun, the complexity of the resulting mixture, and in some cases, surface effects. A need for understanding the mechanism of these high temperature reactions still remains a basic problem. The kinetics and energetics of a number of reactions investigated at low temperatures appear to be at least partially understandable. However, considerable deviation from theory is indicated as the reaction temperature is increased.

The outstanding feature that distinguishes high temperature kinetics from low or moderate temperature kinetics is the much larger amount of energy present in the reaction system. As the result of this high energy content, possible deviations from low temperature kinetics may arise. The sources of these deviations are listed as follows:

1. Reaction intermediates that may be somewhat stable at low temperature may decompose rapidly at elevated temperature, supplying chain carriers that may completely change the kinetics of the reaction.
2. Non-equilibrium energy distributions may appear among reactants and products in fast, high temperature reactions.
3. Diatomic and triatomic radicals may be formed in addition to the polyatomic radicals which are usually observed at low temperature.
4. Large numbers of atoms and radicals may be produced which are unknown at lower temperatures.

The conventional kinetic systems are impractical for the study of high temperature reactions since the reactants must be heated rapidly to a high temperature without appreciable reaction occurring before the desired temperature is attained. The single impulse shock tube which has been described by Glick, Squire, and Hertzberg[1] offers a means of considerable flexibility for obtaining more fundamental chemical data. A wide range of reaction temperature is possible, concentrations of reactants can be varied within wide limits and surface effects are eliminated. With the single impulse shock tube, the reaction occurs following the reflected shock wave, and then is quenched by a strong rarefaction. The reaction products can be flushed from the tube and analysed.

Apparatus and Materials

The single-impulse shock tube was made of two-inch stainless steel pipe; three-foot sections were assembled and held in proper alignment by bolted flanges. The general construction is essentially that described by Glick, Squire and Hertzberg.[1] A few minor modifications were required to overcome certain mechanical difficulties.

The arrangement used in these studies was determined by the reaction time desired. A typical arrangement proceeding from one end of the apparatus to the other, is as follows: Expansion tank (twenty gallon capacity; six-foot high pressure driver section; three-foot buffer section (I); three-foot reaction section; six-foot buffer section (II); end plate. Two SLM quartz piezo-electric pressure pick-ups were mounted in buffer section II to measure the velocity of the shock wave by feeding the proper signal to the start and stop of a Berkeley EPUT and Timer model No. 7360. A shock-proof mounting was required for the crystal pressure pick-ups.

The position of the reaction section was chosen after a study of pressure-time traces during the operation of the tube with the pressure pick-up in different positions. These traces were made by using the Kistler Instrument Company piezo calibrator. The output of the calibrator was recorded photographically with a Tektronix Model 535 oscilloscope with No. 53C plug-in dual beam preamplifier unit. The position which was chosen for the reaction section resulted in the reaction occurring in a section which was free from anomalous pressure peaks in the trace.

Two special quick-opening valves were used to isolate the reaction mixture from the buffering gas prior to reaction.

These values were plug type valves in which the plug was bored exactly to the inside diameter of the shock tube. Leakage across the valve and to the atmosphere was eliminated by the use of O-rings in appropriate grooves.

All of the hydrocarbons used with the exception of cyclopropane, were research grade chemicals supplied by Phillips Petroleum Company. The compressed gases were commercially available. The azomethane used was prepared by the oxidation of dimethylhydrazine with mercuric oxide according to the method of Renaud and Leitch.[2]

Experimental Procedure

In preparation for a reaction, all parts of the system were evacuated, flushed with helium, evacuated again, and then filled with helium to the required pressure. The reaction mixture was prepared by introducing helium, and the reactants, into a stainless steel cylinder and mixing by imposing a strong thermal convection. The buffer and reaction sections were all filled to exactly the same pressure, and the quick-opening valve was opened ten-fifteen seconds before the bursting of the main diaphragm.

The reaction products were flushed from the shock tube in a stream of helium through two traps cooled in liquid nitrogen; the second trap was filled with adsorbent charcoal which had been activated by heating to 300°C. in a stream of helium.

The contents of the traps were transferred to gas holders for analysis. Conventional gas chromatographic methods were used; the following analyses were performed with the respective columns:

1. Linde Molecular Seive 5A, 117°: hydrogen, carbon monoxide, and methane.
2. Silica gel 40°: ethane, ethene, and carbon dioxide.
3. Dowtherm A 40°: propane, propene, and all the C_4 hydrocarbons, pentane, and the pentenes.
4. Polyethylene glycol 40°: oxygenated compounds.

A Gow-Mac filament type cell was used with the first three columns; a very sensitive thermistor cell was used in the search for oxygenated compounds.

In almost all of the runs, the composition of the mixture in the reaction section was approximately five mole percent or less.

Other reaction products that could not be separated by gas chromatography were determined by other conventional methods of analysis. The reacted gas was passed into water and formaldehyde was determined as the 2,4-dinitrophenylhydrazone; the acid equivalent, by titration; and peroxides, by titrating with hydrogen iodide according to the procedure of Satterfield, Wilson, LeClair and Reid.[3]

Results

Thermal Decomposition of Azomethane

Azomethane was thermally decomposed at temperatures ranging from 437.5 to 635.2°C. and reaction times of 0.6 to 3.8 milliseconds. At the lower temperatures and at low concentration the dominant reaction leads to the formation of ethane. At higher temperatures and higher initial concentrations, methane, ethylene and propane are formed in large amounts. Linear relationships are obtained when the log azomethane concentration at a particular temperature is plotted against the reaction time. The rate expression for the thermal decomposition of azomethane was determined to be

$$k = 1.24 \times 10^{15} \exp \frac{-46,200}{Rt} \quad \text{sec}^{-1}.$$

Methyl Radical Reaction with Oxygen

Methyl radicals, which were generated by thermally decomposing azomethane, were allowed to react with oxygen at 522°C. and at various oxygen-radical ratios. The results for a 5:1 oxygen-azomethane ratio are given in Table I. The acid formed from the methyl radical-oxygen was determined in only one experiment. From 442×10^{-6} m of azomethane under the above conditions, 26.6 microequivalents of acid was formed. To test the stability of some of the reaction products under the reaction conditions, several reactions between methanol and oxygen and carbon monoxide and oxygen were carried out. For the water-catalysed reaction of CO and oxygen at 632°C. practically all of the CO was recovered unchanged. At 1300°C., however, more than 90 percent of the CO was converted into CO_2.

Table I
Reaction of Methyl Radicals and Oxygen in the Shock Tube at P_{41} = 14.66, T = 522°C.
(Oxygen-Azomethane Ratio = 5:1)

Exp. No.	12-50-(3)	(4)	(5)[b]	(6)	(7)
Reaction Time (milliseconds)	2.6	2.2	0.8	1.5	3.0
Azomethane, μm.					
initial	416	464	440.4	456.4	476
unreacted	14.5	42.8	a	a	a
Products					
C_2H_6	45.6	35.4	a	18.9	72.7
CH_4	96.3	79.0	a	52.4	117.3
CO	197	176	a	138.4	286.4
CO_2	27.6	20.5	a	11.2	82.7
H_2	176	181.6	a	118.2	a
C_2H_4	8.3	9.3	a	6.4	33.2
HCHO	273	a	92.8	378.2	235.0
CH_3OH	a	2.0	a	a	a
Carbon balance	85.8	46.8	10.6	69.1	98.2

[a] Experimental difficulties prevented analysis of these compounds.

b A complete set of analyses for formaldehyde at this temperature shows a maximum in concentration at 2 millisec.

Cyclopropane and n-pentane Reactions

The isomerization of cyclopropane to propylene occurs readily at 760°C. and higher although at long reaction times methane, ethylene, butene and hydrogen are also formed. The methyl radical-induced decomposition of cyclopropane was also studied. At 760°C. the induced reaction leads to heavy carbon deposits on the walls of the shock tube. When the induced reaction was carried out with added oxygen traces of acetaldehyde, formaldehyde and acrolein were detected as the 2,4 DNPH derivatives.

The products formed by the reaction of n-pentane with oxygen are those generally expected of hydrocarbon oxidation at high temperature. A series of experiments were carried out at 877°C.

in which the reaction time was varied from 2.2 to 3.4 milliseconds. The only oxygenated products found were carbon monoxide and carbon dioxide. Oxygenated products with any vestige of the original carbon skeleton are absent even at very short reaction times.

Discussion

The thermal reaction of azomethane in the shock tube appears to proceed by a unimolecular process when the initial azomethane concentration is reasonably low, the reaction time is short and the reaction temperature is not too high. The formation of propane in the reaction system at the higher temperatures and at long reaction times suggest that ethyl radicals are present in great abundance. Products involving methyl addition to azomethane to form tetramethylhydrazine were not detected in any of the experiments which indicates that this reaction is not important at these high temperatures.

The Arrhenius activation energy of 46,200 cal for the thermal reaction is in reasonably good agreement with the literature values.

The reaction of methyl radicals and oxygen at high temperatures is extremely complicated. There is an increase in the rate of decomposition of azomethane in the presence of oxygen somewhat over that of the pure thermal reaction. Although the results are not quantitative nor complete, this evidence suggests that chain reactions involving methyl radicals, oxygen or reactive intermediates become important at these high temperatures.

Previous investigators have explained the major products of the reaction of methyl radicals and oxygen by these reactions

$CH_3 + O_2$	$\longrightarrow$	CH_3OO	I
$CH_3 + O_2$	$\longrightarrow$	$HCHO + OH$	II
CH_3OO	$\longrightarrow$	$HCHO + OH$	(1)
$HCHO$	$\longrightarrow$	$H_2 + CO$	(2)
$CH_3 + HCHO$	$\longrightarrow$	$CH_4 + CHO$	(3)
$CHO + OH$	$\longrightarrow$	$HCOOH$	(4)
$2\ CH_3OO$	$\longrightarrow$	$2\ CH_3O + O_2$	(5a)
$2\ CH_3O$	$\longrightarrow$	$CH_3OH + HCHO$	(5b)
$CH_3O + RH$	$\longrightarrow$	$CH_3OH + R$	(5c)
$CHO + O_2$	$\longrightarrow$	$CO_2 + OH$	(6)

A number of reaction paths are available to account for the products found in low yield in this reaction and are of minor importance.

Considerable uncertainity still exists as to the nature of the initial reaction of methyl radicals and oxygen. At temperatures from 0°C. to at least 200°C., reaction I is attractive since the subsequent reactions (eq. 5a, 5b) can adequately explain methanol formation. Reaction II leads to no plausible mechanism by which methanol is formed. Only traces of methanol were formed in the oxidation reactions at 503°C. Methanol is relatively stable at this temperature, but only traces of methanol were found. Reactions 5b and 5c do not appear important at this temperature.

Methoxy radicals, formed from dimethylperoxide and thermally decomposed yield formaldehyde and methanol as major products. When oxygen is present, only traces of methanol are detected and CO_2 becomes the major product.

A comparison of the CO_2 analyses from methyl and methoxy radical experiment supplies evidence that the total amount of methyl radicals that go through a methoxy intermediate is probably a good deal less than 5 percent.

The large amount of formaldehyde formed in all stages of the reaction reflects its importance as an intermediate in the oxidation mechanism. The reaction of methyl radicals and formaldehyde, and possibly the formyl radical, partially explain the high methane concentration. When the easily abstractable hydrogen of formaldehyde become readily available, especially at the later stages of the reaction, methane becomes a major product.

Reaction involving peroxide, hydrogen peroxide or hydroperoxide formation apparently do not take place to any appreciable extent at these temperatures.

The conversion of CO to CO_2 at 632°C. is a very slow reaction and although a small amount of CO_2 may be formed from CO, other reactions leading to CO_2 are much more likely to occur.

Although many of the radicals described have been identified in combination reactions by mass spectrometry the importance of many of these species in a chain mechanism at high temperature still cannot be confirmed.

Pentane was chosen for this study since it is intermediate between the simple hydrocarbons and higher molecular weight

hydrocarbons which are important liquid fuels. Pentane, a relatively simple hydrocarbon undergoes reactions that are difficult to interpret. Oxygenated organic products, aldehyde, keton, or acids are absent in the products. Evidently, once a pentane molecule becomes a radical in the presence of oxygen at high temperature it rapidly undergoes complete degradation to carbon monoxide and carbon dioxide. A certain amount of radical decomposition leads to olefin plus a lower alkyl radical. The rather uniform rate of oxidation of pentane over a wide range of oxygen concentration suggests that the radical chains are long.

Certain high temperature combustion studies can be carried out successfully in the chemical shock tube. The oxidation reaction can be carried only to the desired stage and stopped.

While the experimental results do not permit a reaction mechanism to be proposed, an insight of the high temperature problem, with all of its complexities, has been obtained.

References

1. Glick, H., Squire, W. and Hertzberg, A., Fifth Symposium (International) on Combustion, p. 393.
2. Renaud, R. and Leitch, L. C., Can. J. Chem., 32, 545 (1954).
3. Satterfield, C. N., Wilson, R. E., LeClair, R. and Reid, R. C., Anal. Chem., 26, 1792 (1954).

Boundary Layer Effects on Pyrolysis Behind Reflected Shock Waves in Narrow Tubes

K.E. McCulloh and R.E. Ferguson
National Bureau of Standards, Washington, D.C.

Introduction

In some experiments on the thermal decomposition of propane in a flow system at temperatures between 1100°K and 1400°K, the usual difficulty was experienced in evaluating the role of surface reactions in the chain decomposition. To try to avoid this difficulty, further experiments were performed using a small diameter, low-pressure shock tube with helium as the driver gas, and employing the reflected shock wave technique to heat a propane-argon mixture to calculated temperatures in the range 1800°K to 2260°K. A study of the products and the dependence of extent of decomposition on calculated temperature behind the reflected shock wave revealed strong evidence of non-ideal behavior, undoubtedly related to Duff's [1] observations of the marked effects on the main stream of boundary layer development behind the incident shock wave. Measurement of the distance between contact surface and incident shock confirmed the conclusions drawn from the chemical evidence: that in narrow low-pressure shock tubes the loss of gas from the hot flow region behind the incident shock to the boundary layer is appreciable, and only part of the reactant gas is heated to high temperature by the reflected shock wave.

Experimental

The goal was to study the decomposition of C^{13}-labelled propane; since only a small amount was available, a small (25 mm i.d.) low-pressure shock tube was employed. Reaction temperatures in the neighborhood of 2000°K were obtained behind the reflected shock wave. The low-pressure section, 120 cm long, was of standard-wall Pyrex tubing selected for uniformity of bore. The brass driver section was 61 cm long. Diaphragms (one-mil cellophane) were punctured by a solenoid-driven needle.

Helium at an initial pressure of 1.3 atm was used as the driver gas in all experiments. The ambient temperature was 300 ± 2°K. Initial pressures of the reactant gas mixture in the low-pressure section ranged from 3.3 to 7.5 mm Hg depending on the desired shock strength. This mixture contained in all cases 90.0 mole per cent argon (Matheson research grade) and 10.0 mole per cent propane. Gas chromatographic analyses confirmed the absence of significant impurities in these gases. Vacuum handling of reactants and products was adequate to avoid introduction of impurities exceeding one mole per cent of the initial propane in any given experiment.

Incident shock wave speeds were determined from oscillograms which displayed timing marks at 10 μ sec intervals together with signals from three shock wave detectors located 75, 95, and 115 cm from the diaphragm. The detectors were thin-film nickel oxide resistors which have been described elsewhere [2].

These measurements indicated that shock wave attenuation was negligible, less than one per cent in 20 cm of travel. It appeared that small discrepancies (7 or 8 per cent)

between observed velocities and those calculated from the initial pressures could be adequately explained by assuming that slight flow obstructions resulted from incomplete diaphragm removal. Measurements made with a detector in the end plate showed that the high-temperature dwell time after the shock was reflected was one m sec or greater.

Products were collected for analysis by pumping the entire contents of the shock tube through two traps in series, both cooled with liquid nitrogen. The first, a 4-loop reentrant trap, collected condensables; the second contained Linde Molecular Sieve 5A to retain methane and argon. Condensables were determined quantitatively by gas chromatography, using a thermal conductivity detector calibrated separately for each product of interest.

Calculations

Using the usual one-dimensional shock wave theory, conditions behind the incident and reflected shock waves were computed from the observed incident shock wave speeds. Calculations were made assuming unreacted gas in internal thermal equilibrium at high temperature. Enthalpy data for propane below 1500°K were taken from published tables [3], and values at higher temperatures were computed on the basis of Pitzer's vibrational assignment [4] and Pitzer and Gwinn's treatment of hindered rotation [5].

Since ideal one-dimensional shock tube behavior was not realized in these experiments, these calculations should not be taken very seriously. The calculated reflected shock temperatures are presented here only to provide a rough indication of experimental conditions. The observed incident shock wave speeds and the calculated reflected shock temperatures in three experiments are listed at the top of the table.

Results of Three Experiments on Decomposition of Propane by the Reflected Shock Wave Technique

	Run 1	Run 2	Run 3
Shock wave speed (incident)	1.12 mm/μ sec	1.19 mm/μ sec	1.31 mm/μ sec
Calculated T behind reflected shock	1800°K	1960°K	2260°K
Propane (initial)	0.581 cm^3	0.414	0.255
Propane (final)	.283	.204	.127
Fraction decomposed	.513	.507	.502
Products			
Ethane	.029	.014	.006
Ethylene	.197	.142	.077
Acetylene	.019	.031	.041
Propylene	.036	.015	.004

Results and Discussion

Since incident shock wave attenuation was negligible in preliminary experiments, serious departures from one-dimensional flow were first suspected when attempts were made to understand the product analyses. Referring to the table, one sees some apparent discrepancies. On the one hand, the conversion of propane is only 50 per cent and is virtually independent of incident shock speed and calculated reaction temperature in the three experiments. On the other hand, that the reaction temperature is actually increasing with increasing shock strength is fairly obvious from the trend in product distribution, showing acetylene increasing at the expense of other products as calculated temperature goes up.

It is difficult to reconcile these observations and to explain the surprisingly low extent of decomposition if ideal shock tube behavior is assumed.

Considering first the low conversion of propane to products: one can estimate a minimum rate of decomposition by assuming that propane disappears by first-order unimolecular dissociation to ethyl and methyl radicals, with an activation energy of 85 kcal (rather a high estimate) and a frequency factor of 2×10^{13} sec^{-1}. The half-life of propane with these assumptions, leaving out all consideration of chain reactions, would be less than 10^{-4} sec at 2000°K. In our experiments, the minimum available reaction time at the high temperature (one m sec or greater) amounts to at least ten half-lives even using this unrealistically low estimate of rate. The conclusion is almost inescapable that only about half the propane is heated to the calculated reaction temperature.

If this is so, the results obtained can be viewed as follows: It is as if the reactant gas were divided into two parts, one of which is restricted to sufficiently low temperatures that little pyrolysis occurs, while the other is decomposed to high conversion. The two portions are then mixed (by the sampling procedure) and the apparent per cent conversion is determined by analysis of the mixture. The measured extent of decomposition would thus be governed by the original division of the sample.

A mechanism to explain qualitatively these results can be devised starting from Duff's observations [1]. From his report of the close pursuit of the incident shock wave by the contact surface we infer that main stream-boundary layer interactions impose a severe limitation on the quantity of gas that can exist in the intervening hot flow region. The influence of the boundary layer on the main stream is not simply encroachment of the former on the latter; in addition there is an actual flow toward the wall of gas in the main stream. The reactant gas thus tends to concentrate near the wall where some of it is bypassed by the central core of cold driver gas before the reflected shock wave arrives.

In our experiments, reaction occurs only behind the reflected shock; hence only that portion of reactant gas that remains in the hot flow region until it is traversed by the reflected shock will undergo decomposition at a rate characteristic of the calculated reflected shock temperature. That which has been lost to the boundary layer behind the incident shock may undergo little or no decomposition on passage of the reflected shock wave.

In order to estimate in another way the importance of such effects in the present experiments, some additional runs were made, with conditions as in Run 2 of the table, but with the third detector (115 cm station) mounted in midstream to permit measurement of the time between arrival of the incident shock and the contact surface at this station. The results varied from run to run, but the observed time interval never exceeded one-half the value given by one-dimensional theory. It was evident that a significant fraction of the reactant gas had been lost from the hot flow region.

In another experiment gas was sampled from near the center of the end plate, where by the above mechanism the apparent conversion of propane should be high. A small sample bulb with stopcock was attached to the end plate; with the stopcock open the diaphragm was burst, and then the stopcock was closed. The condensable part of the sample recovered from the bulb contained 27 mole per cent propane; that from the rest of the shock tube contained 63 mole per cent unreacted propane. Again, marked loss of gas from the hot flow region was indicated.

Conclusions

This investigation presents rather extreme examples of difficulties which are introduced by boundary layer effects. It is difficult to estimate the extent to which one must go, either by employing a tube of larger diameter or by working at higher pressure, in order to reduce below a tolerable limit the loss of reactant gas from the hot flow region. The obvious desirability of avoiding dynamical similarity with these experiments indicates that an answer cannot be obtained by simple dimensional analysis.

However, the very fact that extreme cases are presented should give some insight into the direction in which interpretation of experiments can err when boundary layer effects are ignored. For example, it is not difficult to see how an illusory indication of low octivation energy for decomposition could result if an unsuspected fraction (not too strongly dependent on shock strength) of the reactant gas were lost from the hot flow region.

The observed variations from run to run of the duration of hot flow can introduce other experimental complications as well. These variations presumably result in part from the finite but ill-defined rate of diaphragm rupture.

In conclusion, it is important to emphasize that none of the effects reported here would have been suspected on the basis of the shock wave velocity measurements, which gave no clear indication of incident shock attenuation or unusual disagreement between calculated and observed incident shock velocities. From the available evidence we must conclude that shock wave velocity measurements do not provide a reliable criterion for appraising the importance of departures from uniform flow in the hot gas when small, low-pressure shock tubes are employed. Even with larger tubes, especially if activation energies are to be derived from the data, independent measurements should probably be made to determine whether loss of reactant gas to the boundary layer is significant.

Acknowledgment

We are indebted to R. Gilbert Kaufman for his help with analyses of products and calibration of the gas chromatography system.

References

[1] R. E. Duff, Phys. Fluids 2, 207 (1959).
[2] K. E. McCulloh, Rev. Sci. Instruments 31, 780 (1960).
[3] American Petroleum Institute Research Project 44, Carnegie Institute of Technology, Pittsburgh, Pa., December 31, 1952.
[4] K. S. Pitzer, J. Chem. Phys. 12, 310 (1944).
[5] K. S. Pitzer and W. D. Gwinn, J. Chem. Phys. 10, 428 (1942).

CHEMICAL REACTION STUDIES WITH A HYDROMAGNETIC SHOCK TUBE

By James L. Lauer and Robert L. James
Sun Oil Company, Marcus Hook, Pennsylvania

INTRODUCTION

To gain quick qualitative information about high-temperature reactions, the hydromagnetic shock tube originally designed by Fowler and later modified by Kolb has been found useful.[10] In this tube a shock wave is produced by the rapid discharge of a high-voltage condenser through an arc formed between two electrodes perpendicular to the tube axis and located at one end of the tube. Compared to the mechanical or diaphragm shock tube, the hydromagnetic tube is but a small toy, generally less than 2 feet long and having only one chamber. Series of equivalent shock waves can be passed through a gaseous reaction mixture and significant yields of product obtained. Effective contact times are very short (shorter than normally obtainable with an electric arc) and exceedingly high temperatures can be reached. These advantages are partly offset, however, by non-uniform shock velocity, the influence of the electric arc on the reaction, the requirement of low gas pressure, all of these making quantitative analysis of the entire process exceedingly difficult.

However, when the reaction products were stable and the reaction studied was one of high activation energy, much could be learned from a few experiments with the hydromagnetic shock tube. The only parameters determined were product composition and shock velocity. Details of the procedure, applied mostly to the pyrolysis of methane, are explained in the following sections.

APPARATUS

Figure 1 is a schematic drawing of our hydromagnetic shock tube. It is a modification of the so-called "Tee" or Kolb[9] tube, the principal difference being that it is constructed of standard Pyrex pipe parts making for easy disassembling, cleaning, and exchanging. The electrodes along the bar of the tee-tube are connected in parallel with a high-voltage, low-inductance condenser (1.6 or 15 microfarads, 25 kv). A high-pressure gap, containing nitrogen between two stainless steel electrodes is interposed between one of the tube electrodes and the high-voltage side of the condenser to function as a switch. The entire tee-tube is filled with the gas mixture to be studied, which is usually at pressures of from 10 to 100 mm of Hg. To effect a discharge, the condenser is charged from a d.c. power supply and the gap switch triggered by means of an auxiliary electrode (not shown) brought to high potential by an automotive ignition coil attached to a battery. The discharge current returns to the ground side of the condenser through a strap located along the tee-tube between the two electrodes. As the current passes, it induces a magnetic field in the electrode section in a direction such as to produce an unbalanced force on the ions in the arc. This force propels the ions and the gas molecules colliding with them down the stem of the tee-tube. This "magnetic driving" accounts for about one-quarter to one-half the energy in the shock wave. Mainly, however, the shock wave is generated by the "pinch" effect of the discharge: The arc, constituting a rapidly varying current,

constricts about its axis ("pinch"), thereby heating the gas there to a very high temperature and bringing it to a pressure higher than that prevailing in the rest of the tube. Later expansion of this gas results in a shock wave propagating down the tube.

The dimensions of the apparatus were arrived at after considerable experimentation in which we tried to balance high shock velocity with convenience and safety of operation. The diameter of the tee-tube is 1 inch; the length of the stem portion can be varied by using different sections of pipe, but is usually between 1/2 and 2 feet; the gap between the electrodes is about 1/2 inch wide. All electrical leads are brass straps, 1-inch wide and 1/16-inch thick, to reduce inductance losses.

Shock arrival times were measured with a Tektronix Model 545A oscilloscope, using an inductive pickup (a few turns of wire) from the ground lead of the condenser to start the trace and a pressure or photo pickup at different locations along the tube to give an indication of the shock's position. Generally a Kistler piezoelectric pickup was used at the end of the tube where it faced the shock wave directly.

Figure 2 is a photograph of the apparatus during the passage of a very strong shock wave. The sharp, luminous front representing the farthest travel of excited ions and molecules is clearly shown. Figure 3 is the oscillogram for this particular experiment. The first sharp downward excursion of the trace corresponds to the arrival of the primary shock wave at the end of the tube, the second and third (smaller) excursions correspond to the arrival of the shock wave after traversal of 3 and 5 tube lengths, or — in other words — after 2 and 4 reflections at the tube ends.

THEORY

Fowler and coworkers[2,3] were the first to investigate the phenomenon of the so-called "Rayleigh Afterglow," i.e., the luminosity produced outside of the electrode region in a short-lived gas discharge and lasting considerably beyond the duration of the discharge. They established that the afterglow was due to gas molecules excited by very intense shock waves originating in the discharge. Their shock velocity and luminous front velocity measurements were in general agreement with the theory of shock and detonation waves. Several years later, Kolb,[9] in an effort to produce very intense shock waves and thereby very high temperatures in deuterium (hoping to start a nuclear fusion reaction) modified the Fowler tube, chiefly by adding the return strap and other features to get the effect of "magnetic driving." Simultaneously, Harris[12] developed a theoretical analysis of the Fowler tube by solving the following problem: "A given amount of energy W is deposited instantaneously in a very narrow slab of fluid in a tube of unit cross section. We wish to find the subsequent motion of the fluid." Using the methods of similarity analysis and approximations reasonable for strong shock waves (among others, that all the mass is concentrated at the shock front and that it has the velocity and internal energy prevailing there), Harris found that the shock radius R of a one-dimensional wave should vary with time according to the expression

$$R = \left(\frac{3}{2}\right)^{2/3}\left(\frac{\gamma+1}{2}\right)^{2/3}\left(\frac{W}{2\rho_0}\right)^{1/3} t^{2/3} \qquad (1)$$

where γ is the heat capacity ratio (assumed independent of temperature) and ρ_0 the gas density ahead of the shock front. (Equation (1) is analogous to an expression derived by G. I. Taylor[13] for the propagation of spherical blast waves in the wake of atomic bomb explosions.)

Kash[6] tried to check Harris' equation with the Kolb tube and found that an empirical relation between R and t, viz.,

$$t = AR^n \qquad (2)$$

was a truer representation of his data than Equation (1), which, however, was in good agreement with the general trends (e.g., changes in W and ρ_o). Recently, Agobian and Lifschitz[1] have performed similar experiments and have come to agree with Kash. They also made a brief analysis of the reasons for the deviation of their results from Harris' formula.

Our own results with methane, nitrogen and other gases always showed agreement with Equation (2). However, under some conditions of low pressure and high discharge energy, our results have come very close to agree with Equation (1).

By combining the "blast wave" equation (Equation 1) with first order kinetics, it was possible to test at least the reasonableness of kinetic constants either assumed or found in the literature. While the procedure used was admittedly quite approximate, it proved to be consistent in itself and with other data in the case of methane pyrolysis. The theory behind it is, therefore, briefly sketched here and the method of calculation illustrated in Paragraph (f) of the next section of this paper.

Differentiation of Equation (2) with respect to time yields an equation for the shock velocity, viz.

$$\dot{R} = \left(\frac{1}{nA}\right)^{\frac{1}{n}} t^{\frac{1}{n}-1} \qquad (3)$$

which is related to the ratio of temperatures behind and in front of the shock front by the "strong shock" formula[10]

$$\frac{T}{T_o} = \frac{2\gamma(\gamma-1)\dot{R}^2}{(\gamma+1)^2 a_o^2} \qquad (4)$$

a_o and T_o being the sound velocity and temperature in the medium ahead of the shock front. Equation (4) holds for $(\gamma-1)\dot{R}^2/2a_o^2 \gg 1$, a condition fairly well satisfied in our experiments over the region where reaction took place.

A monomolecular decomposition is described by

$$-d\ln c = k\,dt \qquad (5)$$

where c is the concentration or partial pressure of the decomposing material, t the time, and k the reaction velocity constant defined by the Arrhenius formula

$$k = z\,e^{-E_a/R'T} \qquad (6)$$

(z is the frequency factor, Ea the activation energy per mole, R' the universal gas constant, T the absolute temperature). By making the assumption of Harris and considering all the mass concentrated at the shock front, it is permissible to substitute T from Equation (4) into Equation (6) and use the resulting k in Equation (5). Thus one gets after integration:

$$\frac{1}{z}\ln(c_o/c) = \int_{t_o}^{t_1} e^{-BE_a t^{2-2/n}}\,dt \qquad (7)$$

with $B = \dfrac{(\gamma+1)^2 a_o^2 (nA)^{2/n}}{2R'\gamma(\gamma-1)T_o}$ and (7a)

$$A = \frac{4}{3}\cdot\frac{1}{\gamma+1}\cdot\left(\frac{2\rho_o}{W}\right)^{1/2} \quad \text{for } n = \tfrac{3}{2}. \qquad (7b)$$

The integral of Equation (7) can be written in the form

$$I = \int_{t_o}^{t_1} e^{-\alpha t^\beta} dt = \frac{1}{\alpha^{1/\beta}\beta} \int_{\alpha t_o^\beta}^{\alpha t_1^\beta} e^{-y} y^{\frac{1}{\beta}-1} dy$$

$$= \frac{1}{\alpha^{1/\beta}\beta} \left[\gamma\left(\frac{1}{\beta}, \alpha t_1^\beta\right) - \gamma\left(\frac{1}{\beta}, \alpha t_o^\beta\right) \right] ; \quad \frac{1}{\beta} > 0 ;$$

where the incomplete gamma functions can be expressed in terms of confluent hypergeometric functions according to the formula

$$\gamma(C, x) = x^{C-2} e^{-x} (C-1)\, {}_1F_1[1; C-1; x] - (C-1) e^{-x} x^{C-2} - x^{C-1} e^{-x} \qquad (9)$$

$$\text{When } n = \frac{3}{2} \;, \quad \frac{1}{\beta} = C = \frac{3}{2}$$

Equation (9) was derived from recurrence relations given in Slater's "Confluent Hypergeometric Functions." It is already in a form suitable for use with the tables contained in the same treatise.[14]

The isentropic index γ used in Equation (7) is an "effective" γ over the portion of the shock tube for which the reagent concentration is changed from Co to C by passage of the shock wave. Concentrations are found by analysis of the tube's contents, for varying tube lengths or varying positions of a barrier within the tube (cf., following section). Thus, extents of reaction in different portions of the tube can be calculated (shock strength attenuates with distance from the arc region).

EXPERIMENTAL RESULTS

(a) Relative Amounts of Reaction in Electrode and Shock Tube Portions

In order to determine the relative extent of reaction in the electrode and shock tube sections of the tee-tube, we placed a loosely fitting barrier in the shock tube at various distances from the electrodes in such a way as to reflect oncoming shock waves. The composition of the gas mixture after discharge was found to depend strongly on the position of the barrier. When the tube had been originally filled with methane, it was possible to double the proportion of acetylene in the final mixture by placing the barrier a certain distance from the arc (around 5 inches under our conditions). This effect of the barrier (the barrier did not change tube volume) was a maximum at a certain distance from the electrodes and decreased more sharply with decrease than with increase of distance from the position of maximum influence. The effect of the barrier dropped to zero at about five times the distance of the maximum from the electrodes. This effect on reaction rate we ascribed to reactions taking place in the wake of a shock wave derived from the primary shock wave by reflection at the barrier. When the barrier was far from the electrode region, the shock wave was too weak to cause further reaction; when it was very close to the electrode section, a shock wave had not yet formed and reaction was due to the arc.

By this procedure, we were able to estimate for the conditions of discharge voltage, pressure, electrode distance, etc., what the relative influences of arc and shock wave on the (high-temperature) reaction were and over what distance down the tube reaction took place.

(b) Effect of Increased Electric Energy Expenditure on Extent of Reaction

As mentioned earlier, the hydromagnetic shock tube permits passage of successive shocks through the same gas mixture. Thus it is possible to increase the energy input in two ways: (1) by increasing the discharge energy (higher capacitance, higher condenser voltage) and (2) by increasing the number of discharges per experiment, every discharge occurring at the same potential. Both methods increased the concentration of acetylene in the final gas mixture (analyses were done on aliquot samples from the tube either by mass spectrometry or by gas chromatography). However, the latter method was more instructive, for, as Table I shows, the gradual substitution of ethylene for acetylene was demonstrated. Table I also illustrates the effect of increase in shock strength by the introduction of "magnetic driving." When the return strap had been removed from the electrode portion, the yields of product were considerably lower.

(c) Effect of Initial Pressure on Extent of Reaction

As expected from the theoretical analysis (Equation (1)), higher initial pressures (higher ρ_0) should result in shorter shock radii at a given time (lower shock velocities) and hence lower temperatures and less reaction. This result is indeed obtained (Table II). However, probably because the methane decomposition reaction proceeds with an increase in volume, the decrease of acetylene concentration is even greater than one would otherwise predict.

(d) Shock Velocities

Figure 4 contains plots of arrival times in nitrogen of shock waves against breakdown voltage for various pressures. On the logarithmic scales, the curves are reasonably straight lines of slopes in agreement with predictions from Equation (1).

The variation of arrival time in methane with distance is shown in Figure 5. The curves are straight lines on a logarithmic plot. Thus the slope of these lines corresponds to n and the intercept to A of Equation (2). Over the distances shown, the exponent n is nearly independent of pressure and of breakdown voltage, as predicted theoretically. It is also nearly equal to 1.5, the theoretical value. A varies with pressure and discharge voltage according to Equation (1).

When a series of discharges and shock waves were passed through methane, arrival times at a fixed location changed as composition and pressure of the gas mixture changed, the result being a gradual decrease of arrival time or increase in shock velocity. By measuring both total pressure change and shock velocity for every shock passed through a given gas mixture, it was often possible to learn enough about the extent of reaction without further analysis; e.g., if one wanted to know what influence a change in the concentration of a particular reagent would have on the yield of a particular product.

An example of such a study is the effect of hydrogen on the pyrolysis of methane, which is illustrated in Table III. Increases in the hydrogen/methane ratio led to higher conversion of methane, but more to ethylene than to acetylene. The proportions of the products could be deduced from pressure and velocity measurements only.

(e) Pyrolysis of Hydrocarbons

The pyrolysis of methane in the hydromagnetic shock tube was used in the preceding sections to illustrate the method. Ethylene, acetylene, hydrogen and carbon were the principal products. Any change of conditions leading to an increase of temperature behind the shock wave (lowering of pressure, increase of breakdown

potential) resulted in an increase of acetylene and hydrogen production and a decrease of ethylene and carbon production. The converse was also found to be true. The heat capacity ratio of the higher paraffins is smaller than that of methane. According to Equation (1) the shock velocity should, therefore, be lower, which in turn would produce a lower temperature in the wake of the shock wave (Equation (4)). Thus, higher paraffins would be expected to yield relatively more ethylene and carbon than would methane under otherwise identical conditions. This was indeed the result obtained. Under the same conditions, however, olefins yielded more carbon than the corresponding paraffins. Evidently not only heat capacities but also energies of formation and kinetics of pyrolysis play an important role. When the differences of experimental conditions were taken into account, our work on hydrocarbon pyrolysis appeared to be in general agreement[6] with that of Greene, Taylor, and Patterson, who used a conventional shock tube. Our pyrolysis work is still continuing and will form the subject of a later paper.

(f) Kinetic Parameters in the Pyrolysis of Methane

In a series of experiments with pure methane at a breakdown voltage of 16 kv and 60 mm of pressure, shock arrival times were measured as a function of distance along the tube axis and from the slopes and intercepts of the curves (Figure 5) the parameters $A = 0.512 \times 10^{-6}$ and $n = 1.5$ were obtained (cf., Equation (2)). For a distance of about 13 cm from the arc section (26 microseconds arrival time), an effective γ of 1.15 was calculated. (Because the value of n obtained was the theoretical one, it was possible to calculate the energies per unit area of shock front by differentiating Equation (1) and forming $\rho_0 R\dot{R}^2$. For breakdown voltages of 10 to 18 kv, the ratio of this energy to the condenser energy proved to be very nearly constant (Table IV), thus lending further support to the validity of the blast wave treatment). Using literature values for the other quantities in Equation (7a), B turned out to be 0.322. Taking Ea = 93 kcal (a reasonable value), αt^{β} of Equation (8) came out 26.6. Taking a time spread of 10 microseconds, the integral of Equation (8) could be approximated by:

$$I \sim (t_i - t_o)\, e^{-\alpha t^{\beta}} \sim 10^{-5} \times e^{-26.6} \sim 10^{-16.6} \qquad (10)$$

During this period about 1% of the methane was converted to other products (cf., Figure 6*); hence, from Equation (7)

$$z \simeq \ln(C_o/C) \times 10^{16.6} = 10^{14.6} \qquad (11)$$

This result for the frequency factor is in remarkably close agreement with Heath and Kevorkian's[7] 1.32×10^{14}, considering the drastic approximations made. The error in z is probably about 2 orders of magnitude.

We do not recommend this procedure for the determination for reaction kinetics; many better methods are available[4]. We have included this example only to illustrate the consistency of the description of the phenomena observed.

*The maximum in this figure is probably caused by shock wave reflections. Their effects have been removed in the above estimate.

CONCLUDING REMARKS

As said at the outset, the purpose of this paper was to illustrate a technique for the study of high temperature reactions. Accordingly, we have refrained from presenting many data obtained on specific reactions, especially since we have not yet arrived at definite conclusions. For example, our obtaining more carbon in the pyrolysis of methane than in the pyrolysis of paraffins of higher molecular weight under otherwise equal conditions could also be regarded as evidence in favor of Porter's theory of carbon formation.[12] For, if acetylene is a necessary intermediate whose rapid polymerization leads to carbon, as Porter asserts, then molecules containing C_2 linkages would have a better chance of forming carbon. Much more evidence is needed to support or reject this speculation.

To obtain quantitative information, we recently inserted a diaphragm into the shock tube. It thus became a "conventional" tube, with the high-pressure section electrically heated by the arc discharge. However, it differs from the conventional shock tube by the higher Mach numbers and by the possibility of reflecting primary shock fronts arriving at the tube's end as rarefaction rather than compression waves (because of the great temperature difference in the two chambers at the time of diaphragm rupture). A method of "tailored interface" by adjusting tube length is thus made available. This work will be the subject of a later communication.

REFERENCES

(1) Der Agobian, R., and Lifschitz, L.: Comptes Rendus 248, No. 19, p. 2734 (May 1959)

(2) Fowler, R. G., et al.: Phys. Rev. 88, 137 (1952)

(3) Fowler, R. G., and Seay, G. E.: Proc. Oklahoma Acad. of Sci. 35, 111, (1954)

(4) Glick, H. S., Squire, W., and Hertzberg, A.: 5th Int. Symp. Combustion, p. 393, Reinhold, New York, 1955.

(5) Greene, E. F., Taylor, R. L., and Patterson, W. L., Jr.: J. Physic. Chem. 62, 238 (1958)

(6) Harris, E. G.: NRL Report 4858, October 1956.

(7) Heath, E., Kevorkian, V., and Boudart, M.: Presented before Division of Industrial and Engineering Chemistry, American Chemical Society, Boston, April 1959; J. Phys. Chem. 64, 964 (1960)

(8) Kash, S. W., Magnetohydrodynamics, p.89, Stanford University Press, 1957

(9) Kolb, A. C., Magnetohydrodynamics, p.76, Stanford University Press, 1957

(10) Lauer, J. L.: Bulletin of the American Physical Society, Series II, Vol. 4, No. 3., p. 138 (March 1959)

(11) Liepmann, H. W. and Roshko, A.: Elements of Gas Dynamics, p.65, Wiley, New York, 1957

(12) Porter, G.: AGARD Memo AG 13/M9 (1954); 4th Symp. Combustion, p.248, Williams & Wilkins, Baltimore 1952

(13) Sedov, L. I.: "Similarity and Dimensional Methods in Mechanics", Academic Press, New York 1960

(14) Slater, L. J.: "Confluent Hypergeometric Functions", Cambridge University Press, 1960

(15) Taylor, G. I.: Proc. Roy. Soc. London A201, 159 (1950)

TABLE I

Composition of Gas Mixture Resulting from Passage of Series of Shock Waves through Methane

18 kv. Breakdown Potential
Starting Pressure: 60 mm Hg

	Composition in Percent by Volume				
	Original	After 1 Shock	After 5 Shocks	After 20 Shocks	
Magnetic Driving	---	Yes	Yes	Yes	No
Constituents					
H_2	---	6.1	25.0	50.9	42.0
CH_4	100	92.6	70.6	36.6	51.4
C_2H_6	---	0.2	0.1	0.4	0.3
C_2H_4	---	0.2	0.6	1.7	1.4
C_2H_2	---	0.9	3.6	10.0	7.5
di-C_2H_2	---	---	0.1	0.4	0.2
Final Pressure (mm Hg)	60	63	70	89	76
Arrival Time at Tube's End (μ secs.)	670	665	640	590	-

TABLE II

Effect of Initial Pressure on Product Distribution of Pyrolyzed Methane

Composition after 20 Shocks of 18 kv. Breakdown Potential

	Initial Pressure, Percent by Volume		
Constituents	20	60	120 mm Hg
CH_4	19.5	46.7	48.9
C_2H_2	61.2	43.6	26.6
C_2H_4	5.7	10.5	16.6

TABLE III

Effect of Hydrogen on Pyrolysis of Methane at Constant Total Pressure

18 kv. Breakdown Potential

Constituents	Composition after 5 Shocks in Percent of Methane Charged		
	No Initial H_2	10% H_2	30% H_2
CH_4	60.7	54.3	48.6
C_2H_2	26.0	19.6	18.3
C_2H_4	4.2	21.4	26.3
C	7.5	6.8	2.8

TABLE IV

Shock Arrival Times in Methane at 25 cm Distance as Functions of Breakdown Potentials

Breakdown Potential (kv)	6.0	10.0	13.0	16.0	18.0
Condenser Energy, E_o (joules)	270	750	1270	1920	2430
Parameter A (μ-sec. $cm^{-3/2}$)	1.24	0.808	0.624	0.512	0.448
Arrival Time (μ-sec.)	155	101	78	64	56
Shock Velocity (mm/μ-sec.)	1.07	1.65	2.14	2.61	2.98
(Mach No.)	2.38	3.68	4.75	5.79	6.62
Energy in Shock Wave, $\rho_o R^2$ (joules/cm^2)	1.622	3.515	5.74	8.74	11.42
$\rho_o R^2/E_o$ (x 10^{-3})	6.01	4.68	4.52	4.55	4.70

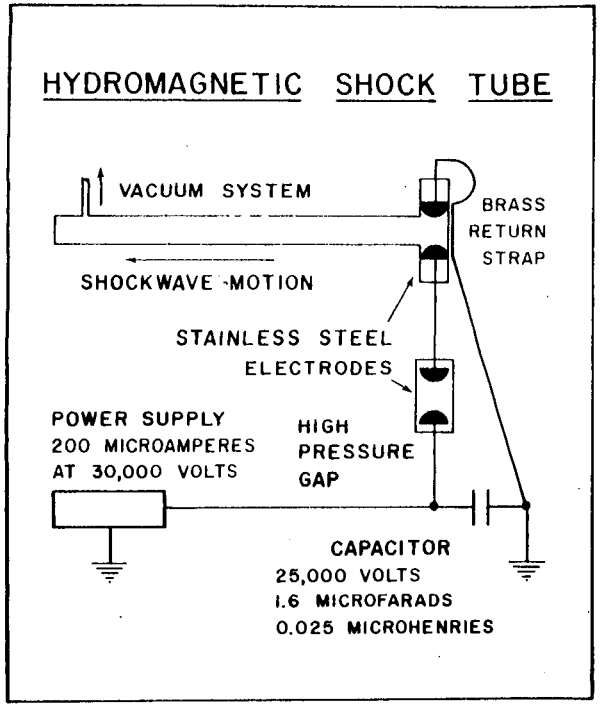

FIGURE 1.

SCHEMATIC ARRANGEMENT

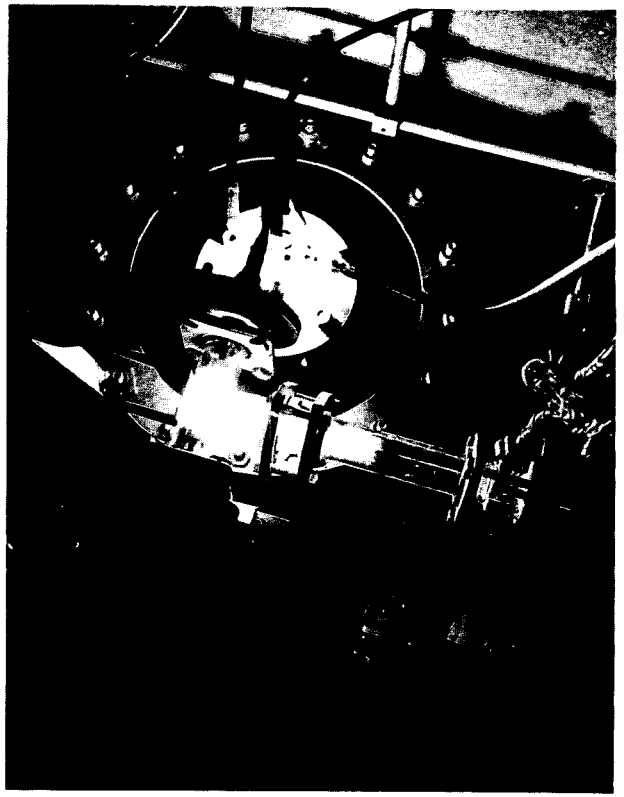

FIGURE 2.

A PHOTOGRAPH SHOWING PROPAGATION
OF THE LUMINOUS FRONT

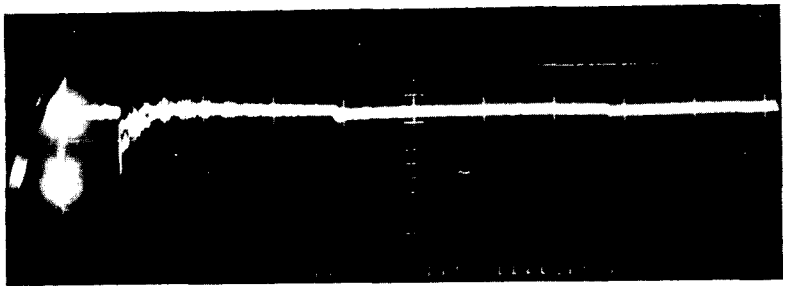

FIGURE 3.

OSCILLOGRAM SHOWING THE ARRIVAL
OF THE PRIMARY AND REFLECTED SHOCKS

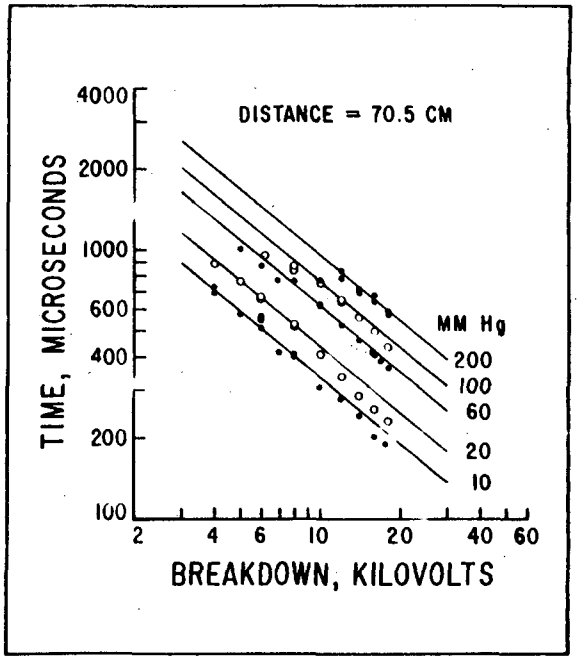

FIGURE 4.

SHOCK ARRIVAL TIMES IN NITROGEN

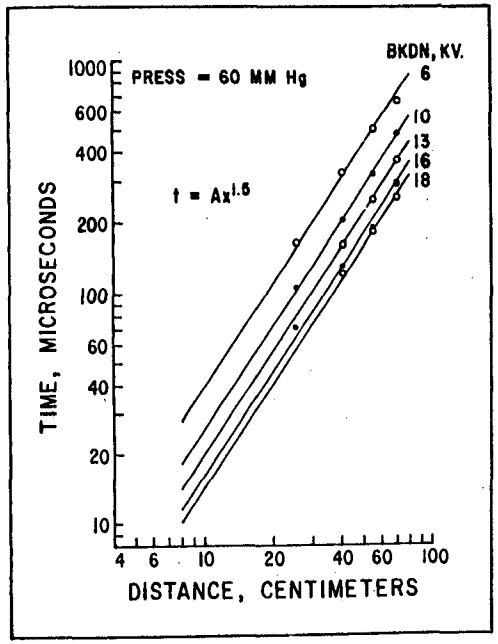

FIGURE 5.

SHOCK ARRIVAL TIMES IN METHANE

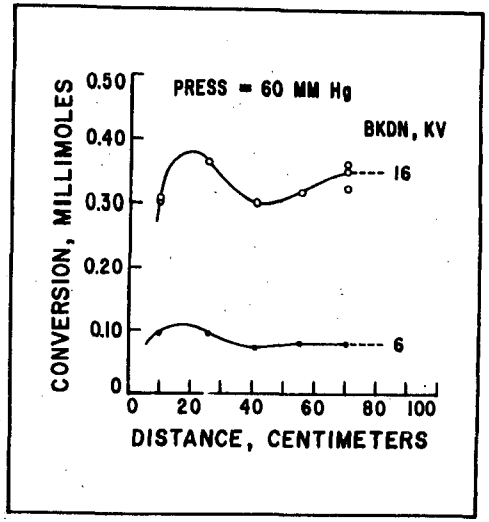

FIGURE 6.

EFFECT OF TUBE LENGTH
ON THE CONVERSION OF METHANE

PYROLYSIS OF METHANE AND THE C_2 HYDROCARBONS

Gordon B. Skinner
Monsanto Chemical Co., Research and Engineering Division,
Dayton 7, Ohio

INTRODUCTION

Since its invention by Glick, Squire and Hertzberg (1), the single-pulse shock tube has been adopted by many investigators for chemical kinetic studies, so that it is rapidly developing into a standard laboratory tool. In this type of shock tube a sample of gas can be heated rapidly, held under known temperature and pressure conditions for a known time in the range of 0.1 to 10 milliseconds, cooled rapidly, and then removed for analysis. Optical and other measurements can be made on the gas during the heating time. In earlier shock tubes gas samples of known history could not be recovered. It is undoubtedly the ability to recover samples of reacted gas that has made this type of tube so popular with chemists, along with the fact that the shock tube is one of the few techniques for obtaining entirely homogeneous reaction data.

This paper is a review of recent shock-tube work as it applies to the pyrolysis of these simple hydrocarbons.

EXPERIMENTAL

Our shock tube is shown schematically in Fig. 1. It was made of 3-inch stainless steel pipe, the reaction section being 12 feet long and the driver section adjustable in length between 6 and 28 feet, so dwell times up to 15 milliseconds could be obtained with helium driver gas. The surge tank had a volume of about 50 cubic feet.

For measuring the incident shock speed, two SLM pressure transducers spaced 55 and 7 inches from the downstream end were used (a and b, Figure 1). The amplified signals from these were used to start and stop a microsecond timer, and also to start two oscilloscopes. One of these measured the pressure by means of a third SLM gauge, c, 3 inches from the downstream end, (see Figure 2) while the other measured the output from a photocell, d, mounted outside a window in the side of the shock tube, also 3 inches from the end (see Figure 3). Directly opposite the photocell window was a small tube leading to a quick-opening valve, e, from which samples of gas could be drawn for analysis.

Gas samples were analyzed before and after reaction by a vapor chromatograph. In spite of the fact that the driver gas was in direct contact with the sample during the experiments, no more than 5% driver

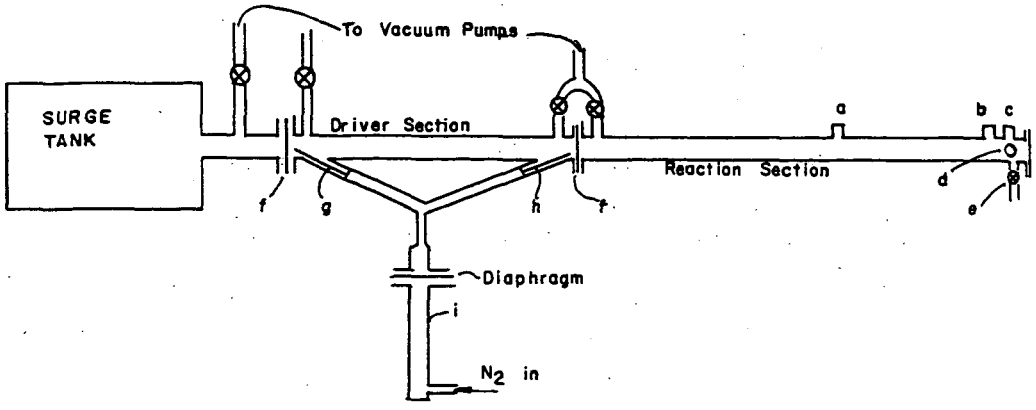

FIG. 1.
Schematic Drawing of Shock Tube

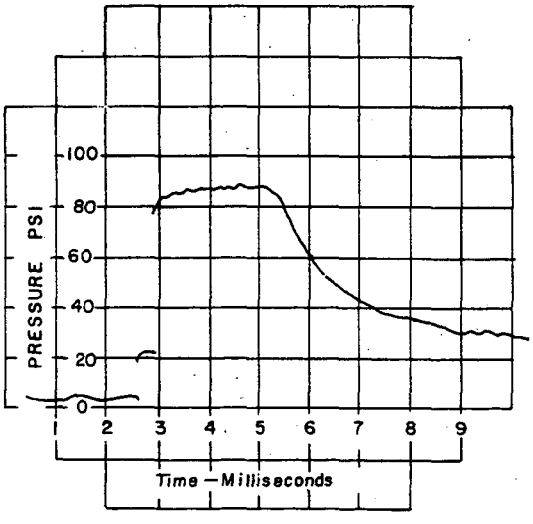

FIG. 2.

TYPICAL PRESSURE RECORD

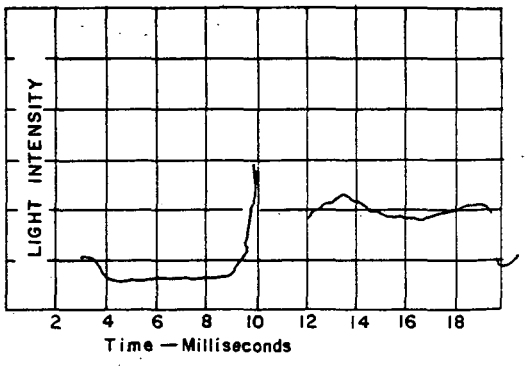

FIG. 3.

TYPICAL PHOTOMULTIPLIER RECORD

gas was found in the reactant gas after the runs, and in most cases the amount was less than 1%. As would be expected, the longer time runs showed the greatest contamination.

In a typical run, all sections of the shock tube were first evacuated, and then the sample and driver gases were added. Since the "tailored interface" technique (1) was used to give a pulse of uniform temperature, small amounts of nitrogen were usually added to the helium driver gas, to match it with the sample and pressure ratio. The two diaphragms f were then ruptured at the proper times, by the plungers g and h operated by the auxiliary shock tube i, and a sample of gas taken for analysis a few seconds later. The oscilloscope traces were recorded with Polaroid cameras.

Strehlow and Cohen (2) have published a discussion of the reflected shock wave technique. They found that the most nearly ideal conditions for kinetic studies occurred when the sample gas was nearly all monatomic, while diatomic gases could be studied with some accuracy if measurements were taken near the end wall of the shock tube. With polyatomic gases, perturbations in the reflected shock wave due to boundary layer interactions were so great that temperatures could not be calculated with any accuracy. Polyatomic gases such as hydrocarbons must be highly diluted with a monatomic gas such as argon to give reasonably ideal conditions, and also to reduce the average specific heat of the sample gas to permit heating with reasonable driver/sample pressure ratios. It seems to have been satisfactorily demonstrated (3,4) that if these conditions are fulfilled, gas temperature calculated by the standard methods (5,6) are accurate to about 2%. However, we have found that in many runs the pressure, while coming to nearly the theoretical value just behind the shock wave, subsequently fluctuates for reasons we do not quite understand. We have corrected the calculated temperature by assuming that these fluctuations cause temperature changes according to the standard isentropic equations, and feel that these corrected temperatures are more accurate than uncorrected ones. Temperatures were also corrected for heat of chemical reaction.

RESULTS AND DISCUSSION

Methane. The rate of methane decomposition has been studied in three very similar single-pulse shock tubes by different investigators (7,8,9). There is agreement that the reaction is first-order in methane concentration, and that there is little inhibition of the reaction by products in the temperature range studied. The first-order rate constants are shown in Figure 6. On the whole, agreement among the three sets of data is reasonable, and though the activation energies calculated, 85 Kcal. (7), 93 Kcal. (9), and 101 Kcal. (8), differ, this may well be due to experimental error. None of these activation energies requires an unreasonable value of the frequency factor to give the observed rates. While the lower activation energies seem to fit in better with data obtained by other methods at lower temperatures (10,11), the possibility remains that some heterogeneous reaction occurred in the lower-temperature experiments, despite the investigators' best attempts to avoid it.

Figure 5 shows the product distribution in the pyrolysis of methane for heating times of 1.5 milliseconds at different temperatures, in terms of moles of each product formed per 100 moles CH_4 decomposing. Experiments at longer times show relatively more C_2H_2

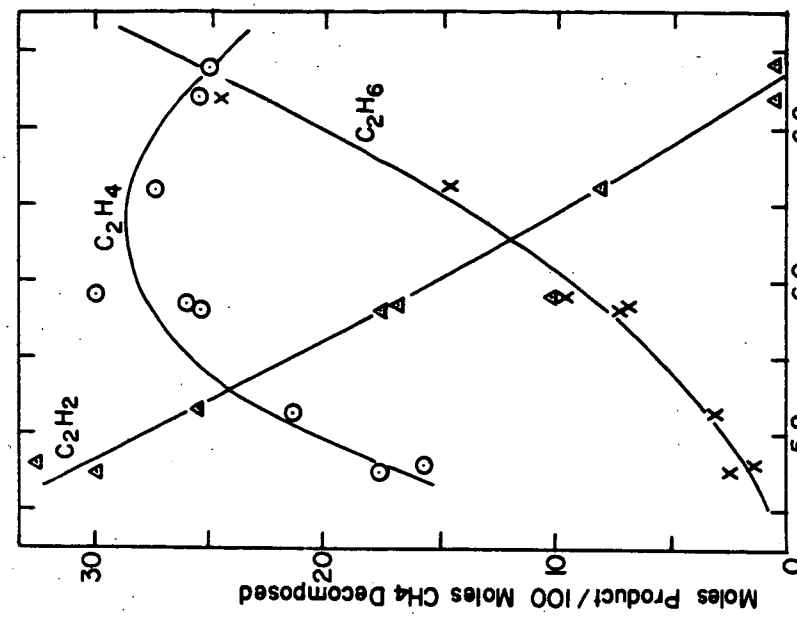

FIG. 5.
Product Distribution in Methane Pyrolysis

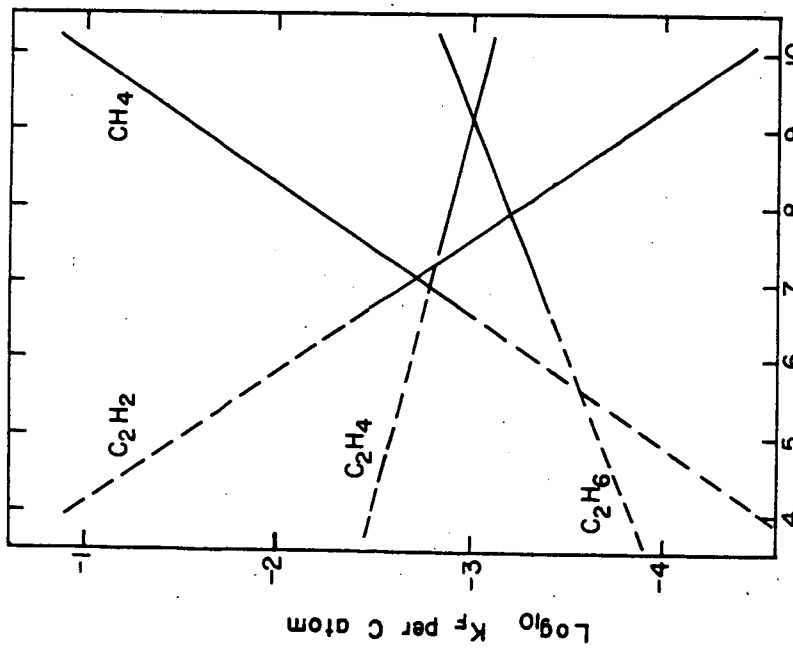

FIG. 4.
Equilibrium Data for CH_4, C_2H_6, C_2H_4, and C_2H_2

and C_2H_4, and less C_2H_6, suggesting that C_2H_6 is an unstable intermediate. Methane pyrolysis thus seems to occur stepwise

$$CH_4 \rightarrow C_2H_6 \rightarrow C_2H_4 \rightarrow C_2H_2 \rightarrow C \qquad (1)$$

although the C_2H_6 has a very short lifetime at high temperatures. There is a relation between the product yields of Figure 5 and the thermodynamic equilibrium data of Figure 4, which shows the relative stability of each molecule as a function of temperature, the species appearing highest on the graph being most stable. These data are taken from the NBS tables (12) although a very similar graph was made earlier by Kassel (13). The stepwise nature of the pyrolysis reaction is confirmed by comparison of these two Figures, since C_2H_6 and C_2H_4 show up more prominently in Figure 5 than would be expected from the equilibrium curves of Figure 4 alone.

The mechanism of conversion of CH_4 to C_2H_6 is still unsettled. Largely on the basis of our observed activation energy of 101 Kcal., we have preferred the series of reactions

$$CH_4 \rightarrow CH_3 + H \qquad (\Delta H \sim 101 \text{ Kcal.}) \qquad (2)$$

$$H + CH_4 \rightarrow CH_3 + H_2 \qquad (3)$$

$$2CH_3 \rightarrow C_2H_6 \qquad (4)$$

On the other hand, Kevorkian and co-workers (9) have preferred the reaction sequence

$$CH_4 \rightarrow CH_2 + H_2 \qquad (\Delta H \sim 85 \text{ Kcal.}) \qquad (5)$$

$$CH_2 + CH_4 \rightarrow CH_3 + H \qquad (6)$$

$$2CH_3 \rightarrow C_2H_6 \qquad (7)$$

because it agrees better with their lower observed activation energy. These two reaction sequences both give first order kinetics with "chain length" of two, and it will require either some sort of direct observation on the reacting gas, or very accurate kinetic measurements, to decide between the two.

Ethane. Pyrolysis of ethane has for some time (14) been thought to occur by a free-radical chain mechanism, as follows:

$$C_2H_6 \rightarrow 2CH_3 \qquad (8)$$

$$CH_3 + C_2H_6 \rightarrow C_2H_5 + CH_4 \qquad (9)$$

$$C_2H_5 \rightarrow C_2H_4 + H \qquad (10)$$

$$H + C_2H_6 \rightarrow C_2H_5 + H_2 \qquad (11)$$

$$2C_2H_5 \rightarrow C_4H_{10} \text{ or } C_2H_4 + C_2H_6 \qquad (12)$$

$$H + C_2H_5 \rightarrow C_2H_6 \text{ or } H_2 + C_2H_4 \qquad (13)$$

A number of shock tube experiments (15) have given further verification of this reaction scheme. It has been found (as Steacie and Shane (16) for example found at lower temperatures) that one mole of

CH_4 is produced for each 20-25 moles of C_2H_6 in the first stages of pyrolysis. As pyrolysis proceeds, the rate constant falls off to less than a tenth of its original value, and the fraction of methane produced increases markedly. Ethane pyrolysis is strongly inhibited by methane, as would be expected from the above free radical steps and reaction 3. Inhibition by C_2H_4 also occurs. Quantitative calculations were made by using rate constants for the free radical reactions derived from various sources (and some estimates) which showed that these experimental observations should be expected from the above mechanism. Finally, with the assigned rate constants, the experimental results of several investigators could be reproduced over a wide range of temperatures, as shown in Figure 7.

From a series of experiments in a flow reactor in which ethane has been pyrolyzed in the presence of a small amount of radioactive methane, Brodskii and co-workers (17) have concluded that the above chain reaction is not the main one in the temperature range of 770-890°C. We are not altogether satisfied with their interpretation of their experimental data, and are making calculations to see if their observations can be interpreted in terms of the chain mechanism.

Ethylene. Shock tube studies on ethylene pyrolysis between 900 and 1600°C (18) show that there are two major reactions, one the formation of acetylene, which is a first-order reaction with an activation energy of 46 Kcal. over the upper part of the temperature range, the other the formation of 1,3-butadiene, which is second-order with an activation energy of about 25 Kcal. Butadiene formation is, of course, favored at low temperatures and high pressures, and acetylene at high temperatures and low pressures. Acetylene formation has been most thoroughly studied.

In contrast to ethane pyrolysis, this reaction does seem to be a molecular one in the classical sense, without the formation of free radicals. The most direct evidence for this is that the Arrhenius rate equation holds all the way from 2 to 95% ethylene decomposition, while for a chain reaction the rate should fall off at high conversions. Moreover, the product distribution (almost all hydrogen and acetylene at high temperatures and low pressures) remained the same up to 95% decomposition. The activation energy for acetylene formation is just slightly more than the heat of reaction (44 Kcal. at 1500°K.) (12), and we have not been able to think of a free-radical mechanism which would give this activation energy.

Experiments with an ethylene-acetylene mixture show that butadiene is not formed by reaction of ethylene with product acetylene, but comes more directly from ethylene, either by a straight bimolecular reaction, or perhaps through dimerization to butylene followed by loss of hydrogen. No butylenes were found, so they are unstable intermediates if they form at all.

Acetylene. Pyrolysis of acetylene has been studied in shock tubes by Greene, Taylor and Patterson (19) and by the author (20), between 900 and 2000°C. There is agreement that the overall reaction is second-order, and the observed rate constants are about the same. Acetylene is quite stable at high temperatures, compared to ethane and ethylene. The only difference in the two sets of data is that we found vinylacetylene and hydrogen to be the major pyrolysis products, while Greene found diacetylene to be a more important product than vinylacetylene. The latter compound seems without doubt to be the

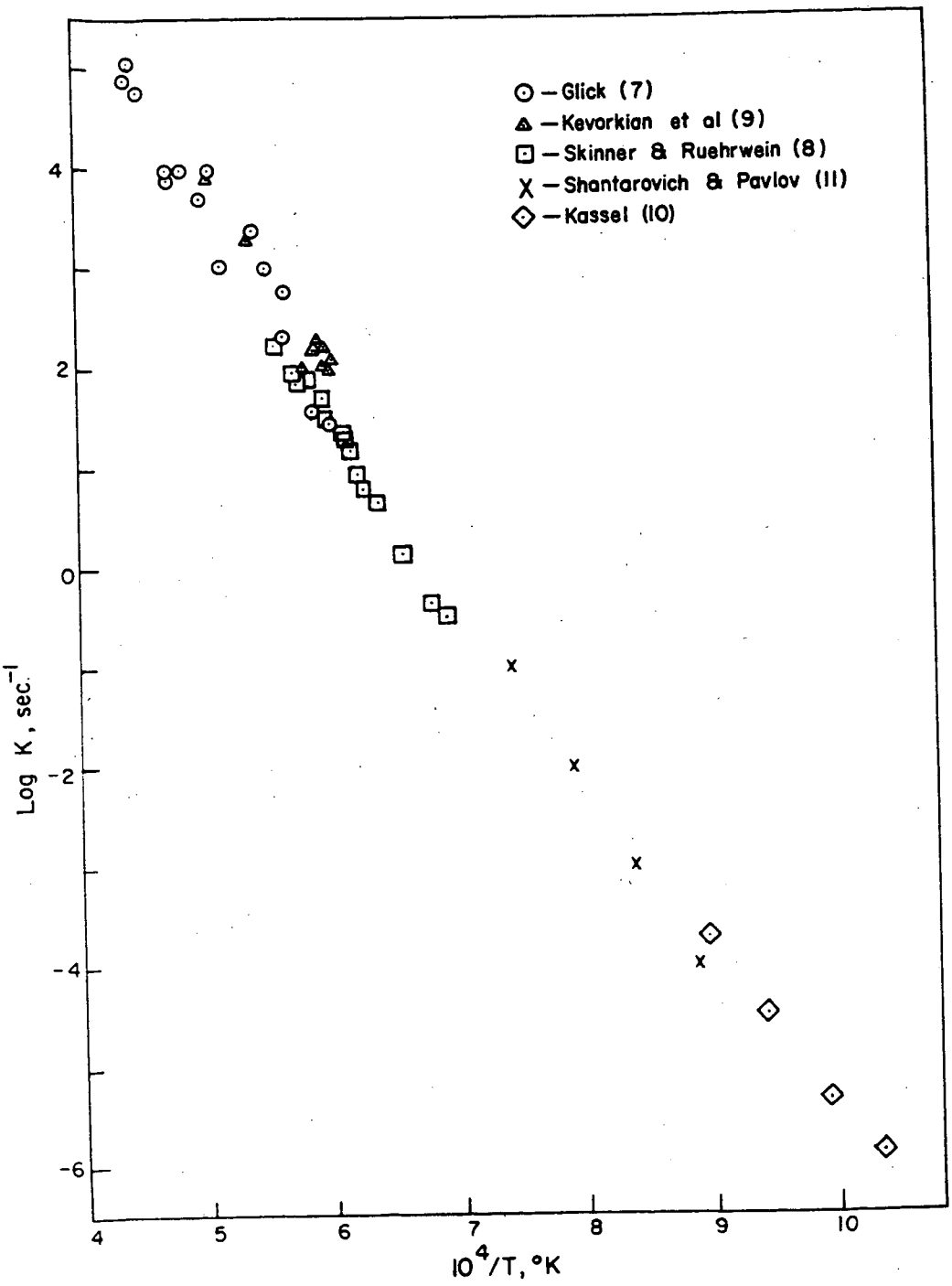

FIG. 6. Rate Constants for Methane Pyrolysis

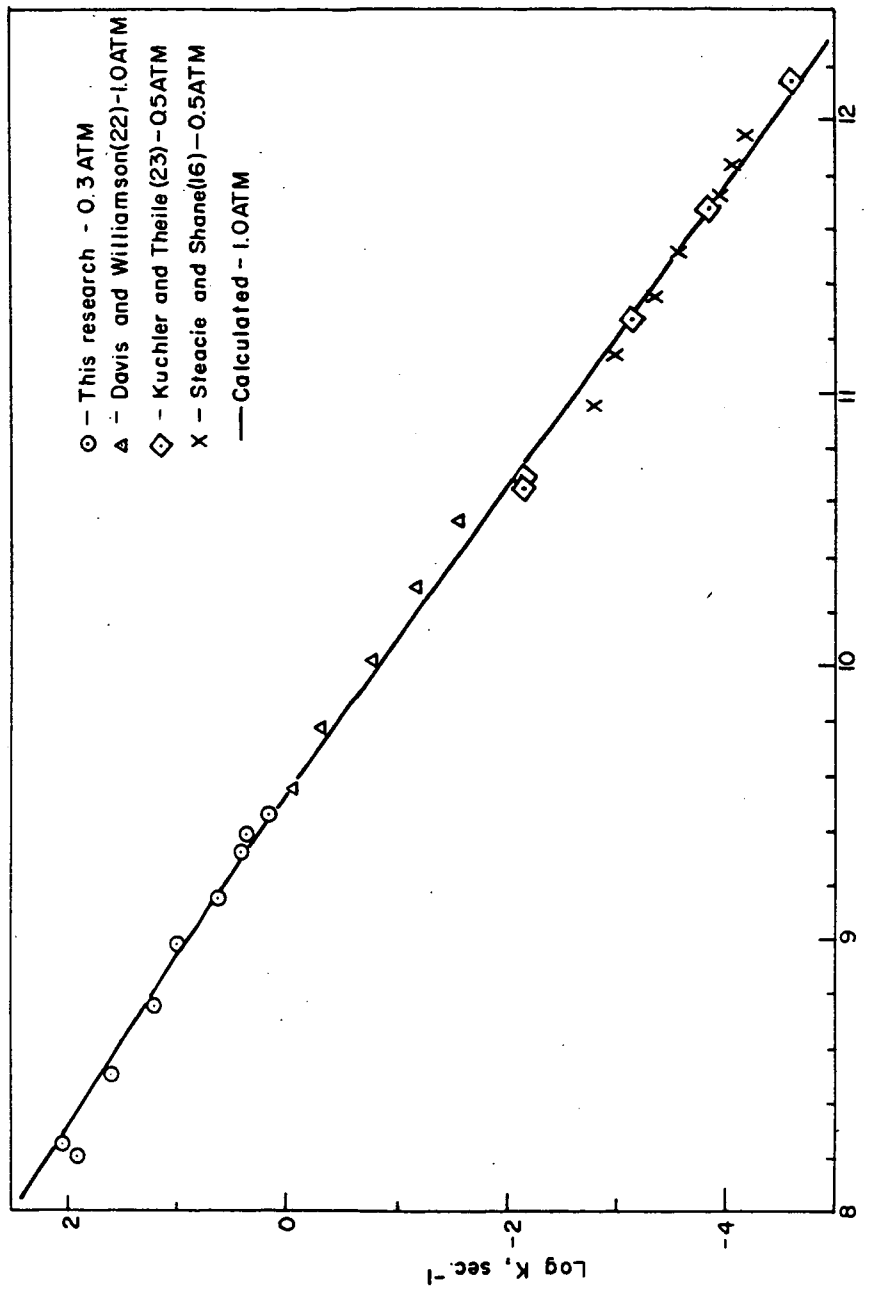

FIG. 7 Initial Rate Constants for Ethane Pyrolysis

first pyrolysis product of acetylene in this temperature range, since it appears at low conversions before any hydrogen is observed. The subsequent steps have not been defined, but probably involve further polymerizations and condensations to produce benzene and condensed aromatic compounds which eventually may be thought of as carbon, as discussed by Smith, Gordon and McNesby (21). These pyrolysis products intermediate between acetylene and carbon catalyze the decomposition reaction, so the rate increases as decomposition proceeds. When hydrogen was added to the acetylene, butadiene rather than vinylacetylene was formed, and the overall rate of acetylene decomposition was less than in the absence of hydrogen. That is, hydrogen inhibits acetylene decomposition by converting reactive vinylacetylene to relatively unreactive butadiene.

In conclusion, shock tube studies have added much to our understanding of the high temperature pyrolysis reactions of these simple hydrocarbons. On the other hand, many interesting problems remain to be solved.

REFERENCES

(1) H. S. Glick, W. Squire and A. Hertzberg, Fifth Symposium (International) on Combustion, 1954, p. 393

(2) R. A. Strehlow and A. Cohen, J. Chem. Phys. 30, 257 (1959)

(3) G. B. Skinner, J. Chem. Phys. 31, 268 (1959)

(4) T. A. Brabbs, S. A. Zlatarich, and F. E. Belles, J. Chem. Phys. 33, 307 (1960)

(5) G. Rudinger, Wave Diagrams for Nonsteady Flow in Ducts, Van Nostrand, New York (1955)

(6) G. H. Markstein, ARS Journal 29, 588 (1959)

(7) H. S. Glick, Seventh Symposium (International) on Combustion, 1958, p. 98

(8) G. B. Skinner and R. A. Ruehrwein, J. Phys. Chem. 63, 1736 (1959)

(9) V. Kevorkian, C. E. Heath and M. Boudart, J. Phys. Chem. 64, 964 (1960)

(10) L. S. Kassel, J. Am. Chem. Soc. 54, 3949 (1932)

(11) P. S. Shantarovich and B. V. Pavlov, Zhur. Fiz. Khim. 30, 811 (1956)

(12) National Bureau of Standards, Selected Values of Chemical Thermodynamic Properties, Series III (1947)

(13) L. S. Kassel, J. Am. Chem. Soc. 55, 1351 (1933)

(14) E. W. R. Steacie, Atomic and Free Radical Reactions, 2nd ed., Reinhold, New York (1954)

(15) G. B. Skinner and W. E. Ball, J. Phys. Chem. 64, 1025 (1960)

(16) E. W. R. Steacie and G. Shane, Can. J. Res. B18, 203 (1940)

(17) A. M. Brodskii, R. A. Kalinenko, K. P. Lavrovskii and V. B. Titov, Russian J. of Phys. Chem. Nov. 1959, p. 474 (Russian p. 2457)

(18) G. B. Skinner and E. M. Sokoloski, J. Phys. Chem. 64, 1028 (1960)

(19) E. F. Greene, R. L. Taylor and W. L. Patterson, J. Phys. Chem. 62, 238 (1958)

(20) G. B. Skinner and E. M. Sokoloski, J. Phys. Chem. 65, (1961)

(21) A. S. Gordon, S. R. Smith and J. R. McNesby, Seventh Symposium (International) on Combustion, 1958, p. 317

(22) H. G. Davis and K. D. Williamson, Fifth World Petroleum Congress, Section IV, Paper 4, 1959

(23) L. Kuchler and H. Theile, Z. physik. Chem. B42, 359 (1939)

COMPOSITIONS OF C/H SYSTEMS AT HIGH TEMPERATURES. SHOCK TUBE DATA AND A THEORETICAL ANALYSIS.

S. H. Bauer, R. E. Duff[R], M. Cowperthwaite, and W. Tsang
Department of Chemistry, Cornell University, Ithaca, New York
and
[R]University of California, Los Alamos Scientific Laboratory,
Los Alamos, New Mexico

INTRODUCTION

During the past seventy-five years, numerous experiments have been performed on the pyrolysis of hydrocarbons, of both low and high molecular weights. In reports describing these investigations, there are listed a large variety of products so obtained. It was readily demonstrated that the pyrolytic processes are very complex, involving numerous interconversions of the hydrocarbons. The rates of decomposition of the initial material and that of the production of the host of products depended on many factors. Two general types of techniques have been used for the kinetic studies. In the fixed-volume experiments, the material was subjected to modest temperatures for relatively long contact times. Pressure changes were noted, and after quenching the residues were analyzed. Somewhat later, flow techniques were introduced, and the operating temperatures were raised to the neighborhood of 1000°K. with a corresponding decrease in contact time. Along with the inherent analytical difficulties due to the complexity of the reactions, there appeared a disturbing problem. Both in the fixed-volume and the flow through a hot tube experiments, the heterogeneous reactions induced by the heated walls could not be readily separated from the homogeneous reactions which were of primary interest. Also, the gas samples could not be uniformly heated due to limitations on the rate of heat transfer from the walls. It has been generally established that the decomposition is initiated by rupture of carbon-hydrogen and carbon-carbon bonds. The radicals thus produced initiate chains which produce the complex mixture of products. Further details may be found in numerous papers and books[1,2,3].

The chemical properties of the radicals produced in the pyrolytic reactions are not only of direct interest to those concerned with the behavior of organic compounds but also constitute essential information to those who would analyze the course of the hydrocarbon decomposition. During the past twenty years, much effort has been expended in the study of gaseous radicals. Generally, these have been produced by photochemical dissociation of selected gases; their chemical properties have been deduced from the subsequent reaction of the radicals with the ambient gas. These techniques have been extended to cover an appreciable range in radical type, temperature, and medium.[4,5,6,7] Production *via* photochemical processes is often limited by the light intensity available, so that the concentration of radicals generated is quite small. Use of intense photoflashes[8,9] and electrical discharges[10]

permits the production of appreciable concentrations. We thus anticipate extended current activity in the investigation of the chemical properties of radicals. Were this information available now, it would mitigate but not solve the pyrolysis problem, since it is abundantly clear that the pyrolytic processes in hydrocarbons exposed to temperatures of 1000°K. or below are complex because many competing rates are involved.

During the past decade, a new technique has been developed, the utilization of shock tubes for chemical kinetic investigations. The upper temperature range is easily extended to about 5000°K. Shock tube heating has the added attractive features that the gas is homogeneously and rapidly heated to a uniform temperature (in less than a microsecond) and the reactions occur so rapidly that there is no time for confusion by a heterogeneous process which may occur on the walls. During a temperature pulse, the time required to attain a temporary state of equilibrium may be 100 microseconds to several milliseconds. Hence, these kinetic studies require the development of specific analytical methods, which have microsecond resolution. The single-pulse technique[11] avoids the necessity for such rapid and specific analytical procedures. The shocked gases are rapidly quenched after a selected dwell time of (1-5) milliseconds and the residual gases analyzed by conventional techniques. The quench rates obtained, (1-4) x 10^5°K/sec., are barely adequate for terminating those steps in the complex mechanisms which have appreciable activation energies. Atom abstractions, free-radical rearrangements, and recombinations continue. Hence, the interesting product distributions which have been reported must be interpreted with care.[12,13,14,15,16,17,18,19] As an example, one may cite the range of 'first-order' decomposition rate constants reported for the pyrolysis of methane. The early hot tube experiments at around 1000°K. gave an activation energy of 79 kcal.[20]; then in succession, shock tube values (for the temperature range 1200-2100°K.) were reported which ranged from 85 kcal.[14] to 93 kcal.[17] to 101 kcal.[16] There were differences in the magnitudes of the rate constants (factors of 3 to 5), such that were one to draw the best straight line through all the shock tube data the deduced activation energy would be about 104 kcal. It is presumed that the primary step produces CH_3 radicals, and the product distribution following the quench depends on the height and width of the temperature pulse to which the methane was subjected; the amount of acetylene increases with a rise in temperature, the yield of ethylene passes through a maximum, and ethane is found in small amounts only.

The higher hydrocarbons, although studied in many laboratories, have not been as extensively investigated as methane. A shock tube pyrolysis of ethane[18] (1059-1410°K.) indicated a decomposition rate which was first order in the reactant, with an activation energy of 60 kcal. The primary step is presumed to be the fission of the C-C bond to produce two CH_3's. This is followed by a sequence of free-radical reactions. There are a number of serious loopholes in the proposed mechanism, not the least being that the proposed rate constant for the dissociation of ethane is inconsistent with the measured rate constant for the association of two methyl radicals.[21] The products found after the quench were ethylene, acetylene, methane, hydrogen, and some 1,3-butadiene. The pyrolysis of ethylene[19] was similarly investigated; acetylene and 1,3-butadiene were the principal products, the acetylene being formed via a first-order step with an activation

energy of approximately 46 kcal., while the butadiene was generated via a net second-order reaction. The proposed mechanism is that $C_2H_4 \longrightarrow C_2H_4^* \longrightarrow C_2H_2 + H_2$.

The large variety of products and the often conflicting conclusions deduced from different experiments suggest that the reported differences are not due to poor technique; rather, they reflect the sensitivity of these studies to different experimental conditions. Since the pyrolysis reactions follow very complex mechanisms, small differences in experimental parameters selectively favor different controlling steps, and the differences in rates and product distributions are thereby considerably amplified. This point of view has been corroborated by our studies of the C/H system.

In the experiments performed in our laboratory[22], one of the objectives has been the search for conditions under which the pyrolytic process may prove relatively simple. It was presumed that the higher the temperature the simpler the species which must be considered. In our study of the pyrolysis of ethylene over the temperature range 3000-4000°K., we followed spectrophotometrically the changes which occur in the gas. Timewise, the method has adequate resolution, but it is not sufficiently distinctive to permit identification of many of the species which nonetheless are present under these conditions. Principally, we used the characteristic absorption by C_2 as a means of determining its population in the v = 0 vibrational state of the $^3\pi_u$ electronic state. Two postulates were made in setting up this experiment. (a) With regard to translation, rotation, and vibration of all the molecular species involved, equilibrium is rapidly attained in the shock front, in a time small compared to the changes in concentration of C_2, and (b) equilibrium is not attained with regard to the precipitation of carbon even at the end of our observation time (which is of the order of 1 millisec.). The latter may be justified on the basis of data reported by Kistiakowsky and confirmed in other laboratories[23].

The computations described below provide a glimpse of the complex kinetics which may be operative by ascertaining the equilibrium compositions of systems containing carbon and hydrogen which are being approached through the involved kinetic processes. Since the variety of molecular fragments which are conceivable is enormous, the equilibrium composition may serve to point to those species which are present in appreciable concentrations as the dominant ones in propagating chains. One might anticipate that in the long history of the study of hydrocarbons such computations would have been made. Only two attempts have been described recently[24,25], and in neither did the authors consider the full range of species required to provide an adequate analysis. Furthermore, in the more general computations described by Kroepelin and Winter[24], questionable values were used for the thermodynamic functions of those species which were included.

KINETICS OF PRODUCTION OF C_2 FROM ETHYLENE

Shock tube studies reported below were made in a conventionally instrumented shock tube, 1-1/2'' in diameter. The driver length was 35.5'', and the sample section was 129.3''. The driver gas (hydrogen) ranged in pressures from 5 to 15 atm. The driven gas consisted of a mixture of 92% argon and 8% ethylene. The impurity level in the

ethylene as established by mass spectrometric analysis was less than 0.4%. It was particularly desirable in these studies to avoid contamination by oxygen; we estimate that the oxygen impurity was less than 0.1%. Shock speeds of the forward-moving wave were measured by means of narrow platinum film gauges supported on pyrex rods mounted flush with the inside of the shock tube. These speeds ranged from 1.30 to 1.55 mm. per microsecond.

A schematic of the experimental arrangement is shown in Fig. 1. To record the changes in the absorption spectrum of the sample which had been subjected to a shock, two types of configurations were used. In the first, a continuum of wave lengths was generated by discharging a condenser (1.0 μf, 10 KV) through a small quartz tube through which argon was flowing at a pressure of approximately 50 mm. Hg.[26] This produced an intense emission which initially rose sharply and fell to half of the peak intensity in about 10 microseconds. The light which passed through the shocked gas was picked up by a mirror and sent to a grating spectrograph (Fig. 1, right corner) in which a camera was substituted for the photomultiplier tube. By delaying the source trigger pulse, the argon continuum was generated at predetermined times after passage of the reflected shock past the observation ports. The transmission spectra were then photographed (at 16 A° per millimeter dispersion) over the range λ3900 to λ 6000, thus providing a record of the absorption intensity as a function of wave length at specified intervals after initiation of the reaction. The photographs show a general absorption which is fairly uniform over the longer wave lengths but increases rapidly below some critical wave length which depends on the time interval. Upon this background, there was clearly superposed a well developed Swan band system. As far as we can tell, no measurable absorption due to C_3 was discernable at λ 4050, although there are indications from preliminary experiments that a small amount of absorption due to this species did appear during the higher temperature runs.

To study the rate of appearance of C_2, a characteristic source was placed at the position indicated in Fig. 1. The light was split with a half-silvered mirror, so that the JAco monochromator phototube monitored the intensity of a small wave length interval near λ5165, while the small grating spectrograph with the phototube attachment monitored the intensity of the mercury line at λ5460. The characteristic source was generated by a discharge of a 2 μf condenser at about 12 KV through a tube filled with butane, helium, and mercury. The outputs of the two 1P28 photocells were led to a 100 KC electronic switch, so that the relative absorption by the shock sample of the two characteristic emission regions was displayed on one oscilloscope record. The optical window was 0.5 A° wide and set at the band head of the (0,0) band of the $^3\pi_g \longrightarrow {}^3\pi_u$ transition for C_2. The percent absorption recorded in this manner is thus a measure of the population of the C_2 species present in the zero vibrational level of the $^3\pi_u$ state. Because a continuum absorption is superposed on the characteristic absorption, a correction for the former should be made. It was convenient to monitor the background absorption at the λ5460 mercury line. The error introduced by the displacement of 300 A° is of secondary significance, since the essential kinetic data were derived during the induction period, when the background absorption was negligible. Since the populations of the lower states for these lines change with the temperature, a correction was made in reducing the percent absorption to relative concentration.

Fig. 2 is a sketch of a typical reduced oscilloscope trace. The solid line is the intensity recorded at the C_2 band head, and the dashed line is that recorded at the λ5460 mercury line. The characteristic features of these curves which will be subjected to analysis are indicated in the figure. One may add that after the induction time τ the difference between the dashed and solid curve is very nearly constant for periods up to one millisecond, indicating that a steady-state concentration in C_2 was reached at a time prior to the beginning of the continuum absorption at this wave length.

Although an absolute calibration for the concentration of C_2 is not available, since no reliable f value for this band is known, one may nevertheless determine relative rates of production from the initial slope of the oscilloscope trace. To deduce the order of the reaction for the production of C_2, $d/dt\ (\log I_0/I)_i$ was plotted vs. $\log \rho_3$ (the density of the shocked gas in the reflected shock region). The data are consistent with a first-order rate of production of C_2 (with respect to ρ_3) during the early stage of the pyrolysis. It follows

$$\left(\frac{dC_2}{dt}\right)_i = \frac{2.3}{\langle\mu\rangle \ell} \frac{d}{dt} (\log I_0/I)_i = k_1 \rho_3$$

The activation energy for the production rate constant k_1 may be obtained, as in Fig. 3, from a plot of

$$\log \left[\frac{1}{\rho_3} \frac{d}{dt} (\log I_0/I)_i\right] \quad \text{vs.} \quad 1/T.$$

The deduced value for the activation energy is 68 ± 10 kcal., obtained from the best visually estimated straight line through all the points.

From traces such as Fig. 2, it was evident that a steady-state concentration of C_2 was attained after a time varying from 50 to 300 microseconds. The approach to a limiting value (designated D_{ss}) implies that some process removes C_2, eventually at a rate equal to that of production. It was demonstrated that the order of the scavenging reaction is close to unity and that the rate for removal of C_2 proceeds with essentially zero activation energy.

Attention is called to another feature which appears in the oscilloscope traces. In Fig. 2, an induction time (τ) was defined as the first appearance of absorption, monitored at the λ5460 mercury line. This background absorption is presumed to be due to large molecular-weight polyaromatic or conjugated high molecular fragments. We infer from qualitative observations that the length of the induction period decreases with decreasing wave length, and in the ultraviolet the background absorption can be detected even in the incident shock region. With the passage of time, the edge of the intense absorption region shifts toward the red, and the entire level of absorption increases. We estimate from the total absorption curve recorded at 300 microseconds after passage of the shock that the dominant species are polyaromatic nuclei which contain on the average four condensed aromatic rings or their equivalent in the form of a highly conjugated polyene chain. The induction time multiplied by the reflected shock density appears to be constant for shock temperatures above 3000°K.

POSSIBLE MECHANISM FOR THE FORMATION OF C_2

Since the data have been gathered for the reflected shock, the question arises as to whether the incoming shock had processed the material with which the shock tube was filled. Between the passage of the incoming and reflected shocks, no detectable quantity of C_2 was generated, nor was there any absorption apparent in the visible. Nonetheless, the incoming shock had processed the ethylene and had produced some new products, since a small amount of absorption was detected in the limit of our working region in the ultraviolet. For the elapsed time (between the forward and reflected shocks at the position of our observation port) of the order of 300 microseconds, a major portion of the ethylene (perhaps as much as 80%) must have been converted to acetylene plus hydrogen. This estimate is based on the first-order rate constant for the molecular reaction $C_2H_4 \longrightarrow C_2H_4^{\ddagger} \longrightarrow C_2H_2 + H_2$.[19]

$$-\frac{d(C_2H_4)}{dt} = k_2\,(C_2H_4)\ ; \quad \log k_2 = 8.87 - \frac{10{,}150}{T}$$

The resulting mixture is then heated a second time by the reflected shock to produce the following 'initial' composition (indicated by the symbol ρ_3) in the reflected shock front. At $t = 0$,

$$\rho_3 = \frac{np_3}{RT_3}\left[2\,x_{H_2} + 26\,x_{C_2H_2} + 28\,x_{C_2H_4} + 40\,x_{Ar}\right]$$

wherein the mole fraction of the argon (x_{Ar}) by far dominates the magnitude in the bracket.

Since our results indicate a pseudo-unimolecular rate of appearance for C_2 in the $^3\pi_u$ state, one might be tempted to write

$$C_2H_2 + X \rightleftharpoons C_2H_2^{\ddagger} + X$$
$$\qquad\qquad\quad \vdots\!\!\rightarrow C_2 + H_2$$

However, this cannot be the process we observe. In the first place, the activation energy expected for this step is 140 kcal., compared with the experimental value of 70 kcal. Secondly, due to the spin conservation restrictions, the C_2 which is generated in such a step would of necessity be in a $^1\Sigma$ state, since both the reactant (acetylene) and the second product formed (H_2) are in singlet states. It may well be that some acetylene decomposes in this manner to produce C_2 molecules in the ground $^1\Sigma_g^+$ state, but the collision-induced transition to the $^3\pi_u$ state would be expected to require many molecular encounters and take considerable time. One must conclude that C_2 was produced in the $^3\pi$ state via a chain reaction, that the over-all initial production rate was pseudo first order, and that during the subsequent pyrolysis a steady state was reached wherein the C_2 was consumed as rapidly as it was produced. We shall propose a combination of reactions which form a chain for which one would anticipate an activation energy of around 70 kcal.

	ΔH_0°, kcal.
Initiation:	
$C_2H_2 \longrightarrow C_2H_2^* \longrightarrow C_2H + H$	114.0
$2\ C_2H_2 \longrightarrow C_4H_2 + H_2$	2.6
$H_2 + \begin{Bmatrix} H \\ C_2H_2 \end{Bmatrix} \rightleftharpoons 2\ H + \begin{Bmatrix} H \\ C_2H_2 \end{Bmatrix}$	103.3
Enhancement of the carrier:	
$H + C_2H_2 \longrightarrow C_2H + H_2$	10.7
Propagation:	
$C_2H + C_4H_2 \longrightarrow C_4H_3 + C_2$	72.5
$C_4H_3 + C_2H_2 \longrightarrow C_4H_2 + C_2H_3$	21.4
$C_2H_3 + C_2H_2 \longrightarrow C_2H_4 + C_2H$	10.0
$C_2H_4 \longrightarrow C_2H_4^* \longrightarrow C_2H_2 + H_2$	39.8

The controlling activation energy in the propagation sequence should be of the order of 72 kcal., as estimated for ΔH_0°. This mechanism is consistent with the observations made in our laboratory and the data reported in the literature. However, it is evident that there are many other possible chains. Furthermore, there must be many steps involving the transfer of H atoms which require small activation energies; these reach a steady-state condition rapidly and in effect attain a local equilibrium. Before attempting to select between possible alternate mechanisms and an analysis of the details of the termination steps, we consider it worthwhile to answer the fundamental question: what is the composition of the system toward which this kinetic condition is drifting?

ESTIMATION OF MOLECULAR PARAMETERS OF C/H FRAGMENTS:

In our first attempt[22] to compute the equilibrium composition of C/H systems at elevated temperatures, we considered 43 species. This and subsequent analysis showed that particularly for carbon-rich systems the list was incomplete and that a second approximation was necessary. Therefore, it is our objective to estimate the heats of formation and the molecular parameters, such as the moments of inertia and vibrational frequencies, with sufficient certainty to permit the computation of the thermodynamic functions in the ideal gas state as they depend on the temperature, for the large number of low-molecular weight species consisting of carbon and hydrogen. The temperature range we intend to cover is 500-5000°K. The species considered are listed in Table I. The molecular parameters and heats of formation were taken from the literature wherever available. A considerable amount of guessing was needed to complete the list. Estimates were made with the help of analogies, bond dissociation energies derived from kinetic data, and mass spectrometer appearance potentials, with due allowance for resonance stabilization.

In Table I, we have also listed values for the heats of formation. Those shown in parentheses are based directly on experimental measurements, whereas the ones given in square brackets were estimated by means of an empirical theory. Thus, experimental values which link two states (for example, $C_3H_3 \longrightarrow C_3 + 3\ H$) were divided into unit steps ($C_3H_3 \longrightarrow C_3H_2 + H \longrightarrow C_3H + 2\ H \longrightarrow C_3 + 3\ H$) on the basis of empirically assigned parameters. The justification for this procedure and the consequent deduction of structures and vibrational frequencies are given in detail elsewhere. It is essential to recognize that the best guess no matter how tenuous its basis is by far a better approximation than the omission of that species from the computation, since the latter merely implies that an excessively large value has been arbitrarily assigned to its heat of formation. The reasons for the omission of some species (footnote to Table I) will become evident from the inspection of the computations and comparison of estimated heats of formation for these species with the corresponding isomers which were included. Typical results based on computations of the equilibrium compositions for various C/H ratios are presented in the following section. It can be shown that all the isomers of comparable stability must be included in the solutions of the simultaneous equations which give the composition at equilibrium. Indeed, this is even so if the isomers have the same thermodynamic functions; however, under this simplifying condition, a contraction can be made so that the sum of the concentrations of all the closely similar isomers may be obtained by the use of an effective equilibrium constant.

It is well known that equilibrium constants can be calculated for all possible reactions between any given set of species when for each species the moments of inertia, symmetry number, electronic degeneracy, vibrational frequencies, the corresponding degeneracies, and heat of formation at 0°K. are known. It should be realized that the equilibrium constants are more sensitive to changes in some of the molecular parameters than others. Because of their weighting in the partition function, the vibrational frequencies need be known only roughly. It is also fortunate that for these C/H species one has to consider a narrow range of interatomic distances, so that the rotational contributions to the partition functions may be computed with acceptable accuracy. For many molecules, the heats of formation may be estimated at best to within several kilocalories; consequently, this parameter exercises a maximum influence on the computations. However, for the high molecular-weight species containing more than two hydrogen atoms, it is not so sensitive a variable, because these fragments will be present in very small amounts. Changes even in an order of magnitude in their concentrations will have a negligible effect on the equilibrium amounts of the prevalent species.

In estimating the heats of formation, we had to postulate reasonable molecular structures and assign to them electronic configurations. Full use was made of experimental values to provide empirical bond dissociation energies and correction factors ascribed to changes in the basic configurations due to hybridization, delocalization, and other nonbonded interactions. This procedure led to a self-consistent set of values for the heats of formation, the interatomic distances, and the fundamental vibrational frequencies. To check this procedure in a number of cases, we computed the enthalpy changes to be expected for specified dissociations and compared them with experimentally available enthalpy increments for the corresponding steps. For some molecular fragments, the heats of formation were estimated following independent paths and checked against each other.

An illustration of the procedures evolved for estimating heats of formation is the set of values deduced for crucial parameters in the C_3 sequence. The changes in electron configurations associated with the successive removal of hydrogen atoms from propene to generate C_3 are indicated in Fig. 4. Experimental values are available for

$$D(H_2C{=}C(H)CH_2{-}H) \approx (76\text{-}79) \text{ kcal.}$$

$$D(H_2C{=}C{=}C(H){-}H) = 81.2 \text{ kcal.}$$

$$D(HC{\equiv}C{-}CH_2{-}H) = 82.8 \text{ kcal.}$$

Consider the first dissociation shown in Fig. 4. The observed value (78 kcal.) may be expressed as the sum $(98 + a - \gamma)$, where γ = 23.1 kcal. denotes the energy gained by the nonbonded interactions present in the $H_2C\text{-}CH\text{-}CH_2$ radical. To remove the second hydrogen atom, one must expend 104 kcal. (ethylenic C-H) and γ kcal. (stabilization energy) but regains α kcal., which leads to a BDE of 65.3 kcal. This compares favorably with 64.4 kcal. deduced by taking direct differences between experimental quantities. Similar arguments for the production of the $CH_2\text{-}C{\equiv}CH$ radical from methyl acetylene and allene lead to ε = 20.5 kcal. and δ = 22.8 kcal., respectively. These and other similarly deduced parameters were used to evaluate BDE's for analogous steps in the higher C_n sequences.

As a gauge of the reliability of this semi-empirical method, consider the reaction

$$Me(H)C{=}C(H)Me \longrightarrow Me(H)C{=}C{=}CH_2 + H_2$$

The estimated value for its ΔH°_0 is 143.8 kcal., compared with the experimental value of 143.0 kcal. For the reaction

$$Me(H)C{=}C{=}CH_2 \longrightarrow H_2C{=}CH{-}C{\equiv}CH + H_2$$

the estimated ΔH°_0 is 135.6 kcal., while the experimental value is 136.5 kcal. The self-consistency of the method may be judged by comparing estimates of the heats of formation of radicals each generated via several independent paths. Thus, for $H_2\dot{C}\text{-}CH{=}C{=}CH_2$, $(\Delta H^\circ_{0f})_{est}$ = 66.8, 67.7, and 67.7 kcal; for $H_2C{=}C{=}C\dot{H}$, $(\Delta H^\circ_{0f})_{est}$ = 71.7, 70.8, 70.8, 71.7 kcal; for $H_2C{=}C{-}C\dot{{\equiv}}H$, $(\Delta H^\circ_{0f})_{est}$ = 103.9 and 101.1 kcal. Further examples are illustrated in Table II; the processes correspond to the steps illustrated in Fig. 5.

The compilation of bond lengths by Costain and Stoicheff[27] for many C/H compounds shows that the C-C and C-H bond lengths for a given bond environment are remarkably constant in different molecules.

Since we have postulated the electronic structures of the unknown species, justifiable estimates of bond lengths and bond angles can be made by comparisons and interpolation with the known bond types listed by these authors.

Although it is well appreciated that in each normal mode all the atoms participate, the (3n-6) unknown frequencies may be assigned to a sufficient accuracy by subdividing the vibrations into classes associated primarily with bond stretching, bond bending, and skeletal motions. Comparison of each vibration with a similar type in molecules whose frequencies are known led to reasonable frequencies. We often assumed that many of the frequencies of a radical produced by the removal of a hydrogen atom will be those of the parent molecule minus the frequencies associated with the C-H bond broken, namely one C-H stretching and two C-H bending frequencies. The correlation of the frequencies of a radical with those of its parent requires consideration of changes in some force constants and in the reduced masses. The hydrogen atom is so light that for most of the compounds in Table I only changes in carbon atom hybridization appreciably affect the molecular frequencies due to corresponding changes in force constants. The deduced frequency change for C-C bonds follows from the assumed changes in hybridization. Skeletal bending frequencies are the most difficult to predict, because they correspond to motions involving the entire molecule. However, these are usually of the order of 300 cm^{-1}, and errors in the partition functions due to incorrect estimates can be neglected because of the high temperatures involved in the computation of equilibrium compositions.

Less error is expected in the estimation of C-H frequencies. The hydrogen atoms may be regarded as oscillating against an infinitely large mass; the vibrational frequency depends practically only on the force constant for the C-H bond and will be approximately constant for species with the carbon atom in a given state of hybridization.

The free energies, as dependent on the temperature, were taken from the literature wherever they were available. This was the case for the stable species in the low-temperature regime (up to 1500°K.). The numerical values as given in the NBS tables were plotted on a large scale and twelve to fifteen values read between the temperature range 500-1500°K. They were then fitted by least squares to the polynomial form

$$\frac{F_T^\circ - H_0^\circ}{RT} = a\,(1 - \ell n\, T) - bT - c/2\, T^2 - d/3\, T^3 - e/4\, T^4 - k$$

$$\frac{H_T^\circ - H_0^\circ}{RT} = a + bT + cT^2 + dT^3 + eT^4$$

Since the same coefficients appear in the expression for the enthalpy and free energy, the magnitude of k may be computed for each temperature; the value used was the average over the equally spaced temperature points. To obtain the corresponding fit coefficients for the stable species over the upper temperature, the usual ideal gas, rigid rotor, and simple harmonic oscillator approximations were made. The thermodynamic functions were computed following an IBM 704 code written by

L. R. Sitney[28]. The same procedure was followed for the unstable species; the computed functions were again least-square fitted to the indicated polynomial form. We thus have two sets of thermodynamic fit coefficients suitable for the two ranges indicated. Details of the computations (the basis for decisions as to the nature of the ground electronic states, the presence and location of low-lying electronic states, corrections for internal rotation, etc.) will be presented in another publication.

THE EQUILIBRIUM COMPOSITIONS

In the computation of equilibrium compositions, we considered two cases. The first and most extensive set of graphs was obtained under the assumption that at the specified pressure and temperature equilibrium was attained for all the species listed, except with respect to the presence of solid carbon. The second set of computations will be performed under the assumption of complete equilibrium including the presence of solid carbon. Although the first case seems artificial, it is significant kinetically. Such a restriction correctly describes a situation in many shock tube and detonation experiments[29] (carbon-rich mixtures) during the intermediate stages of reaction. Since the precipitation of graphite (in highly irregular crystalline form) must await the prior formation of nuclei, the gaseous components attain a pseudo-equilibrium which lasts sometimes for hundreds of microseconds before particles appear. The following ranges in parameters were covered: C/H = 1/10, 1/4, 1/2, 1/1, 1/$\frac{1}{2}$, and 1/$\frac{1}{4}$; p = 10, 1, and 0.1 atm; T = 500-5000°K. in two intervals, 500-1600°K. and 1500-5000°K.

A question remains as to where one may properly terminate the list of species to be included in the equilibrium computation. Evidently, the answer is based on the rate of convergence of the concentrations to a limiting value in the sequence of successive approximations in which more and more species are added. We have found this convergence depends sensitively on the C/H ratio and on the temperature. A comparison of the concentrations deduced in our first computation with the present values indicates that values for the major species for the low C/H compositions were converging rapidly, but that was not the case for the high C/H compositions at the low temperatures.

In performing the computations described below, it is essential that all the isomers be included. Only the isomers which have heats of formation considerably larger than those covered by the computations or such species the dissociations of which are greatly favored by a large entropy increase at the cost of a small enthalpy increment may be omitted.

For a sequence of temperatures and a specified total pressure, the equilibrium (no solid carbon allowed) partial pressures were computed by an IBM 704 program set up by W. Fickett and modified by one of the authors (R.E.D.). Typical graphs are shown in Figs. 6-13; only the upper 8 decades of the partial pressures have been plotted. The 58 species (for which the thermodynamic functions were inserted in the simultaneous equations) were divided into groups on the basis of their hydrogen content. A complete set of such graphs is shown for C/H = 1/2,

but a few selected curves for other C/H ratios were included to demonstrate the effect of change in that parameter on the partial pressures. Variation of the total pressure slightly modified the partial pressures, as expected from 'mass law' considerations.

A general inspection of the curves plotted leads to two important conclusions:

(a) For temperatures above 1500°K., numerous molecular fragments attain significant concentrations. Insufficient attention has been given to the presence of the C_nH and C_nH_2 fragments in the pyrolysis of hydrocarbons. The fact that these and others appear prominently in our plots underlines the importance of including as complete a set as is possible in the computations of the equilibrium partial pressures.

(b) For C_nH_p, those species which have the same p's show on the whole similar trends as a function of temperature. Consider the general equilibrium.

$$n\,C_{(g)} + p\,H_{(g)} \rightleftharpoons C_nH_{p(g)}$$

$$K_{eq(T)} = \frac{(C_nH_{p(g)})}{(C_g)^n\,(H_g)^p} = e^{-\Delta F^\circ_T/RT}$$

$$\ell n\,(C_nH_{p(g)}) = n\,\ell n\,(C_g) + p\,\ell n\,(H_g) - \Delta F^\circ_T/RT$$

Define $G_i \equiv \left(\frac{F^\circ_T - H^\circ_0}{RT}\right)_i + \left(\frac{\Delta H^\circ_{0f}}{RT}\right)_i$; this is known for all the species considered.

$$\ell n\,(C_nH_{p(g)}) = n\,[\ell n(C_g) + G(C_g)] + p\,[\ell n(H_g) + G(H_g)] - G(C_nH_p)$$

For any specified C/H ratio, pressure and temperature, the partial pressure at equilibrium of monatomic carbon gas and monatomic hydrogen is fixed. For any species, $\ell n\,(C_nH_p)$ is linearly dependent on n and p and on the magnitude of the $G(C_nH_p)$ function which expresses the thermodynamic potential of that species at that particular temperature. The observation that the partial pressures of C_nH_p species for equal p have roughly parallel temperature dependences suggests that the $G(C_nH_p)$ function is sensitive to the magnitude of p but varies gradually and regularly with n. Trends of composition with C/H ratio and temperature are given below.

(c) The C_n sequence: as T increases above 2000°K., the concentrations of all C_n's increase. At the highest temperatures, the relative pressures decrease with n. Between 2000-2500°K., C_3 dominates. Below 3500°K., $(C_5) > (C_4)$, $(C_7) > (C_6)$. Per mole of carbon, the sum of the concentrations of the C_n species increases as the C/H ratio increases, as expected.

(d) The C_nH system: the concentration of CH is unexpectedly small. Up to 3000-4000°K. (depending on the C/H ratio), the dominant species are C_3H and C_4H; at higher temperatures, C_2H dominates. Note also that $C_6H > C_5H$, $C_9H > C_8H$. The absolute concentrations are very sensitive to the C/H ratio.

(e) The C_nH_2 system: the curves recorded for C/H = 1/2 are typical. The concentration of these species goes through a maximum between 1500-2000°K. As is well known from the experiments mentioned above, the partial pressure of acetylene rises rapidly as T approaches 1000°K. At higher temperatures, its partial pressure declines gently and is overtaken by CH_2 only for T > 4000°K. Next in prominence is diacetylene.

(f) The C_nH_3 and C_nH_5 systems: these species go through a maximum at a temperature which depends on the C/H ratio, in the vicinity of 1500°K. As the proportion of hydrogen increases, the concentration of species with lower n increases. C_3H_5 is most prominent except for systems which have a small amount of hydrogen. This is a consequence of the symmetry in electron distribution which the molecule possesses; resonance provides it with a high relative stability. Above 2500-3000°K., CH_3 dominates in concentration; it is followed closely by C_2H_3 and C_3H_3.

(g) The C_nH_4 system: on this graph, the concentrations of molecular and atomic hydrogen have also been included. These behave as expected for the equilibrium $H_2 \rightleftharpoons 2\ H$. The hydrocarbons which are usually thought of as being stable rapidly decline in abundance for temperatures above 1500°K. and attain partial pressures below 10^{-3} as T approaches 2000°K; their relative concentrations decrease in magnitude with increasing n. In general, for the stable species, the sum of their concentrations increases as the C/H ratio increases.

(h) The relative concentrations of C_nH_p with p = 6, 8, and 10 follow no obvious trend except that benzene is particularly prominent up to about 1500°K. As expected, its concentration is very high for high C/H. With regard to the relative concentrations of isomers, note that for the C_4H_4 species vinyl acetylene reaches higher concentrations than does butatriene, even though the heat of formation of the former is approximately 4 kcal. higher than the latter. Evidently, the additional flexibility of the vinyl acetylene (internal rotation, etc.) favors this molecule entropywise. For the C_6H_4 species, the same argument holds even though the chain isomers have heats of formation which are 8 kcal. higher than that of benzyne. The concentration of the latter is much smaller throughout the temperature range because of its stiffness and, therefore, lower entropy. In contrast, cyclopropane is always lower in concentration than the propene for two reasons; it has a higher heat of formation and a lower entropy.

(i) The temperature between 1500 and 2500°K. provides an interesting region for the use of single-pulse shock tubes for preparative purposes. The dominant species depends on the C/H ratio. If one starts with naturally occurring hydrocarbons which are rich in hydrogen, the first pass will lead to products which are carbon rich (C_2H_2, C_6H_6, etc.) and hydrogen. A second pass of the resulting hydrocarbons will lead to a further carbon enrichment (C_4H_2, C_8H_2, etc.). Of course, this hinges on the possibility of finding conditions which permit the attainment of this pseudo-equilibrium and quenching without excessive precipitation of carbon.

These computations need extension and further analysis. However, aside from the interesting new species which have to be considered in chain mechanisms, we have established a basis for selecting those species which are present in appreciable concentrations for the generation

of chains. Also, it is evident that the presence of many C/H fragments at equilibrium accounts for the product distributions observed for the quenched mixtures. One should not overlook the relative thermodynamic stabilities of the species and focus only on the kinetic routes by which conceivably they are generated. The emphasis should be on those elementary kinetic steps, which because of their low activation energies attain local equilibrium rapidly.

ACKNOWLEDGMENTS:

This work was supported in part by the Air Force (ARDC) under Contract AF33(616)-6694 and by the U. S. Atomic Energy Commission.

REFERENCES

1. Ed., B. T. Brooks, et al, The Chemistry of Petroleum Hydrocarbons, Vol. II, Reinhold Publ. Co., New York, N. Y. (1955), refer to Chapter 22, E. W. R. Steacie and S. Bywater, and Chapter 25, L. Kramer and J. Happel.
2. A. G. Gaydon and H. G. Wolfhard, Flames, Their Structures, Radiations, and Temperatures, Chapman and Hall, Ltd., London (1953).
3. H. Tropsch and G. Egloff, Ind. Eng. Chem., 27, 1063 (1935).
4. E. W. R. Steacie, Atomic and Free Radical Reactions, 2 vols., Reinhold Publ. Co., New York, N. Y. (1954).
5. A. F. Trotman-Dickenson, Gas Kinetics, Academic Press, Inc., New York, N. Y. (1955).
6. K. O. Kutschke and E. W. R. Steacie, Vistas in Free Radical Chemistry, Pergamon Press, London (1959).
7. Selections from chapters on Kinetics of Homogeneous Reactions, Annual Reviews of Physical Chemistry, Vols. I-X, Annual Reviews, Inc., Palo Alto (1950-59).
8. R. G. W. Norrish and B. A. Thrush, Quart. Rev., X, 149 (1956).
9. S. Claesson and L. Lindquist, Arkiv Kemi, 11, 535, and 12, 1 (1957).
10. N. H. Kiess and H. P. Broida, Seventh Symposium on Combustion, Butterworth Sci. Publ., London (1959), p. 207.
11. H. S. Glick, W. Squire, and A. Hertzberg, Fifth Symposium on Combustion, Reinhold Publ. Co., New York, N. Y. (1955), p. 393.
13. W. J. Hooker, Seventh Symposium on Combustion, loc cit, p. 949.
12. E. F. Greene, R. L. Taylor, and W. L. Patterson, Jr., J. Phys. Chem., 62, 238 (1958).
14. H. S. Glick, Seventh Symposium on Combustion, loc cit, p. 98.
15. G. B. Kistiakowsky, private communication.
16. G. B. Skinner and R. A. Ruehrwein, J. Phys. Chem., 63, 1736 (1959).
17. V. Kevorkian, C. E. Heath, and M. Boudart, ibid, 64, 695 (1960).
18. G. B. Skinner and W. E. Ball, ibid, 64, 1025 (1960).
19. G. B. Skinner and E. M. Sokoloski, ibid, 64, 1028 (1960).
20. L. S. Kassel, J. Am. Chem. Soc., 54, 3949 (1932).
21. A. Shepp, J. Chem. Phys., 24, 939 (1956).
22. S. H. Bauer, et al, WADD Tech. Report 60-107 (April, 1960).
23. G. B. Kistiakowsky and W. G. Zinman, J. Chem. Phys., 23, 1889 (1955).
24. Ed., Y. S. Touloukian, Thermodynamic and Transport Properties of Gases, Liquids, and Solids, McGraw-Hill, New York, N. Y. (1959), article by H. Kroepelin and E. Winter, p. 438.

25. M. N. Plooster and T. R. Reed, J. Chem. Phys., 31, 66 (1959).
26. D. A. Ramsay, Annals N. Y. Acad. Sci., 67, 485 (1957); J. H. Collomon and D. A. Ramsay, Can. J. Phys., 35, 129 (1957).
27. C. C. Costain and B. P. Stoicheff, J. Chem. Phys., 30, 777 (1959).
28. L. R. Sitney, PUBCO-I for Computing the Ideal Thermodynamic Functions of a Polyatomic Gas Molecule, LA-2278, issued May 8, 1959, by LASL.

FOOTNOTES TO TABLE I

[a] A few species were not considered in detail: C_2H_5, C_3H_7, C_4H_7, C_4H_9, $H_3C\text{-}C{\equiv}C$, $HC{=}CH\text{-}CH_2$, $H_2C{=}CH\text{-}C{\equiv}C$, $H_2C\text{-}HC{=}CH\text{-}CH_2$, and a variety of cyclic structures in which there is incorporated large amounts of bond-angle strain energy. Rough estimates indicated that either the heats of formation of these species were considerably larger than those of their isomers which were included or that their entropies were considerably smaller than that of the products into which they could readily dissociate.

[b] Two isomers are possible,

(H-C-C-C-H and 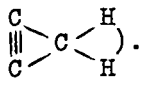).

The estimate cited was made for the linear species, but a rough analysis shows that the heat of formation of the cyclic compound will be rather close to that of the chain.

[c] Two isomers are possible,

(H-C-C-C-C-C-H and 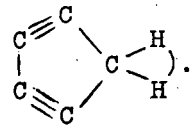).

The estimate cited was made for the linear species, but a rough analysis shows that the heat of formation of the cyclic compound will be rather close to that of the chain.

TABLE I

C/H Species Included in Revised Computation and Their Heats of Formation (ΔH°_{0f})[a]

H (51.62)	C_2 (198)	C_3 (189)	C_4 (238.5)	C_5 (237)	C_6 [287]	
H_2	C_2H [116.7]	C_3H [127.1]	C_4H [154]	C_5H [185.4]	C_6H [211.3]	
	C_2H_2 (54.33)	[b]C_3H_2 [106.7]	C_4H_2 (111.3)	[c]C_5H_2 [165]	C_6H_2 [168.6]	
$C_{graphite}$	C_2H_3 (66.9)	$H_2C-C\equiv CH$ (77.3)	$H_2C=C-C\equiv CH$ [102.5]	C_5H_3 [135.6]	C_6H_3 [158.3]	
$C_{(g)}$ (169.58)						
CH [140.4]	C_2H_4 (14.52)	$H_3C-C\equiv CH$ (46.017)	$H_2C=C=C=CH_2$ [71.3]	$HC\equiv C-C\equiv C-CH_3$ (103.6)	$H_2C=(C)_3<^{H}_{C\equiv CH}$ [132]	
CH_2 [66.8]		$H_2C=C=CH_2$ (47.70)	$H_2C=CH-C\equiv CH$ (75.3)	$H_2C=C=CH-C\equiv CH$ [108.3]	$H_2C=(C)_4=CH_2$ [132.8]	
CH_3 (33.4)				$H_2C=C=C=C=CH_2$ [102.3]	 [124]	
CH_4 (-15.99)		$H_2C-CH-CH_2$ [35]	$H_3C-C\equiv C-CH_2$ [67.8]			
			$H_2C-CH=C=CH_2$ [67.1]			
	C_2H_6 (-16.517)	$H_3C-CH=CH_2$ (8.468)	$H_2C=CH-CH=CH_2$ (29.78)	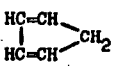 (25.2)	$(CH)_6$ (24.0)	
		$(CH_2)_3$ (17.8)	$(H_3C-C\equiv)_2$ (38.09)			
			$H_3C-CH=C=CH_2$ (42.00)			
			$H_5C_2-C\equiv CH$ (42.74)			
		C_3H_8 (-19.482)	$(CH_2)_4$ (12.5)			
			C_4H_8 (isomers) {(3.48) (0.98) (4.96) (2.24)			
			C_4H_{10} (isomers) (-23.67) (-25.30)			

( ) values deduced in a rather direct manner from experiment

[ ] estimated by analogy, etc.

C_7 [287]	C_8 [339]	C_9 [334]	C_{10} [393]
C_7H [240]	C_8H [267]	C_9H [291]	$C_{10}H$ [324]
C_7H_2 [220]	C_8H_2 [225]	C_9H_2 [271]	$C_{10}H_2$ [282]

TABLE II

Compound	Process	ΔH°_{Of} (kcal.)
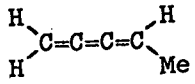	1 + 2	65.7
	8 + 2	66.6
	Heat of hydrogenation	66.5
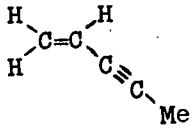	1 + 5	65.5
	8 + 5	66.4
	Heat of hydrogenation	66.4
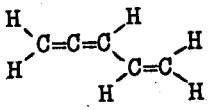	11 + 12	63.2
	11a + 12a	63.3
	Heat of hydrogenation	62.5
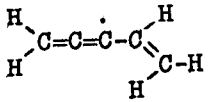	1 + 2 + 3a	96.5
	8 + 2 + 3a	97.4
	1 + 5 + 9	96.7
	11 + 12 + 13	98.5

Compound	Process	ΔH°_{Of} (kcal.)
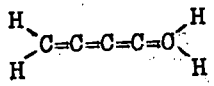	1 + 2 + 3 + 4	104.1
	1 + 2 + 3a + 4a	100.7
	8 + 2 + 3 + 4	105.0
	8 + 2 + 3a + 4a	101.6
	8 + 5 + 6 + 4	101.8
	8 + 5 + 9 + 10	101.8
	1 + 5 + 9 + 10	100.9
	11 + 12 + 13 + 10	102.7
	11 + 12 + 14 + 15	101.8
MeC≡C-C≡CH	1 + 2 + 3 + 7	104.8
	1 + 5 + 6 + 7	101.6
	8 + 2 + 3 + 7	105.7
	8 + 5 + 6 + 7	102.5
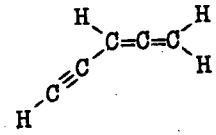	11 + 12 + 14 + 16	108.7
	Heat of hydrogenation	107.9

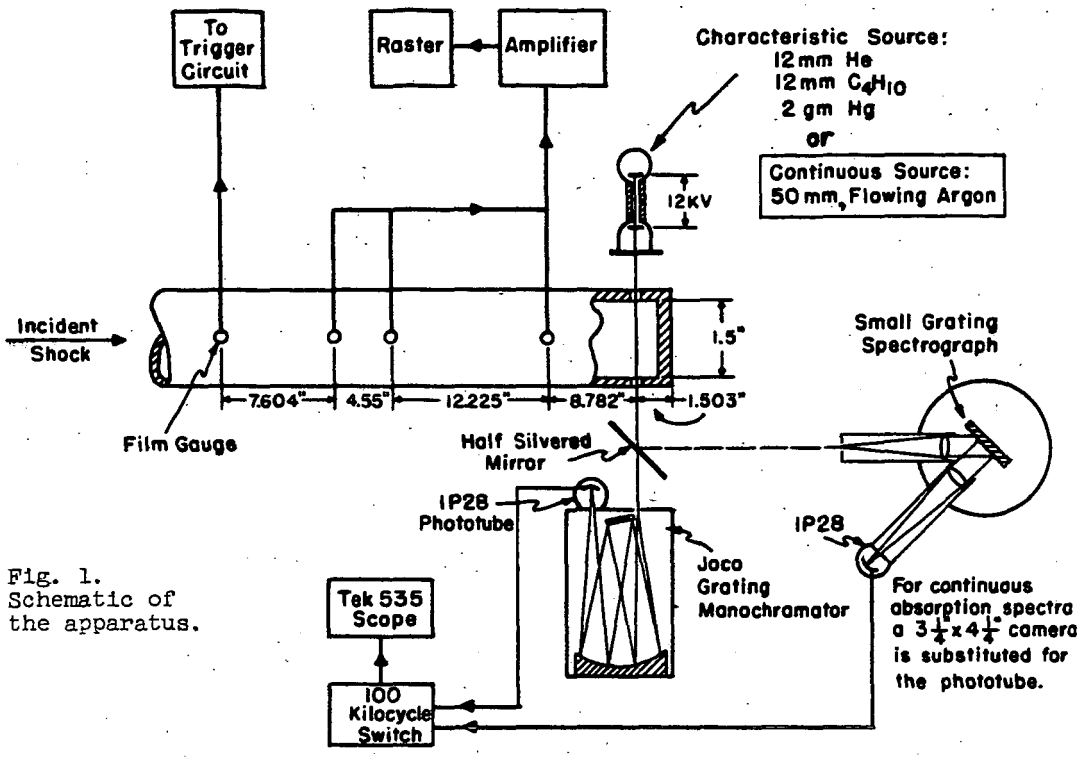

Fig. 1.
Schematic of the apparatus.

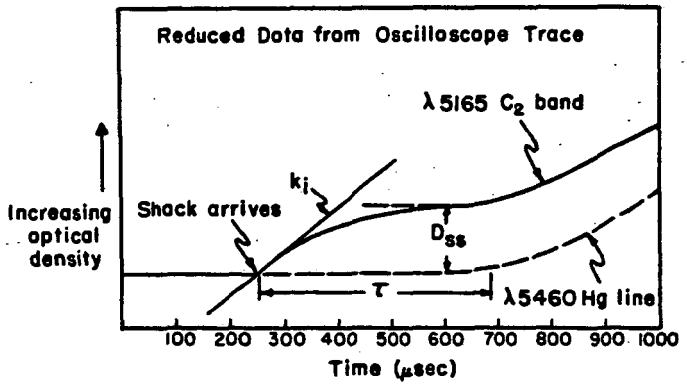

τ = Induction period
D_{ss} = Steady state C_2 conc.
k_i = Initial rate constant for formation of C_2

Fig. 2.

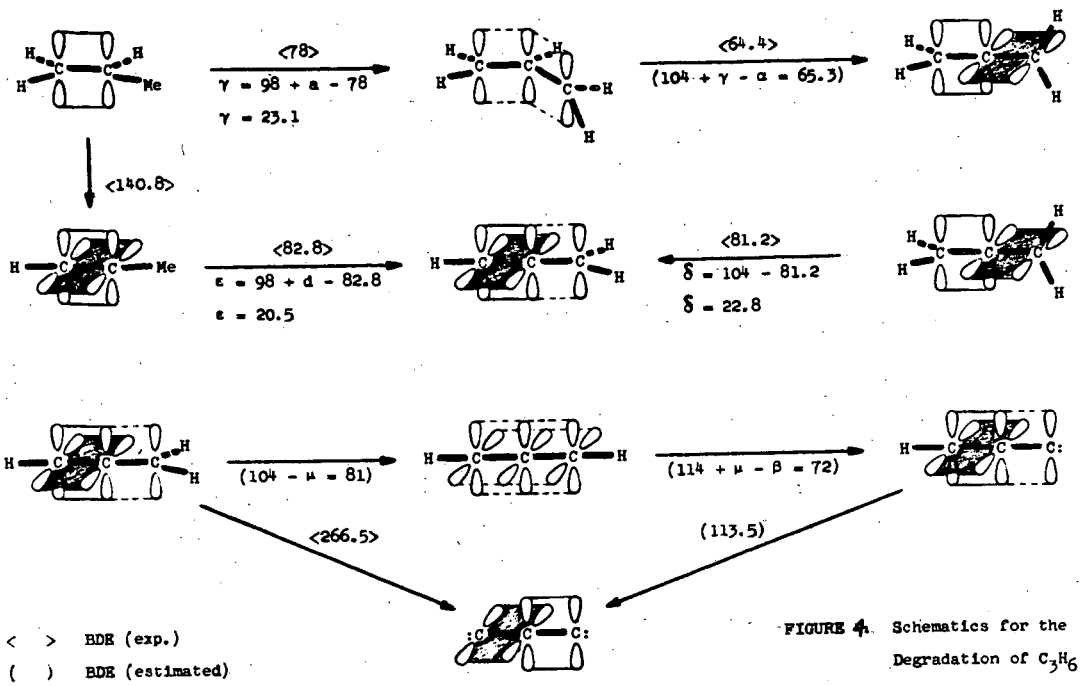

FIGURE 4. Schematics for the Degradation of C_3H_6

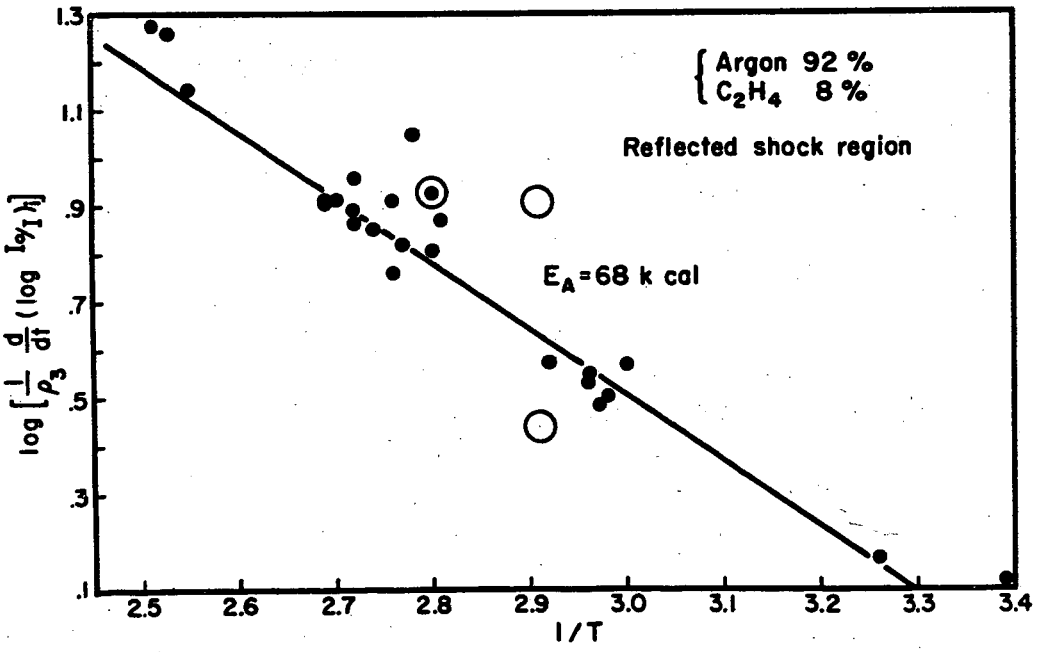

Fig. 3. Activation Energy for the Production of C_2

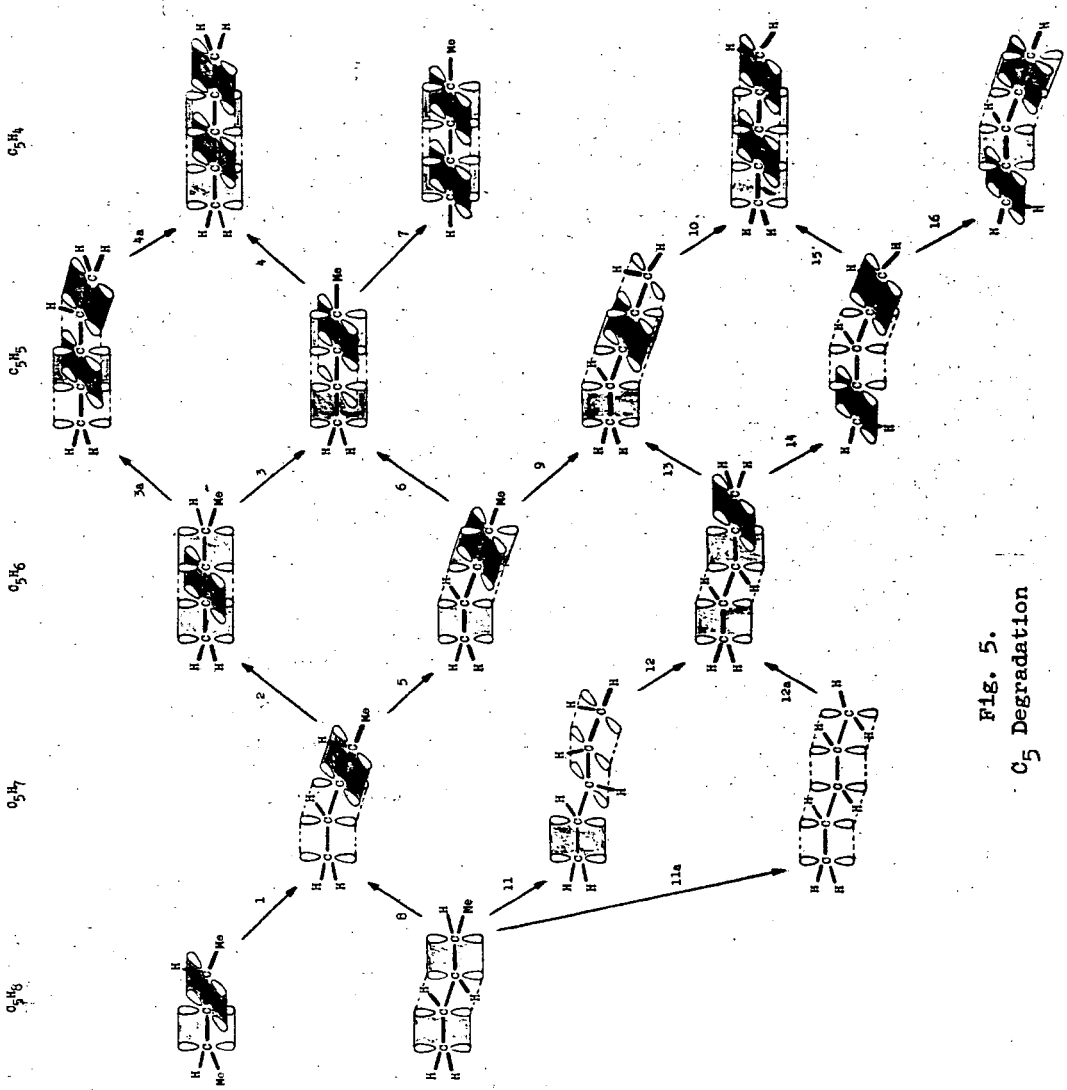

Fig. 5.
C_5 Degradation

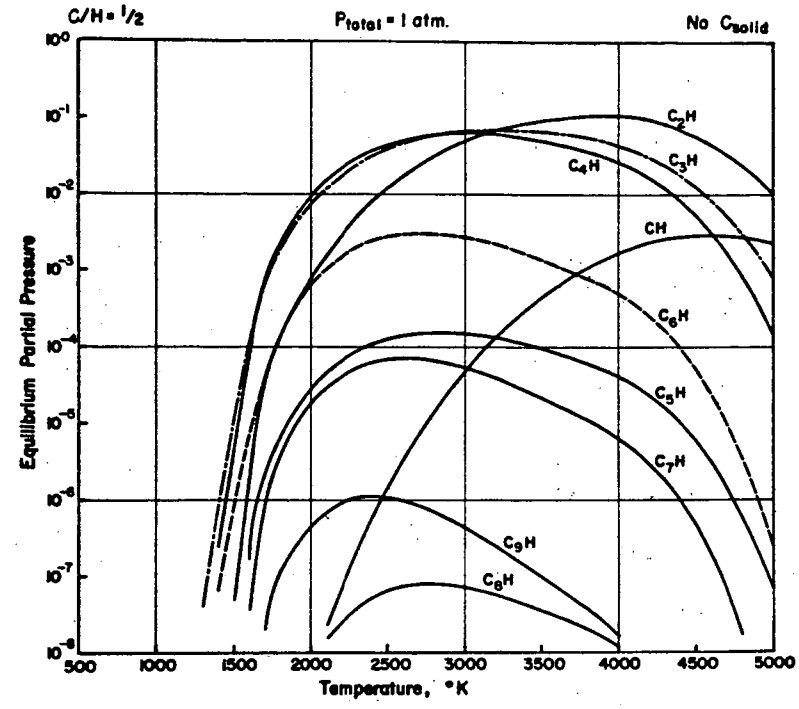
C/H = 1/2
Ptotal = 1 atm.
No Csolid
Equilibrium Partial Pressure
Temperature, °K
C2H
C3H
C4H
CH
C6H
C5H
C7H
C9H
C8H

Fig. 6.

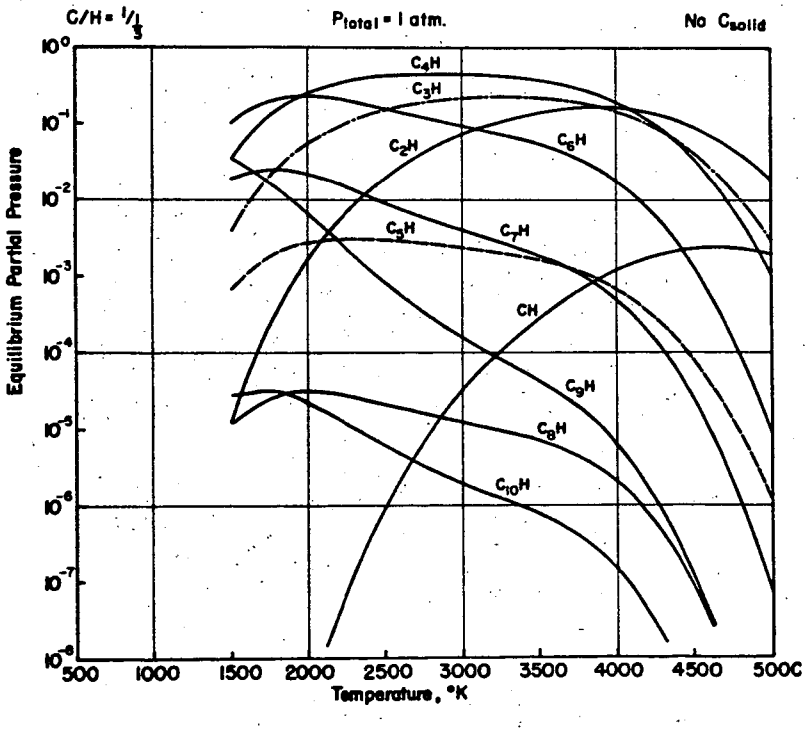
C/H = 1/3
Ptotal = 1 atm.
No Csolid
Equilibrium Partial Pressure
Temperature, °K
C4H
C3H
C2H
C5H
C6H
C7H
CH
C9H
C8H
C10H

Fig.7.

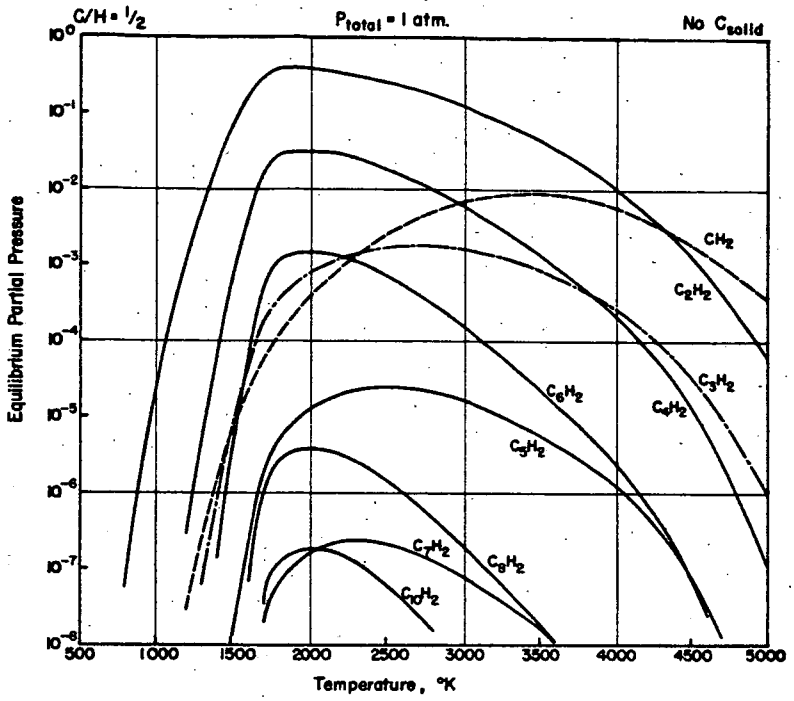
C/H = 1/2
P total = 1 atm.
No C solid
Equilibrium Partial Pressure
Temperature, °K
CH2
C2H2
C3H2
C4H2
C6H2
C5H2
C7H2
C8H2
C10H2

Fig. 8.

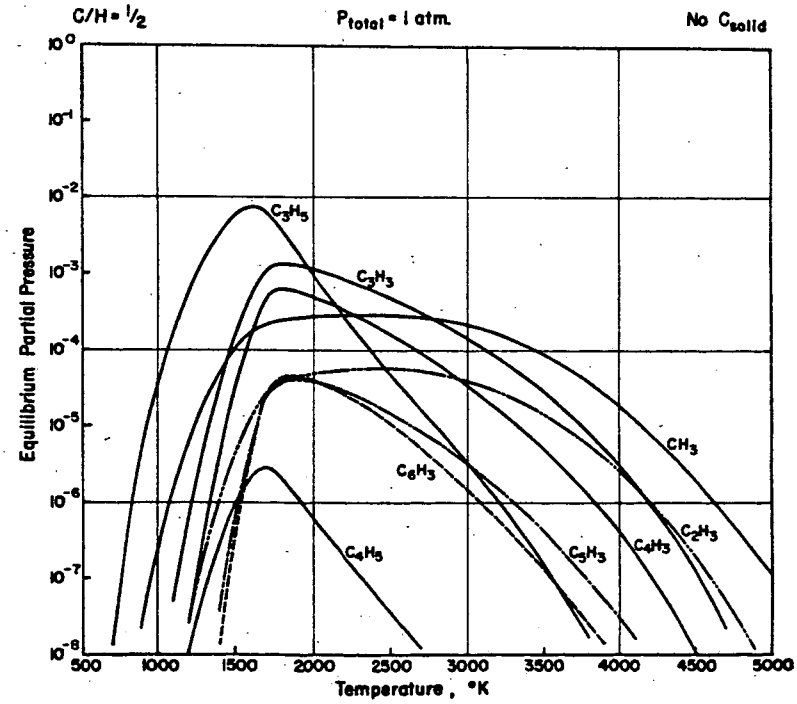
C/H = 1/2
P total = 1 atm.
No C solid
Equilibrium Partial Pressure
Temperature, °K
C3H5
C3H3
CH3
C6H3
C4H5
C5H3
C4H3
C2H3

Fig. 9.

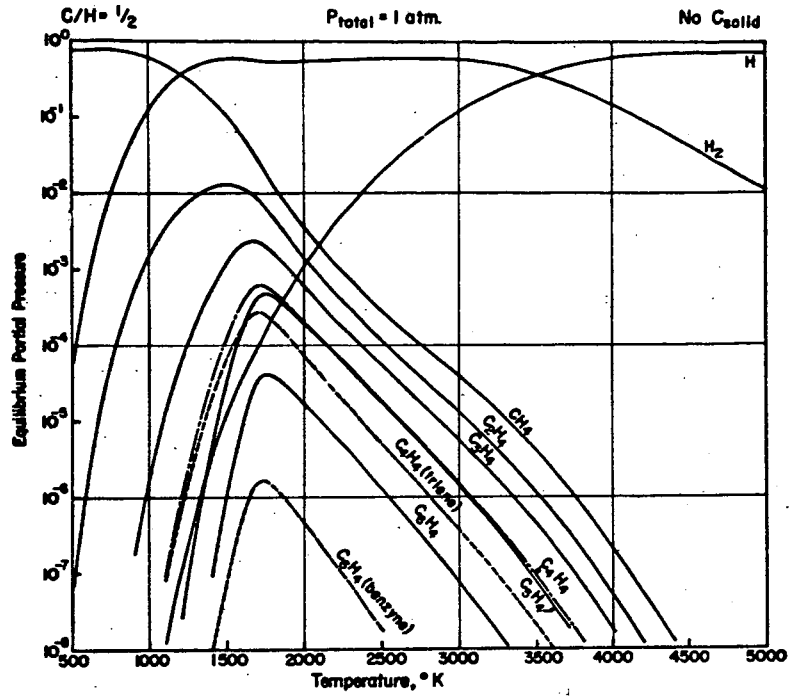
C/H = 1/2
P total = 1 atm.
No C solid
H
H2
CH4
C2H2
C2H4
C4H4 (triacetylene)
C3H4
C6H6 (benzene)
C4H2
C5H12
Equilibrium Partial Pressure
Temperature, °K

Fig. 10.

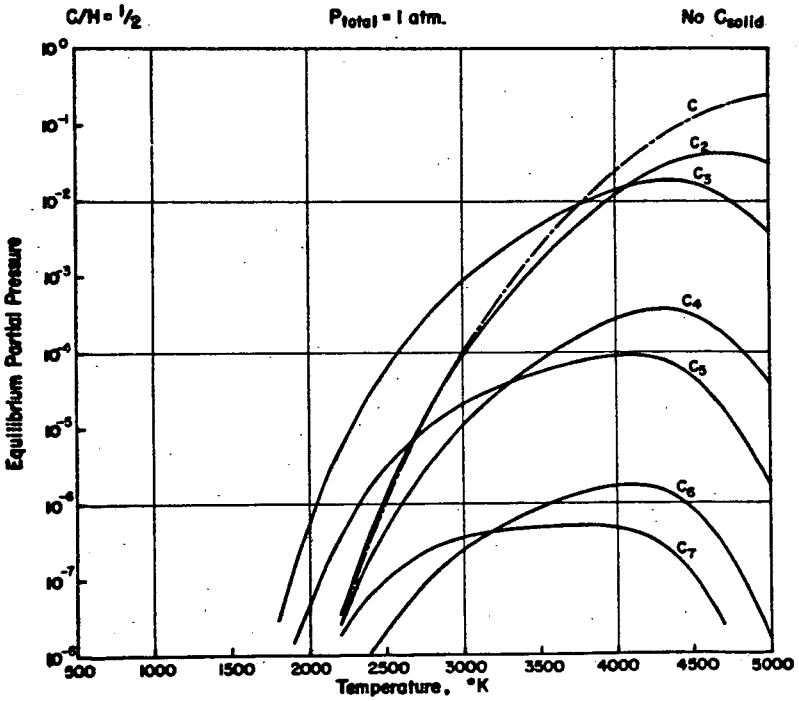
C/H = 1/2
P total = 1 atm.
No C solid
C
C2
C3
C4
C5
C6
C7
Equilibrium Partial Pressure
Temperature, °K

Fig. 11.

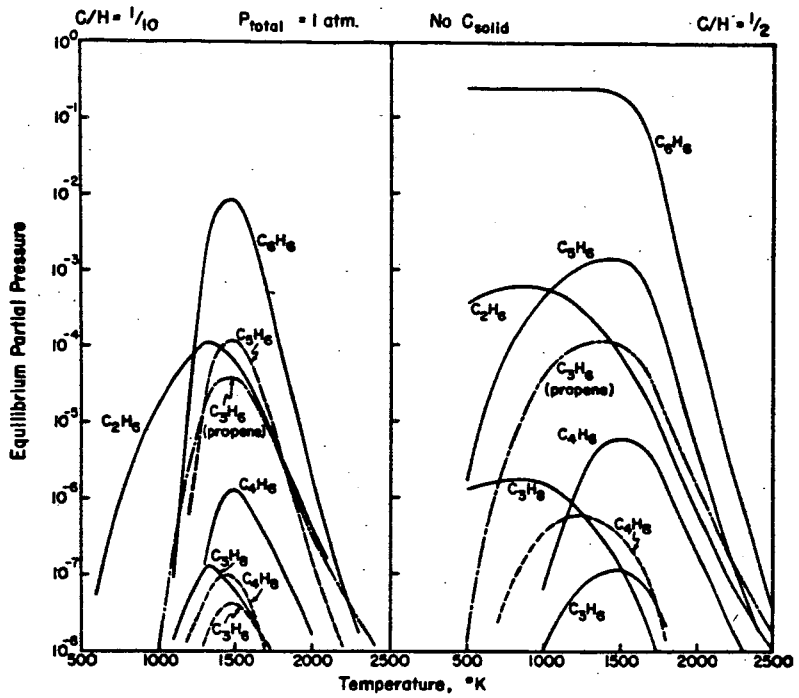
C/H = 1/10
P total = 1 atm.
No C solid
C/H = 1/2
Equilibrium Partial Pressure
Temperature, °K
C6H6
C3H6
C2H6
C3H6 (propene)
C4H6
C5H6
C3H6

Fig. 12.

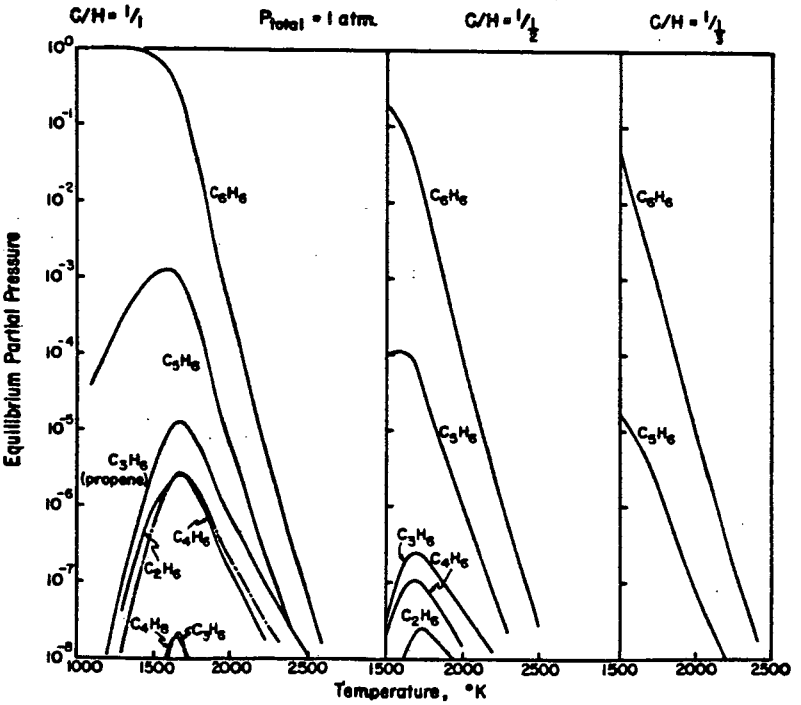
C/H = 1/1
P total = 1 atm.
C/H = 1/2
C/H = 1/3
Equilibrium Partial Pressure
Temperature, °K
C6H6
C3H6
C3H6 (propene)
C4H6
C2H6
C5H6
C3H6

Fig. 13.

THE HYDROGEN-BROMINE REACTION

Doyle Britton and Roger M. Cole

School of Chemistry, University of Minnesota
Minneapolis, Minnesota

INTRODUCTION

The reaction between H_2 and Br_2 is the classic example of a chain reaction. It has been studied here by shock wave techniques both to extend the temperature range over which the rate constants have been determined experimentally and to further test the shock tube method. This reaction has been well reviewed, for example by Pease[1] and by Campbell and Fristrom,[2] and only those pieces of earlier work which are of specific interest will be mentioned below.

The simple reactions which can occur in the hydrogen-bromine system are

$$Br_2 + M = 2Br + M \quad (1)$$
$$Br + H_2 = HBr + H \quad (2)$$
$$H + Br_2 = HBr + Br \quad (3)$$
$$H_2 + M = 2H + M \quad (4)$$
$$HBr + M = H + Br + M \quad (5)$$
$$H_2 + Br_2 = 2HBr \quad (6)$$

(The following notation will be used: K_i is the equilibrium constant for reaction (i) as written; k_{if} is the rate constant for the forward reaction in equation (i); k_{ir} is the rate constant for the reverse reaction. All concentrations will be expressed in moles/liter and all times in seconds unless otherwise noted. The units of the equilibrium and rate constants will be the appropriate combinations of moles/liter and seconds.) If reactions (2) and (3) are regarded as the important propagation reactions and it is assumed that the steady state approximation can be applied to the H atom concentration then

$$\frac{d(HBr)}{dt} = (Br)\,\frac{2k_{2f}k_{3f}(H_2)(Br_2) - 2k_{2r}k_{3r}(HBr)^2}{k_{3f}(Br_2) + k_{2r}(HBr)} \quad (7)$$

Reaction (1) is the source of the bromine atoms. Reactions (4), (5), and (6) are not fast enough to be important and are included in the list for the sake of completeness. At low temperatures or at large relative H_2 and Br_2 concentrations the reverse reaction can be ignored and equation (7) can be rearranged to

$$\frac{d(HBr)}{dt} = \frac{2k_{2f}(Br)(H_2)}{1 + \dfrac{k_{2r}(HBr)}{k_{3f}(Br_2)}} \quad (8)$$

At low temperatures the Br atoms maintain equilibrium with the molecules and $(Br) = K_1(Br_2)^{1/2}$.

If the correct assumptions are made that reaction (1) can be either ignored or studied independently and that all of the equilibrium constants for the various reactions are known, then two kinetic constants need to be determined to characterize the entire reaction. These two constants have generally been k_{2f}(or $k_{2f}K_1^{1/2}$) and the ratio k_{3f}/k_{2r}.

In the earliest work on this reaction Bodenstein and Lind[3] found k_{3f}/k_{2r} to be 10

± 3. Their values of k_{2f} along with those of Bach, Bonhoeffer, and Molwyn-Hughes[4] have been recalculated using modern equilibrium constants[5] and are included in Table V in the discussion. Later Bodenstein and Jung[6] redetermined k_{3f}/k_{2r} and found it to be 8.4 ± 0.6. In both cases it was found to be temperature independent.

There have been three studies of this reaction at high temperatures. Britton and Davidson,[7] in shock tube experiments around 1500°K found that the values of k_{2f} extrapolated from the low temperature values seemed to be low by a factor of about two. They did only a few experiments of a preliminary nature. Plooster and Garvin[8] compressed mixtures of H_2 and Br_2 in a shock tube and measured the induction times for the onset of explosions. The dependence of these times on temperature was reasonably explained on the basis of values of k_{2f} extrapolated from low temperature values, and the assumption that the Br atom concentration increased with time at the high temperatures behind the shock waves, that is, that the steady state approximation did not apply to Br atoms. Levy[9] studied this reaction in a flow system in which the H_2 and Br_2 were preheated before being mixed together. The steady state approximation was a reasonable one in view of this preheating and the results could be explained in terms of the low temperature mechanism. Values of k_{2f} were measured between 600° and 1500°K. The scatter in these values at high temperature was quite large, but in general the agreement with the low temperature results was good. In the experiments reported here it was hoped to improve the accuracy of the high temperature measurements and to extend the range to higher temperatures.

EXPERIMENTAL

The shock tube, the associated vacuum line, and the observation arrangements have all been described previously.[10] In all of the experiments reported here the Br_2 concentration was followed spectrophotometrically at 5000 A. Under the experimental conditions emission at this wave length was negligible. Duplicate observations were routinely made at two stations 40 cm. apart.

Reaction mixtures were prepared by adding Br_2, H_2, HBr and argon to a storage bulb and noting the total pressure after each addition. The mixtures were allowed to mix in the bulbs at least 48 hours before being used, to allow complete mixing.

CALCULATIONS

Calculation of an Apparent Rate Constant in the Reaction between H_2 and Br_2. A shock wave was run in a mixture of Ar, Br_2, H_2, and perhaps HBr, and a trace similar to Figure 1 obtained. The bromine disappearance after the shock front is the sum of two effects, first the dissociation of Br_2 according to reaction (1), and second the formation of HBr according to reactions (2) and (3). These two effects were separated in the following way. All of the concentrations were determined as a function of time. The Br_2 concentration could be read directly from the oscilloscope trace. The compression ratio generally could be assumed to be constant after the shock since the endothermic dissociation of Br_2 which tends to increase this ratio was more or less balanced by the exothermic formation of HBr which tends to decrease this ratio. This also meant that the temperature was much more nearly constant than in a shock involving only the dissociation reaction. The Br atom concentration could be obtained by graphical integration of the Br_2 concentration since

$$\frac{d(Br)}{dt} = 2k_{1f}(Br_2)(M) - 2k_{1r}(Br)^2(M) \qquad (9)$$

and in the reactions between H_2 and Br_2 the last term could be ignored. It must always be remembered in observations on a moving shock wave that the time on the oscilloscope trace, τ, and the time that the gas has been heated, t, are related by $dt = \Delta d\tau$ where Δ is the compression ratio in the shock. The HBr concentration follows from a mass balance of the bromine. The H atom concentration can always be assumed to be negligibly small so that the hydrogen molecule concentration also follows from mass balance. From the concentrations as a function of time d(HBr)/dt and therefore $k^* = 2k_{2f}/[1 + k_{2r}(HBr)/k_{3f}(Br_2)]$ could be calculated at any time. In

the early stages of the reaction, when the Br atom concentration is small, the rate of formation of HBr is small and the uncertainty in k^* is quite large. In the later stages the back reaction is beginning to be important and the errors in estimating the changes in the temperature and density are becoming large. Therefore it was decided to use the value of k^* at 25% disappearance of the Br_2 in each shock as the best value for that shock.

Calculation of the Rate Constant in the Back Reaction, Br + HBr. — The calculations in this case are very similar to those for the forward reaction described in the preceeding section. A shock wave was passed through a mixture of HBr and Br_2, and a trace similar to figure 3 obtained. The change in the Br_2 concentration is again the sum of two effects, the dissociation of Br_2, and the formation of Br_2 from the reaction between HBr and Br. Since both of these reactions are exothermic it is necessary here to correct for the temperature decrease and the density increase that take place as the reaction proceeds. These changes were approximated as being linear with time, which is not correct, but which does not introduce a large error. The Br_2 concentration could be calculated at all times directly from the oscilloscope trace. The Br atom concentration could be calculated from equation (9), this time including the recombination reaction since the reaction between HBr and Br is slower than the dissociation and recombination of Br_2. A numerical, point by point, integration was performed to give (Br) as a function of time. The H atom concentration and the HBr concentration could be calculated from mass balance. The H_2 concentration was plotted as a function of time and $d(H_2)/dt$ could be determined from the plot. The calculated concentrations as a function of the apparent time in the shock wave are shown in figure 4 for the shock shown in the upper trace in figure 3.

The rate constant for the back reaction, k_{3r}, could be calculated from the following rearranged form of equation (7)

$$\frac{d(H_2)}{dt} = \frac{d(H_2)}{\Delta d\tau} = \frac{k_{3r}(Br)\left[(HBr) - K_6(Br_2)(H_2)/(HBr)\right]}{1 + k_{3f}(Br_2)/k_{2r}(HBr)} \qquad (10)$$

The first term in the numerator represents the reaction in question. The second term represents the reverse of this reaction, that is, the reaction which has previously been called the forward reaction. Since at equilibrium only a small fraction of the HBr has disproportionated this second term must be included. The denominator can be estimated from the known value of the ratio k_{3f}/k_{2r} and is not much greater than 1. The rate constant k_{3r} was generally calculated at a point corresponding to about 25% reaction for reasons similar to those given for the forward reaction.

RESULTS

HBr as a Third Body for the Recombination of Br Atoms. Four series of shocks were run to determine the efficiency of HBr as a third body for the recombination of Br atoms. From the initial rise in concentration in the shock waves in essentially pure HBr it was possible to decide that the HBr was vibrationally relaxed at the shock front and that the apparent dissociation rate constants were not complicated by the simultaneous relaxation of the inert gas. Hydrogen bromide is not truly an inert gas since it can and does disproportionate to H_2 and Br_2, but it does not do this until a reasonable number of Br atoms are present, so that the initial slope of the oscilloscope trace does give the desired dissociation rate constant for Br_2. Figure 3 shows the initial dissociation of Br_2 as well as the subsequent decomposition of HBr in a typical shock in an HBr-Br_2 mixture. The point of the inertness of the HBr will be covered more fully in the section Direct Observation of the Back Reaction. The results of these experiments are summarized in Table I. The temperature range in the experiments generally ran from about 1400° to about 1700° K, and the final total concentrations were 10^{-3} - 10^{-2} moles/liter. The 1500° point more or less represents the center of the range.

Table I

Recombination Rate Constants for HBr as Third Body from Shocks in Br_2-HBr Mixtures.

% Br_2	No. of exptl. points	log k_{1r} = A + B/T A	B	k_{1r} at 1500°K ($mole^{-2}$ $liter^2$ sec^{-1})
0.48	12	6.964	2317	3.2×10^8
1.00	11	6.123	3705	3.9
2.00	24	6.760	2831	4.4
4.41	8	7.024	2399	4.2

There are two ways of looking at these data. The first is to take the average k from all the mixtures as the best value. The other is to regard the trend with mole fraction of Br_2 as real and extrapolate to the limits, one limit for HBr as third body, and the other for Br_2 as third body. In Table II this has been done at 1500 and 1600°K for HBr, and also for Ar[10] for comparison.

Table II

Recombination Rate Constants from Br_2 - HBr and Br_2 - Ar Mixtures.

Inert Gas	Temp.	mean k	extrapolated values of k_{1r} k_{HBr} or k_{Ar}	k_{Br_2}
HBr	1500°K	4.0×10^8	3.6×10^8	24×10^8
	1600	3.1	2.8	21
Ar	1500	3.7	2.6	37
	1600	3.2	2.3	30

Two conclusions may be drawn from Table II. First, HBr is only slightly more efficient than Ar as a third body for the recombination of Br atoms, perhaps 10-30% more. Second, there is further support for the suggestion that at these temperatures Br_2 is closer to 10 times more efficient than Ar rather than 3 times as has been suggested.[11] This support is not very strong, but it is consistent with the Ar results within experimental error.

The Forward Reaction, $H_2 + Br_2$. About one hundred shocks were run in various mixtures of Br_2, H_2, HBr, and Ar. The argon was the principal constituent, and was added in every mixture to serve as a heat capacity buffer, and also in order to provide a third body with known efficiency for the dissociation of Br_2. An apparent rate constant $k^* = k_{2f}/[1 + k_{2r}(HBr)/k_{3f}(Br_2)]$ was calculated at the point of 25% reaction as described previously. For any particular mixture the values of k^* were compared as a function of temperature. For one sample mixture, 1% Br_2 - 1% H_2 - 98% Ar, the experimental points are displayed in figure 5 as log k^* versus $1/T$. A straight line has been fitted through these points by the method of least squares. The best straight lines, but not the experimental points, for three other mixtures are also shown in the same figure. All of these straight lines are of the form log k^* = A + B/T and the values of the parameters are listed in Table III.

Table III

Apparent Rate Constants at 25% Reaction.

Composition of Mixture				$\log k^* = A + B/T$	
% Br_2	% H_2	% HBr	% Ar	A	B
1	1	- -	98	11.180	4085 ± 342
1	1	10	88	10.702	3940 ± 592
2	2	- -	96	11.323	4379 ± 257
2	2	10	86	10.894	4069 ± 363

The actual values of k_{2f} and the ratio k_{3f}/k_{2r} were calculated at several temperatures from points taken from the smoothed curves of figure 5. Two independent estimations were made, one by comparing the results of the 1% Br_2 - 1% H_2 shocks with the results of the 1% Br_2 - 1% H_2 - 10% HBr shocks, and the other by comparing the 2% Br_2 - 2% H_2 with the 2% Br_2 - 2% H_2 - 10% HBr. The values obtained are shown in Table IV.

Table IV

Temp. °K	$k_{2f} \times 10^{-8}$ (moles^{-1} liter sec^{-1})			k_{3f}/k_{2r}		
	from 1% Br_2	2%	avg.	1%	2%	avg.
1300	1.16	.98	1.07	9.5	12.7	11.1
1500	3.07	2.76	2.92	8.8	12.8	10.8
1700	6.34	5.88	6.11	8.5	8.2	8.4

Some experiments were also done using higher percentages of bromine and some using excess hydrogen. It was found that when more than 5% of the mixture was reacting the flow behind the shock (or at least the Br_2 concentration) was not smooth even at a distance of forty tube diameters from the membrane. The trace for an extreme case of this type of a shock is shown in figure 2.

As can be seen from the experimental points in figure 5 the spread of the points from the line is about ± 0.1 in log k^*. This must be attributed to the limited accuracy of the shock wave technique. There is further uncertainty introduced by the uncertainty in the value to use for the rate constant for Br_2 recombination. If the value of k_{1r} which was used in the calculations is increased by 5% (this would be the case if Br_2 is five times more efficient than Ar as a third body or if HBr is 50% more efficient) the calculated values of k^* and k_{2f} would be decreased by about 10% and the value of the ratio k_{3f}/k_{2r} would be decreased by about 15%. A conservative estimate of the uncertainty in the constants reported in Table IV is that they are all uncertain by at least 25% and that they are more likely to be too large than too small.

Direct Observation of the Back Reaction. — In many of the shocks in the HBr - Br_2 mixtures it was apparent from the oscilloscope traces that equilibrium had been reached at much higher concentrations of Br_2 than would be expected if the only reaction were the dissociation of Br_2. In four of the shocks in the 0.482% Br_2 - 99.5% HBr mixtures the Br_2 concentration clearly went through a minimum. The most striking example of this is shown in figure 3. In these four shocks the rate constant, k_{3r}, for the reaction between HBr and Br was calculated as outlined in the section on calculations. The results from these four experiments are shown in figure 6 (two points from each experiment). The points show an average scatter of about 10% from $k_{3r} = 8.1 \times 10^9 T^{1/2} e^{-44500/RT}$ which was fit to them by the method of least squares. These values

of k_{3r} can be combined with the previous values of k_{2f} to obtain an independent estimate of the ratio $k_{3f}/k_{2r} = (k_{3r}/k_{2f})K_6$. When the actual values of k_{3r} are combined with the smoothed values of k_{2f} from Table VII the resulting values of the ratio show no variation with tempature and have an average value of 8.3 ± 0.7, which can be compared with the value 10.1 ± 1.7 obtained from the measurements of the forward reaction with and without added HBr.

DISCUSSION

The results of the various studies of the value of k_{2f} are collected in Table V where they are given in two forms, first as $\log k_{2f} = A - B/T$ for convenience in calculation, and second as $k_{2f} = CT^{1/2}e^{-\Delta H/RT}$ since this form has some theoretical justification for a bimolecular reaction.

Table V

The Rate Constant, k_{2f}, for the Reaction between Br and H_2.

temp.	range	ref.	$\log k_{2f} = A - B/T$		$k_{2f} = CT^{1/2}e^{-\Delta H/RT}$	
			A	B	C	ΔH
°K				°K	liter $mole^{-1}sec^{-1}$	kcal/mole
Br + H_2						
500 -	575	5	11.357	4235 ± 46	5.92×10^9	$18.8 \pm .2$
550 -	600	10	10.927	4053 ± 141	2.15	$18.0 \pm .7$
1300 -	1700	this work	11.254	4195 ± 400	3.54	18.3 ± 1.8
500 -	1700	all	11.238	4190 ± 21	3.35	$18.3 \pm .1$

The probable errors would indicate that neither of these two forms is to be preferred over the other on the basis of the experimental data. The agreement between the low temperature results and the high temperature shock wave results is quite good.

The ratio k_{3f}/k_{2r} which was known to be temperature invariant at low temperatures within experimental error has now been shown to be temperature invariant over the temperature range 300 - 1700°K within experimental error. The best low temperature value, 8.4 ± 0.6 is almost exactly the same as the weighted average of the two independent measurements of the ratio at high temperature, 8.3 ± 0.7 and 10.1 ± 1.7.

The activation energy associated with k_{2f} is 18.3 kcal/mole (Table VIII). The heat of the reaction at 0°K is 16.2 kcal/mole. This means that k_{3f} and k_{2r} must have an identical activation energy of about 2 kcal/mole. If the value of the ratio at high temperature differs from that at low temperatures by 10% the activation energies would differ by about 0.1 kcal/mole. This pair of activation energies is an embarrassing case for any rule which tries to predict the activation energy from the bond energy of the bond being broken since D_{Br_2} (=45 kcal/mole) and K_{HBr} (= 87 kcal/mole) differ by a factor of 2.

ACKNOWLEDGEMENTS

We would like to thank the Research Corporation, the Office of Ordnance Research, U. S. Army, and the Graduate School of the University of Minnesota for their support of this work.

REFERENCES

(1) R. N. Pease, "Equilibrium and Kinetics of Gas Reactions," Princeton University Press, 1942, pp. 112-121.
(2) E. S. Campbell and R. M. Fristrom, Chem. Rev. 58, 173 (1958).
(3) M. Bodenstein and S. C. Lind, Z. physik. Chem. 57, 168 (1906).
(4) F. Bach, K. F. Bonhoeffer, and E. A. Molwyn-Hughes, Z. physik. Chem. 27B, 71 (1935).
(5) National Bureau of Standards, "Selected Values of Chemical Thermodynamic Properties," Series III, Washington, 1948, 1954.
(6) M. Bodenstein and G. Jung, Z. physik. Chem. 121, 127 (1926).
(7) D. Britton and N. Davidson, J. Chem. Phys. 23, 2461 (1955).
(8) M. N. Plooster and D. Garvin, J. Am. Chem. Soc. 78, 6003 (1956).
(9) A. Levy, J. Phys. Chem. 62, 570 (1958).
(10) D. Britton, J. Phys. Chem. 64, 742 (1960).
(11) H. B. Palmer and D. F. Hornig, J. Chem. Phys. 26, 98 (1957).

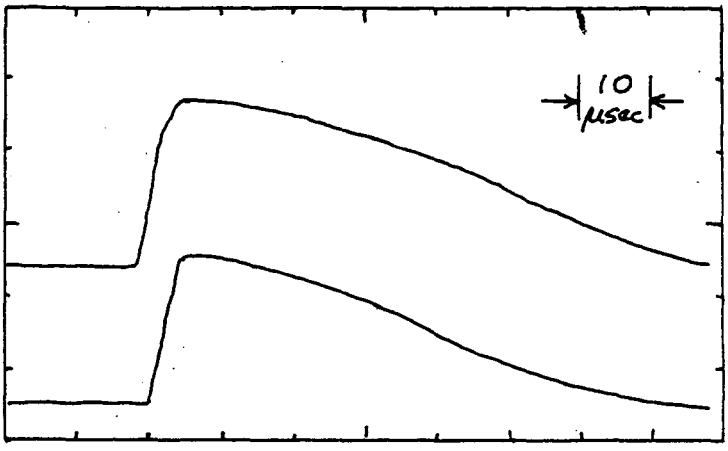

Fig. 1.—Oscillogram of typical shock used for kinetic studies. This shock was run in a 1% H_2 - 1% Br_2 - 98% Ar mixture, and reached a temperature of 1448°K at the shock front. Note the acceleration in the rate of disappearance of Br_2 as more Br atoms are produced. (In all of the oscillograms the lower trace records the Br_2 concentration at the first observation station as a function of time, and the upper trace records at the second observation station, 40 cm from the first.)

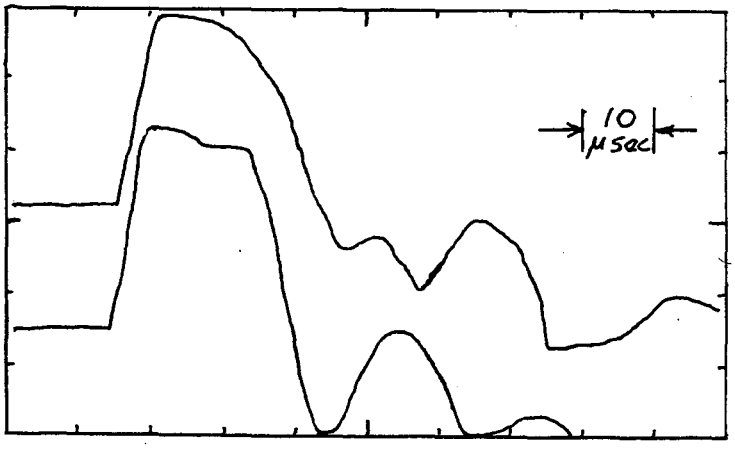

Fig. 2.—Oscillogram of shock in highly exothermic reaction mixture. This shock was run in a 5% Br_2 - 20% H_2 - 75% Ar mixture and reached a temperature of 1424°K at the shock front. It is apparent that no useful kinetic data could be obtained in the shocks in concentrated mixtures.

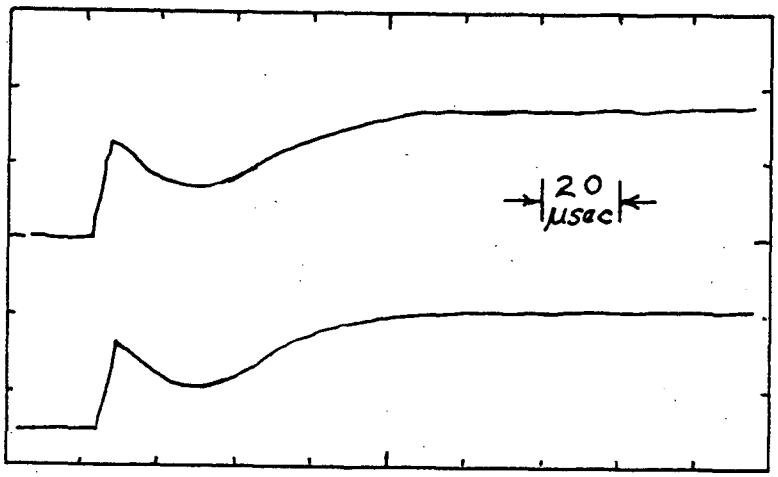

Fig. 3.—Oscillogram of shock showing the reverse reaction. This shock was run in a 0.5% Br_2 - 99.5% HBr mixture and reached a temperature of 1635°K at the shock front. Note the production of molecular Br_2 when the Br atom concentration becomes sufficiently large.

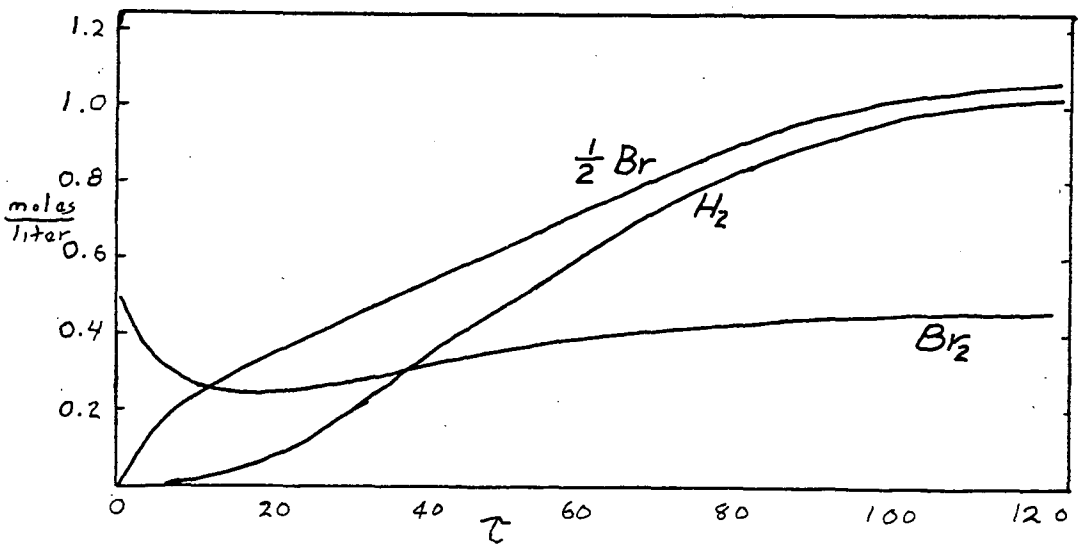

Fig. 4.—Concentrations as a function of time for the upper trace of the shock wave shown in fig. 2. The Br atom concentration is calculated from the known dissociation and recombination rate constants. The H_2 concentration is calculated from mass balance considerations.

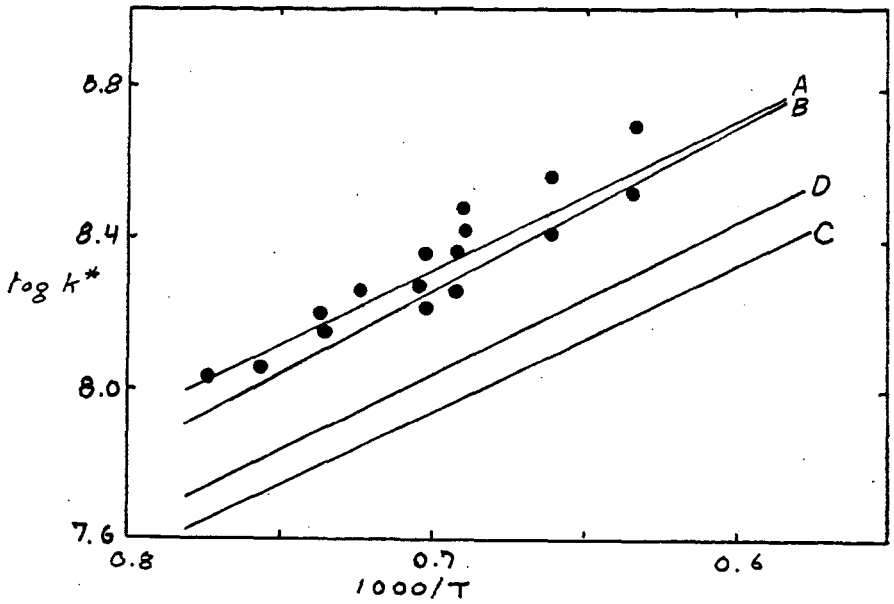

Fig. 5.—Apparent rate constants for the reaction between Br and H_2 at 25% reaction. The points are the experimental points for line A.

A - 1% Br_2 - 1% H_2
B - 2% Br_2 - 2% H_2
C - 1% Br_2 - 1% H_2 - 10% HBr
D - 2% Br_2 - 2% H_2 - 10% HBr

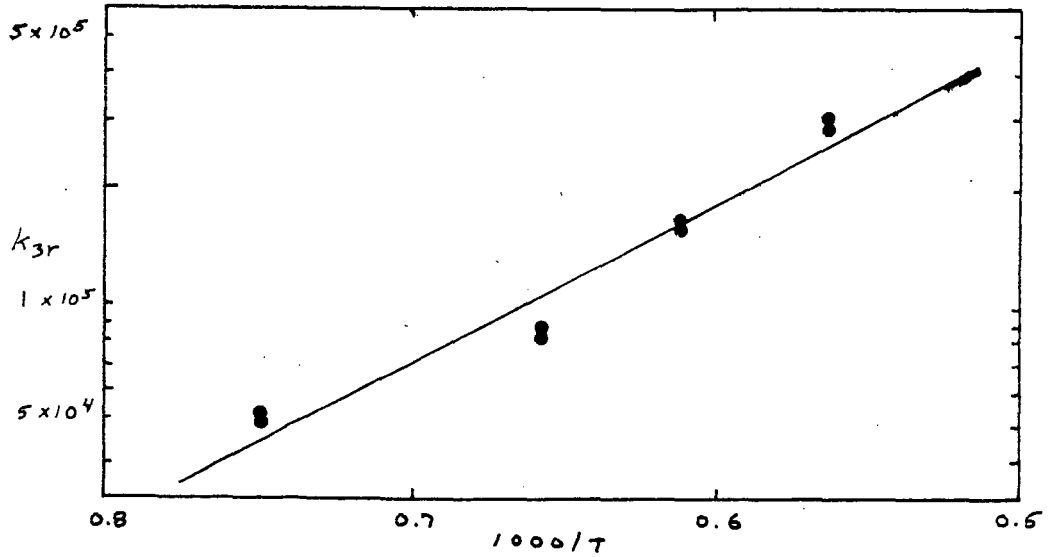

Fig. 6.—Rate constant for the reaction between Br and HBr. The straight line is the least squares line through the points.

A Shock Tube Study of the Vibrational and Chemical Relaxation of Nitric Oxide at High Temperatures*

Kurt L. Wray and J. Derek Teare

Avco-Everett Research Laboratory
Everett 49, Massachusetts

Introduction

Extensive studies of the relaxation region behind normal shocks in air have been carried out at this Laboratory.(1) The experiments include studies on pure air, N_2, O_2, NO, and various mixtures of these with each other and with argon. As a part of this program, we have undertaken a study of the chemical kinetics of NO in the temperature range 3000 - 8000° K, and of the vibrational relaxation of NO in the range 1500 - 7000° K. The experimental technique employed in this investigation was the monitoring of the NO concentration as a function of time by its absorption of 1270 A radiation. The present paper will be restricted to this portion of the overall program, and to a discussion of those reactions which involve the formation, removal or vibrational relaxation of NO.

As we shall see, such systems at high temperatures are fairly involved, and the analysis of the experimental data requires the aid of an electronic computer. To this end, computer programs using an IBM 704 have been written which permit the calculation of the density, temperature, and concentration time history for any given set of pertinent rate constants. These programs include a postulated coupling of vibrational and dissociative processes.(2)

The following is a list of chemical reactions occurring in air which are pertinent to this paper:

$$O_2 + M + 5.1 \text{ ev} \rightleftarrows O + O + M \qquad (1,2)$$

$$N_2 + M + 9.8 \text{ ev} \rightleftarrows N + N + M \qquad (3,4)$$

$$NO + M + 6.5 \text{ ev} \rightleftarrows N + O + M \qquad (5,6)$$

$$NO + O + 1.4 \text{ ev} \rightleftarrows O_2 + N \qquad (7,8)$$

$$N_2 + O + 3.3 \text{ ev} \rightleftarrows NO + N \qquad (9,10)$$

$$N_2 + O_2 + 1.9 \text{ ev} \rightleftarrows NO + NO \qquad (11,12)$$

$$X_2 + M \rightarrow X_2^v + M \qquad (13)$$

It should be pointed out that the collision partner "M" can be any molecule or atom, and part of the unravelling of the kinetics is to evaluate the relative efficiencies of the possible catalysts. Reaction 1,2 has been studied extensively by Camac and Vaughan(3) and others, and the rate constants are well determined. Reaction 3,4 plays but a minor role even at the highest temperatures encountered

*Supported jointly by AFBMD-ARDC-USAF, Contract AF 04(647)-278 and ARPA, monitored by the ARGMA-AOMC-U.S. Army, Contract DA-19-020-ORD-4862.

in the experiments under discussion. Reactions 5-12 all contribute to the formation and subsequent removal of NO behind a shock front in air. Rate constant information for these reactions has been obtained from observations of the decomposition of shock-heated NO.

Vibrational relaxation (reaction 13) plays an important role early in the time history following the shock front. The vibrational relaxation of O_2 and N_2 has been measured by other workers.[4, 5] Robben[6] has measured the vibrational relaxation rate of NO by NO over the temperature range 400 - 1500° K.

Theory of Vibrational Relaxation

It was assumed by Bethe and Teller,[7] and subsequently proven by Montroll and Shuler[8], that if a gas initially has a Boltzmann distribution of vibrational energies, it will relax to a final Boltzmann distribution of energies with all intermediate stages having a well defined vibrational temperature.

The relaxation equation given by the above authors is remarkably simple when written in terms of vibrational energy. If the gas is initially at room temperature, we can write

$$\frac{d \log_e (1 - E_v/E_f)}{dt} = -\frac{1}{\tau} \quad , \tag{14}$$

and, for an harmonic oscillator, we obtain from statistical mechanics

$$\frac{E_v}{E_f} = \frac{e^{\Theta/T_f} - 1}{e^{\Theta/T_v} - 1} \quad . \tag{15}$$

In these equations, E_v is the vibrational energy corresponding to the vibrational temperature T_v at time t, E_f is the vibrational energy corresponding to the final vibrational temperature T_f and τ is the relaxation time. For NO, $\Theta = 2688°$ K.

The relaxation time, τ, is related to a transition probability by the equation

$$\frac{1}{\tau} = Z \, P_{10} \, (1 - e^{-\Theta/T}) \quad , \tag{16}$$

where T is the translational temperature, P_{10} is the transition probability per oscillator per collision for transition between vibrational levels 1 and 0, and Z is the number of collisions suffered by a single oscillator molecule per second with a catalyst particle.

For an NO-Ar mixture, in which two catalytic species are present, the effective relaxation time is related to the relaxation time for each individual catalyst by the equation

$$\frac{1}{\tau} = \frac{f}{\tau_{NO\text{-}NO}} + \frac{1-f}{\tau_{NO\text{-}Ar}} \quad , \tag{17}$$

in which f is the fraction of oscillator molecules in the mixture.

Theoretical formulae for P_{10} have been proposed by Landau and Teller[9] and by Schwartz, Slawsky and Herzfeld.[10] The SSH theory allows P_{10} to be calculated using the Lennard-Jones parameters ϵ and r_0.

$$P_{10} = A \, e^{-BT^{-1/3}} \quad , \tag{18}$$

where, for most molecules A and B are weak functions of temperature.

Experimental Program

The ultraviolet light absorption technique employed in these studies is similar to that used by Davidson and his co-workers[11] who used visible light to measure iodine relaxation rates. Camac[5] has developed the technique extensively using radiation at 1470 A in his O_2 studies. Watanabe, et al,[12] have measured the room temperature absorption coefficients for several gases in the vacuum ultraviolet and found a narrow window in the absorption spectra of O_2 at 1270 A where NO showed strong absorption. Since, in this investigation, we wanted primarily to observe the NO molecule, we chose to work at a wavelength of 1270 A with a bandwidth of 5A.

A schematic diagram of the apparatus is shown in Fig. 1. The shock tube, constructed of stainless steel, was of a circular cross-section having an inside diameter of 3.81 cm. Scored stainless steel diaphragms were used, and they were ruptured by increasing the driver pressure until the diaphragm failed. The usual driver gas was hydrogen or a mixture of hydrogen and nitrogen. The shock speed was determined by means of platinum strip heat transfer gages. The measurements of the position of the shock front could be made to about 1/3 microsecond, which corresponded to 0.3% uncertainty in the shock velocity.

The optical observation station at the shock tube consisted of the following components: (1) light source, (2) slits and CaF_2 windows on both sides of the shock tube, (3) monochromator, (4) phosphor-coated photomultiplier, and (5) recording oscilloscope.

Two types of light sources were used. When it was desired to observe the shock-heated gas for relatively long times, a hydrogen discharge lamp was employed. This lamp produced several strong molecular lines in the 5A wavelength band centered on 1270 A; its intensity which decayed monotonically to zero in about 3 milliseconds allowed a resolution of about 1 μ sec.

When it was desired to observe the leading edge of the shock front, a Lyman lamp was used. The Lyman lamp is a helium discharge light source and it produces a continuum in the wavelength region of interest. This lamp produced a damped oscillating output whose second cycle (the one used) allowed a testing time of about 15 μ sec and was sufficiently intense to allow resolution of a few tenths of a microsecond.

An oscillogram obtained with the U. V. absorption apparatus is shown in Fig. 2. This oscillogram is reproduced here to show the time history over the entire testing time; it does not have a sufficiently fast sweep speed to show the relaxation phenomenon to maximum advantage.

The ground state absorption coefficients for NO, O_2 and N_2 (i.e., room temperature absorption) were determined in this apparatus using the hydrogen lamp on a DC basis with the output of the photomultiplier being monitored by a microammeter, the NO and O_2 gases being introduced into the shock tube. In the case of N_2, however, the absorption by the room temperature gas was insufficient and the path length was increased by introducing the gas into the monochromator.

It was necessary to experimentally determine the absorption coefficients for the various species as a function of vibrational temperature. For this purpose, many shock tube runs were made with NO-Ar and O_2-Ar mixtures and pure N_2. The absorption by the shock-heated gas was measured at a point on the oscillogram corresponding to complete vibrational relaxation but before dissociation starts.

The temperature (vibrational) and density corresponding to this condition were calculated for each run and were used in conjunction with the oscillograms to obtain the curves shown in Fig. 3. The two points at the extreme left of these curves are the room temperature absorption coefficients. We see that vibrationally excited NO absorbs more strongly than does the ground state and that the absorption seems to increase roughly linearly with increasing vibrational temperature. Notice that the absorption coefficient for vibrationally excited O_2 is much larger than for the ground state. This is somewhat unfortunate because it means that under certain conditions (early times in air) the correction for the absorption due to the vibrationally excited O_2 becomes significant.

Although the absorption coefficient of N_2 is completely negligible at room temperature ($k = .014\ cm^{-1}$), our experiments showed it to be a strong function of vibrational temperature ($k = 1.1$ at 6000° K, 3.6 at 8000° K). This absorption correlates with the population of the 11th vibrational state. Vibrationally excited nitrogen thus contributes significantly to the absorption in shock heated air above 6000° K.

By observing the magnitude of the initial jump in the signal due to the compression across the shock front, it was proven that the absorption coefficient is independent of translational and rotational temperature.

Data Reduction

For the purpose of the chemical relaxation studies, computed curves were fitted to a total of 42 experimental time histories in the following six mixtures: 1/2% NO, 1/2% NO + 1/4% O_2, 50% NO, 10% NO, 100% air and 20% air, in all cases the diluent being argon. The temperature range covered was 3000 - 8000° K.

The general equation for the intensity of monochromatic radiation, I, transmitted through a gas sample is

$$I/I_0 = \exp\left\{- L\,(P_1/P_s)\,x\,(\rho_2/\rho_1)\sum_j (k_j f_j)\right\}, \qquad (18)$$

where I_0 is the intensity of radiation with no absorber in the optical path of length L, P_1 is the total initial pressure of the gas, P_s is standard pressure, ρ_2/ρ_1 is the density ratio across the shock, and k_j is the absorption coefficient of species j having a concentration f_j (moles/original mole of mixture).

In general, the density ratio and the quantities k_j and f_j vary throughout the relaxation period. Their values are obtained from a computer program which integrates the chemical and vibrational rate equations subject to the constraints imposed by the conservation equations. The computer output includes T, ρ_2/ρ_1, f_j and df_j/dt, as well as I/I_0 which is used for direct comparison with experimental intensity vs. time histories. The input to the computer includes shock speed, composition, initial pressure, k_j as a function of T_v for the three absorbing species, together with the rate constant information for reactions 1-13. The rate constants for equations 5-12 were varied in a systematic trial and error process which yielded a set of rate constants which satisfactorily fit all the measurements. The high temperature vibrational relaxation rates for NO required in the above computer program were obtained independently as discussed below.

Three NO-Ar mixtures (50% NO, 10% NO and 1% NO) were analyzed for vibrational rate information. The experimental signal (I/I_0) must be related to the quantity $1 - Ev/E_f$, using the NO absorption coefficient of Fig. 3. For each run analyzed it was necessary to construct a plot of I/I_0 vs. $(1 - Ev/E_f)$, and then to cross-plot the I/I_0 vs. time data from the oscillogram. Two typical oscillograms obtained for vibrational analysis are shown in Fig. 4, and the corresponding cross-plots are given in Fig. 5.

According to Eq. 14 such a plot should be a straight line. In general, all the data yielded fairly straight lines when plotted in the above manner. Although these lines seldom went through the value of unity at t = 0, the discrepancies were consistent with transit time considerations. The slopes of these straight lines give the vibrational relaxation (laboratory) time.

Following the usual practice, the data will be presented with the relaxation times in the particle coordinate system and normalized to standard density. In Fig. 6 we have plotted $\tau_s (1 - e^{-\Theta/T})$ vs. $\overline{T}^{-1/3}$ for the three mixtures studied.

Results and Conclusions

The results of our vibrational relaxation experiments as well as those of Robben[6] indicate that the Lennard-Jones parameters appropriate to an NO collision leading to vibrational relaxation are $r_0 = 2.15$ A and $\epsilon/k = 2000^\circ$ K. For this exceptionally high value of ϵ the usual statement that a plot of log $\tau_s(1-e^{-\Theta/T})$ vs. $T^{-1/3}$ should yield a straight line is not valid.

The three solid lines in Fig. 6 are least square fits to the data based on Eq. 17. The curvature in these lines is produced by temperature dependent terms in P_{10} that for most molecules are insignificant compared to the $T^{-1/3}$ dependence. The two dashed curves in Fig. 6 labelled f = 1 and f = 0 are the computed relaxation times for the NO-NO and the NO-Ar collision, respectively, based on the least square fit to the experimental data.

The above relaxation times can be converted into transition probabilities by means of Eq. 16. The calculated probabilities resulting from these experiments are plotted vs. $T^{-1/3}$ in Fig. 7. They are the solid lines labelled P_{NO-NO} and P_{NO-Ar}. It should be pointed out that the P_{NO-NO} curve is very nearly the curve one would get using the data from the NO-rich mixtures alone and assuming that the argon plays no role in exciting the NO. The P_{NO-Ar} curve, on the other hand, is obtained essentially from the 1% data only after subtracting out the large effect due to NO-NO collisions. Hence, the uncertainty in this curve is much greater than the P_{NO-NO} curve. For comparison, Robben's data is also shown in Fig. 7. It covers the temperature range from 400 - 1500° K.

The other two curves shown in this figure are calculated from the SSH theory[10] for the Lennard-Jones parameters indicated in the figure. The lower of these two curves should apply to both NO-NO and NO-Ar transition probabilities.

Robben pointed out in his paper that there is evidence of the formation of an NO dimer (of rectangular geometry) in the solid and liquid state.[13, 14] The Lennard Jones parameters appropriate to the dimer were the ones used to calculate the upper theoretical curve. The low temperature portion of this curve has been drawn as a dotted line as some of the approximations in the SSH theory are not applicable in this temperature range for $\epsilon/k = 2000^\circ$ K.

At high temperatures the slope of the theoretical curve based on the dimer potential compares well with the experimental one. Since the dimer has rectangular geometry, an attractive collision could result only for specifically oriented collision pairs, and a steric factor of about 1/30 implied by Fig. 7 is not unreasonable.

The noise fluctuations in the oscilloscope traces, which were of statistical origin, could produce errors in I/I_0 of as much as ± 4%. This probably represents the greatest source of scatter in the vibrational data, introducing somewhat less than a factor of 2 uncertainty in the relaxation times.

The various mixtures used in the chemical relaxation studies were chosen to emphasize the relative contribution of particular reactions. For example, the

1/2% NO runs provided a determination of the argon contribution to reaction 5, while the 1/2% NO + 1/4% O_2 mixture was used (at Prof. Norman Davidson's suggestion) to emphasize the importance of reaction 7 by providing an abundance of O atoms early in the time history. The NO-rich mixtures emphasize both reaction 12 and the NO catalytic effect in reaction 5. Estimates based on measurements[15] below 2000° K indicated that the bimolecular path (reaction 11-12) should be unimportant above 3000° K, but this proved inconsistent with the present experimental results. In achieving a satisfactory fit, we have made use of recent high temperature measurements[16] of the bimolecular rate constant.

A summary of the rate constants for reactions 1-12 is given in Table I.

Acknowledgements

The authors wish to acknowledge the support given to this work by Dr. M. Camac during the early stages of the experiment. They also wish to thank Mr. A. Magro for his devoted help in the actual operation of the shock tube.

REFERENCES

1. K. Wray, J. D. Teare, B. Kivel and P. Hammerling, Avco-Everett Research Laboratory, Research Report 83, December 1959.

2. P. Hammerling, J. D. Teare, B. Kivel, Phys. Fluids 2, 422 (1959).

3. M. Camac and A. Vaughan, J. Chem. Phys. 34, (1961).

4. V. H. Blackman, J. Fluid Mech. 1, 61 (1956).

5. M. Camac, J. Chem. Phys. 34, (1961).

6. F. Robben, J. Chem. Phys. 31, 420 (1959).

7. H. A. Bethe and E. Teller, Ballistic Research Laboratory, Report X-117 (1941).

8. E. Montroll and K. Shuler, J. Chem. Phys. 26, 454 (1957).

9. L. Landau and E. Teller, Physik. Z. Sowjetunion 10, 34 (1936).

10. R. N. Schwartz, Z. I. Slawsky and K. F. Herzfeld, J. Chem. Phys. 20, 1591 (1952). R. N. Schwartz and K. F. Herzfeld, J. Chem. Phys. 22, 767 (1954).

11. D. Britton, N. Davidson, and Schott, Discussions Faraday Soc. 17, 58 (1954).

12. E. Watanabe, M. Zelikoff, and E. C. Y. Inn, Geophysical Research Papers, No. 21, AFCRC Technical Report No. 53-23.

13. O. K. Rice, J. Chem. Phys. 4, 367 (1936).

14. Dulmage, Meyers, and Lipscomb, J. Chem. Phys. 19, 1432 (1951).

15. F. Kaufman, and J. Kelso, J. Chem. Phys. 23, 1702 (1955).

16. E. Freedman and J. Daiber, Unpublished, Cornell Aeronautical Laboratory, Buffalo, New York.

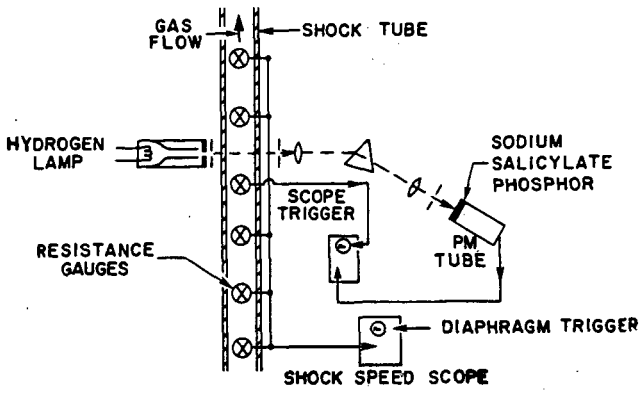

Fig. 1 Schematic diagram of the apparatus used in the ultraviolet light absorption experiments.

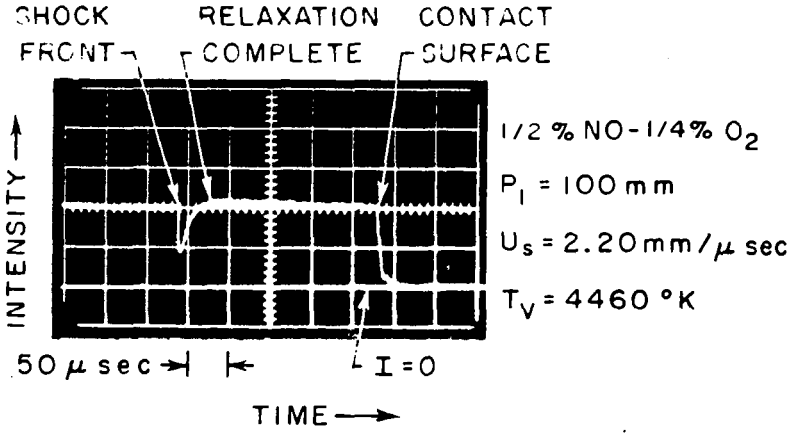

Fig. 2 Typical oscillogram from U. V. absorption experiments showing complete testing time.

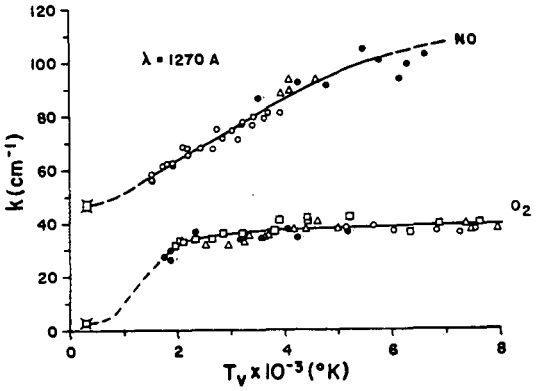

Fig. 3 Absorption coefficients of NO and O_2 per cm. of path length at a density corresponding to P = 1 atm and T = 300° K.

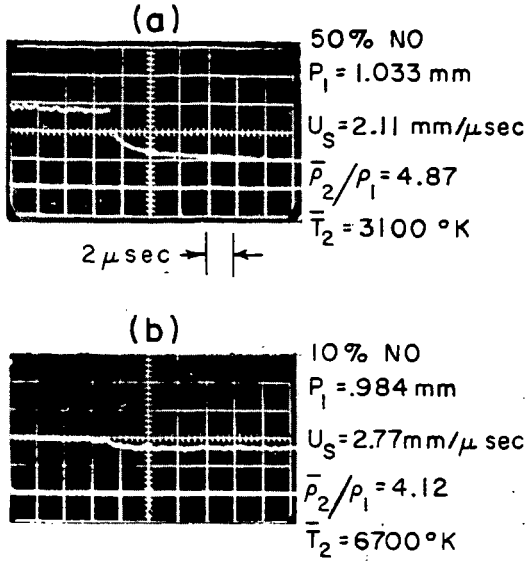

Fig. 4 Typical oscillograms showing the vibrational relaxation of NO.

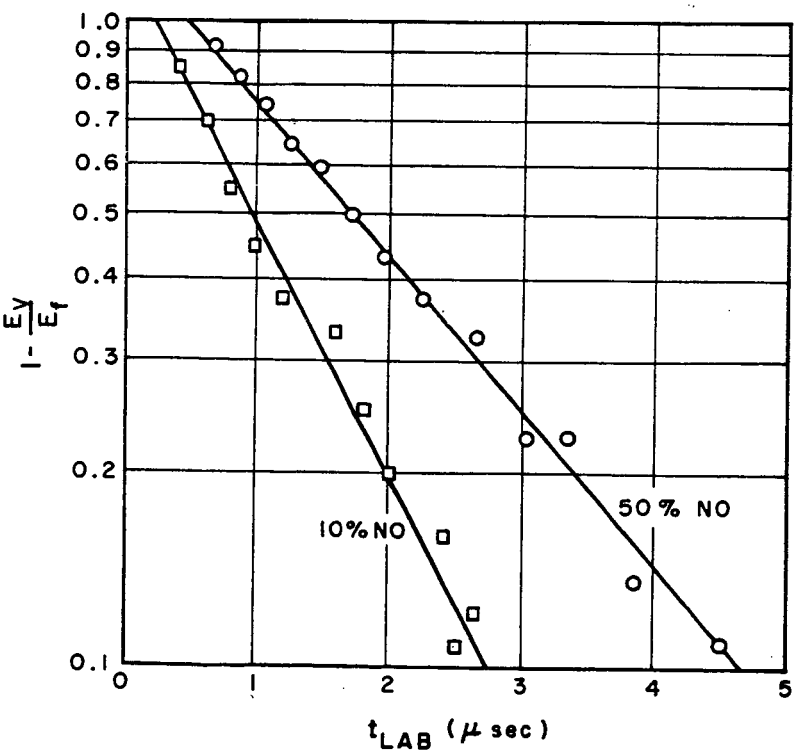

Fig. 5 Experimental plot of $1-Ev/E_f$ against laboratory time. The two cases shown result from the oscillograms of Fig. 4.

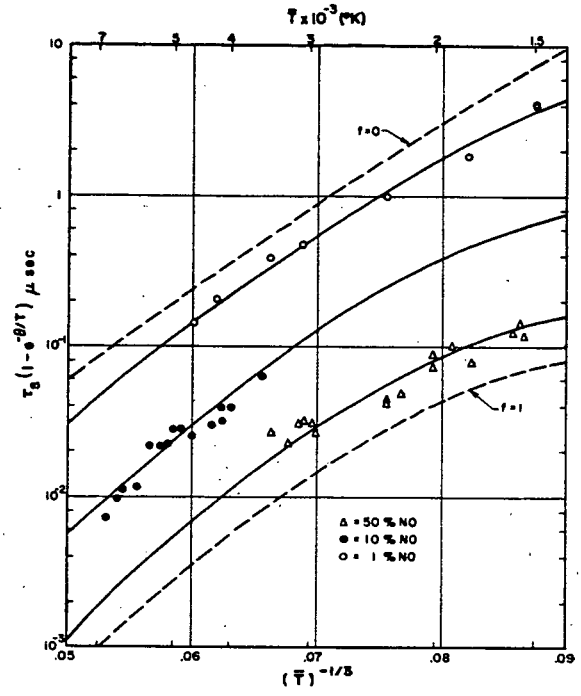

Fig. 6 Experimental vibrational (particle) times standardized to normal density. The solid curves are fitted to the data according to the theory of Schwartz, Slawsky and Herzfeld. The dashed curves show the deduced values of τ for NO-NO (f=1) and NO-Ar (f=0) collisions.

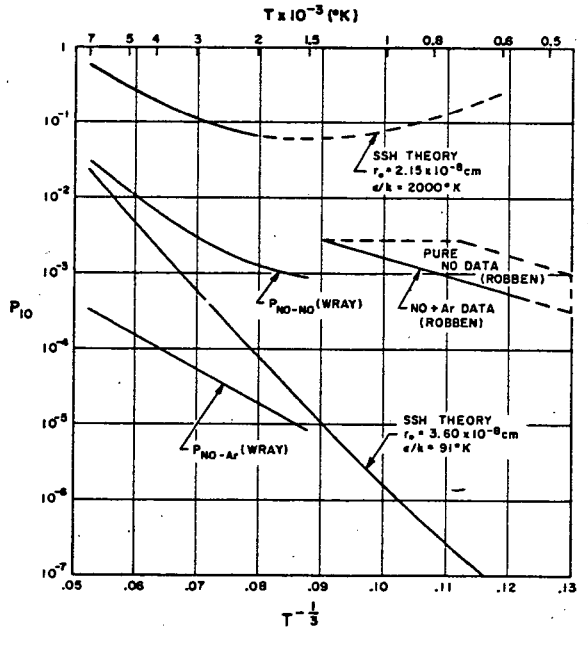

Fig. 7 Experimental and theoretical transition probabilities for de-exciting the first vibrational level of NO.

TABLE I - RATE CONSTANTS FOR CHEMICAL PROCESSES

Reaction	Catalyst M	Rate Constant
$O_2 + M + 5.1\ ev \underset{k_R}{\overset{k_D}{\rightleftarrows}} O + O + M$	Ar, N, N_2, NO	$k_D = \frac{3.6 \times 10^{18}}{T} \exp(-59373/T)\ cm^3/mole\ sec$
	O_2	$k_D = \frac{3.2 \times 10^{19}}{T} \exp(-59373/T)\ cm^3/mole\ sec$
	O	$k_D = \frac{8.9 \times 10^{19}}{T} \exp(-59373/T)\ cm^3/mole\ sec$
$N_2 + M + 9.8\ ev \underset{k_R}{\overset{k_D}{\rightleftarrows}} N + N + M$	Ar, O, O_2, NO	$k_R = 1.7 \times 10^{14} \times (T/4500)^{-1.5}\ cm^6/mole^2\ sec$
	N_2	$k_R = 5 \times 10^{14} \times (T/4500)^{-1.5}\ cm^6/mole^2\ sec$
	N	$k_R = 8 \times 10^{15} \times (T/4500)^{-1.5}\ cm^6/mole^2\ sec$
$NO + M + 6.5\ ev \underset{k_R}{\overset{k_D}{\rightleftarrows}} N + O + M$	Ar, O_2, N_2	$k_R = 3.3 \times 10^{14} \times (T/4500)^{-1.5}\ cm^6/mole^2\ sec$
	NO, O, N	$k_R = 6.7 \times 10^{15} \times (T/4500)^{-1.5}\ cm^6/mole^2\ sec$
$NO + O + 1.4\ ev \underset{k_2}{\overset{k_1}{\rightleftarrows}} O_2 + N$	$k_2 = 1 \times 10^{12}\ T^{0.5} \exp(-3120/T)$	$cm^3/mole\ sec$
$N_2 + O + 3.3\ ev \underset{k_2}{\overset{k_1}{\rightleftarrows}} NO + N$	$k_2 = 1.3 \times 10^{13}$	$cm^3/mole\ sec$
$N_2 + O_2 + 1.9\ ev \underset{k_2}{\overset{k_1}{\rightleftarrows}} NO + NO$	$k_2 = 2.6 \times 10^{23} \times T^{-2.5} \exp(-43030/T)\ cm^3/mole\ sec$	